

Spring 2023

Floodplain Aquifer Storage Capacity in Upper Yakima River Tributaries, Kittitas County, WA

Emily Polizzi
polizzie@cwu.edu

Follow this and additional works at: <https://digitalcommons.cwu.edu/etd>



Part of the [Geomorphology Commons](#), [Stratigraphy Commons](#), and the [Water Resource Management Commons](#)

Recommended Citation

Polizzi, Emily, "Floodplain Aquifer Storage Capacity in Upper Yakima River Tributaries, Kittitas County, WA" (2023). *All Master's Theses*. 1872.

<https://digitalcommons.cwu.edu/etd/1872>

This Thesis is brought to you for free and open access by the Master's Theses at ScholarWorks@CWU. It has been accepted for inclusion in All Master's Theses by an authorized administrator of ScholarWorks@CWU. For more information, please contact scholarworks@cwu.edu.

SHALLOW FLOODPLAIN AQUIFER STORAGE CAPACITY IN UPPER YAKIMA
RIVER TRIBUTARIES, KITTITAS COUNTY, WA

A Thesis
Presented to
The Graduate Faculty
Central Washington University

In Partial Fulfillment
of the Requirements for the Degree
Master of Science
Geological Sciences

by
Emily Claire Polizzi
May 2023

CENTRAL WASHINGTON UNIVERSITY

Graduate Studies

We hereby approve the thesis of

Emily Claire Polizzi

Candidate for the degree of Master of Science

APPROVED FOR THE GRADUATE FACULTY

Dr. Lisa Ely, Committee Chair

Dr. Carey Gazis

Dr. Breanyn MacInnes

Dean of Graduate Studies

ABSTRACT

SHALLOW FLOODPLAIN AQUIFER STORAGE CAPACITY IN UPPER YAKIMA RIVER TRIBUTARIES, KITTITAS COUNTY, WA

by

Emily Claire Polizzi

May 2023

Large wood (LW) restoration projects were recently implemented in the Upper Yakima Basin following the destructive logging practices of the early 20th Century, which stripped Upper Yakima River tributaries of LW. The removal of natural LW increased incision, isolating channels from floodplain aquifers, and degrading resident and anadromous fish habitat. Returning streams to their natural state through instream LW installations is believed to increase floodplain groundwater storage by decreasing channel incision, increasing floodplain-channel connectivity, and raising the water table elevation. Additional storage in floodplain aquifers can help combat the adverse effects of climate change, namely decreasing snowpack and earlier melting. Storing infiltrating snowmelt and river water during peak flow in shallow floodplain aquifers could allow the natural release of groundwater as baseflow through the dry summer. Taneum Creek, Indian Creek, and Teanaway River have established LW projects and are candidates for floodplain aquifer storage. However, a regionally wide spread gray silt layer could affect potential aquifer transmissivity and storage capacity. Through fieldwork, mapping, and grain-size analysis, the groundwater storage volume was quantified taking into consideration the effects of the stratigraphy on groundwater storage, recharge, and flow. Volume estimates indicate a potential floodplain aquifer capacity of 1,040-1,990 acre-feet in the North Fork Teanaway watershed and 352-1,320 acre-feet in Taneum Creek.

ACKNOWLEDGMENTS

This research was funded by the Washington State Department of Ecology (ECY) and the American Water Resources Association Washington Section (AWRA-WA). I would like to thank these organizations for allowing me to dedicate the summer of 2022 and the 2022-2023 academic year to research. I would like to thank my amazing field assistants for dedicating part of their summer to wading around in rivers with me: Brice Liedtke, Bailey Duvall, Connor Hayes, and Austin Halstead. Thank you to my fellow master's students, Edward Vlasenko, Bethany Kharrazi, and Sam Fixler for their field, technical, and moral support during the last two years. I would like to thank my committee members, Dr. Carey Gazis for her groundwater expertise and Dr. Bre MacInnes on her help with laboratory analysis. I would like to thank Dr. Lisa Ely, my advisor and mentor, for her unwavering support and dedication to me through this project. Lastly, I would like to thank my mother, Shannon Nolan, and grandparents, Glenna and Frank Nolan, for always believing in me.

TABLE OF CONTENTS

| Chapter | Page |
|---------|--|
| I | INTRODUCTION 1 |
| | A Brief Summary of the Project..... 1 |
| | Project Objectives 1 |
| | The Upper Yakima River Basin 3 |
| II | BACKGROUND 7 |
| | Yakima Basin Integrated Plan..... 7 |
| | Resident and Anadromous Fish 8 |
| | Climate 9 |
| | Large Wood..... 9 |
| | Tectonics and Lithology..... 12 |
| | Hydrogeologic Setting 13 |
| | Glacial History 19 |
| III | METHODS 21 |
| | Stratigraphy 21 |
| | Piezometer Analysis..... 25 |
| | Sediment Size Analysis..... 26 |
| | Floodplain Mapping 26 |
| | North Fork Teanaway Watershed 27 |
| | Taneum Creek Watershed 29 |
| | Aquifer Storage Capacity Calculation 30 |
| IV | RESULTS 32 |
| | Stratigraphy 32 |
| | Gray Silt 37 |
| | Piezometer Analysis..... 39 |
| | North Fork Teanaway Watershed Floodplain Mapping..... 44 |
| | Taneum Creek Floodplain Mapping 49 |
| | Floodplain Aquifer Volume 54 |
| V | DISCUSSION 57 |
| | North Fork Teanaway Watershed Stratigraphy..... 57 |
| | Taneum Creek Stratigraphy 59 |
| | Gray Silt 63 |

TABLE OF CONTENTS (CONTINUED)

| Chapter | | Page |
|---------|---|------|
| | Floodplain Area..... | 68 |
| | Floodplain Aquifer Volume | 71 |
| VI | CONCLUSION..... | 78 |
| | REFERENCES | 81 |
| | APPENDICES | 84 |
| | Appendix A—Stratigraphic Profiles | 84 |
| | Appendix B—Grain-Size Distribution Graphs | 90 |
| | Appendix C—REM to Floodplain Area Instructions..... | 98 |

LIST OF TABLES

| Table | | Page |
|-------|--|------|
| 1 | LiDAR Metadata..... | 27 |
| 2 | North Fork Teanaway Watershed Radiocarbon Ages | 42 |
| 3 | North Fork Teanaway Watershed Incised Floodplain Area | 49 |
| 4 | Taneum Creek Floodplain Area..... | 53 |
| 5 | Potential Aquifer Storage Capacity in the North Fork Teanaway Watershed | 56 |
| 6 | Potential Aquifer Storage Capacity in the Taneum Creek Watershed | 56 |
| 7 | Potential Aquifer Storage Capacity Comparison..... | 71 |

LIST OF FIGURES

| Figure | | Page |
|--------|---|------|
| 1 | Yakima Basin land cover map | 2 |
| 2 | Historical logging in the Teanaway River | 4 |
| 3 | Upper Yakima River study area map..... | 5 |
| 4 | Yakima Basin mean annual precipitation map | 10 |
| 5 | North Fork Teanaway River Watershed 100k surface geology map..... | 14 |
| 6 | Taneum Creek 100k surface geology map | 15 |
| 7 | North Fork Teanaway River Watershed study area map..... | 17 |
| 8 | Taneum Creek study area map..... | 18 |
| 9 | Taneum Creek lower reach beaver dam map..... | 19 |
| 10 | North Fork Teanaway River and Dickey Creek confluence..... | 22 |
| 11 | Grain-size analysis process..... | 24 |
| 12 | Stratigraphy and grain-size distribution from the North Fork Teanaway and Indian Creek confluence..... | 33 |
| 13 | North Fork Teanaway watershed stratigraphic correlation..... | 34 |
| 14 | Stratigraphy and grain-size distribution from the middle reach Taneum Creek #2 site..... | 35 |
| 15 | Taneum Creek stratigraphic correlation..... | 36 |
| 16 | Taneum Creek middle reach map | 37 |
| 17 | Taneum Creek lower reach meadow transect | 38 |
| 18 | Gray silt grain-size distribution | 40 |
| 19 | Photographs of the gray silt | 41 |

LIST OF FIGURES (CONTINUED)

| Figure | | Page |
|--------|--|------|
| 20 | Taneum Creek upper reach piezometer map | 42 |
| 21 | Teanaway Valley Family Farm well cross-section..... | 43 |
| 22 | TVFF groundwater elevation..... | 44 |
| 23 | North Fork Teanaway geomorphic map | 45 |
| 24 | NFT watershed REM map | 46 |
| 25 | NFT watershed REM extracted floodplain map..... | 47 |
| 26 | NFT watershed floodplain comparison map..... | 48 |
| 27 | Taneum Creek geomorphic map..... | 50 |
| 28 | Taneum Creek REM map | 51 |
| 29 | Taneum Creek REM extracted floodplain map | 52 |
| 30 | Taneum Creek floodplain comparison map..... | 53 |
| 31 | North Fork Teanaway and Indian Creek Confluence Cross-Section..... | 55 |
| 32 | Indian Creek piezometer data | 58 |
| 33 | Taneum Creek grain-size distribution comparison..... | 61 |
| 34 | Taneum Creek photographs | 63 |

CHAPTER I

INTRODUCTION

A Brief Summary of the Project

The Yakima Basin is home to a robust agricultural economy, essential natural resources, the Confederated Tribes of the Yakama Nation, and several municipalities all relying on the consistent quality and supply of water from the Yakima River (Figure 1; YBIP, 2021). Climate change is predicted to bring changing precipitation patterns, which will vastly alter the natural functions of life within the basin. Preemptive measures are being taken through the Yakima Basin Integrated Plan (YBIP) to anticipate and combat climatic threats to important resources through investments in irrigation, conservation, and water storage (YBIP, 2021). My thesis investigates the Upper Yakima River tributaries and addresses the water storage component of the YBIP.

Project Objectives

1. Quantify the sediment composition and storage capacity of floodplain aquifers in the North Fork Teanaway River (NFT), NFT tributaries (Jack, Indian, Middle, and Dickey Creeks), and Taneum Creek, considering a regional confining layer of glacial lacustrine sediment present in both watersheds.
2. Evaluate the effects of the glacial history within the study area and interpret the importance of deposits in terms of groundwater recharge, storage, and flow.
3. Utilize results to inform future restoration projects on the effectiveness of the floodplain to collect, store, and transmit groundwater.
4. Incorporate the results into broader calculations of a water budget for shallow floodplain aquifers in the Yakima Basin.

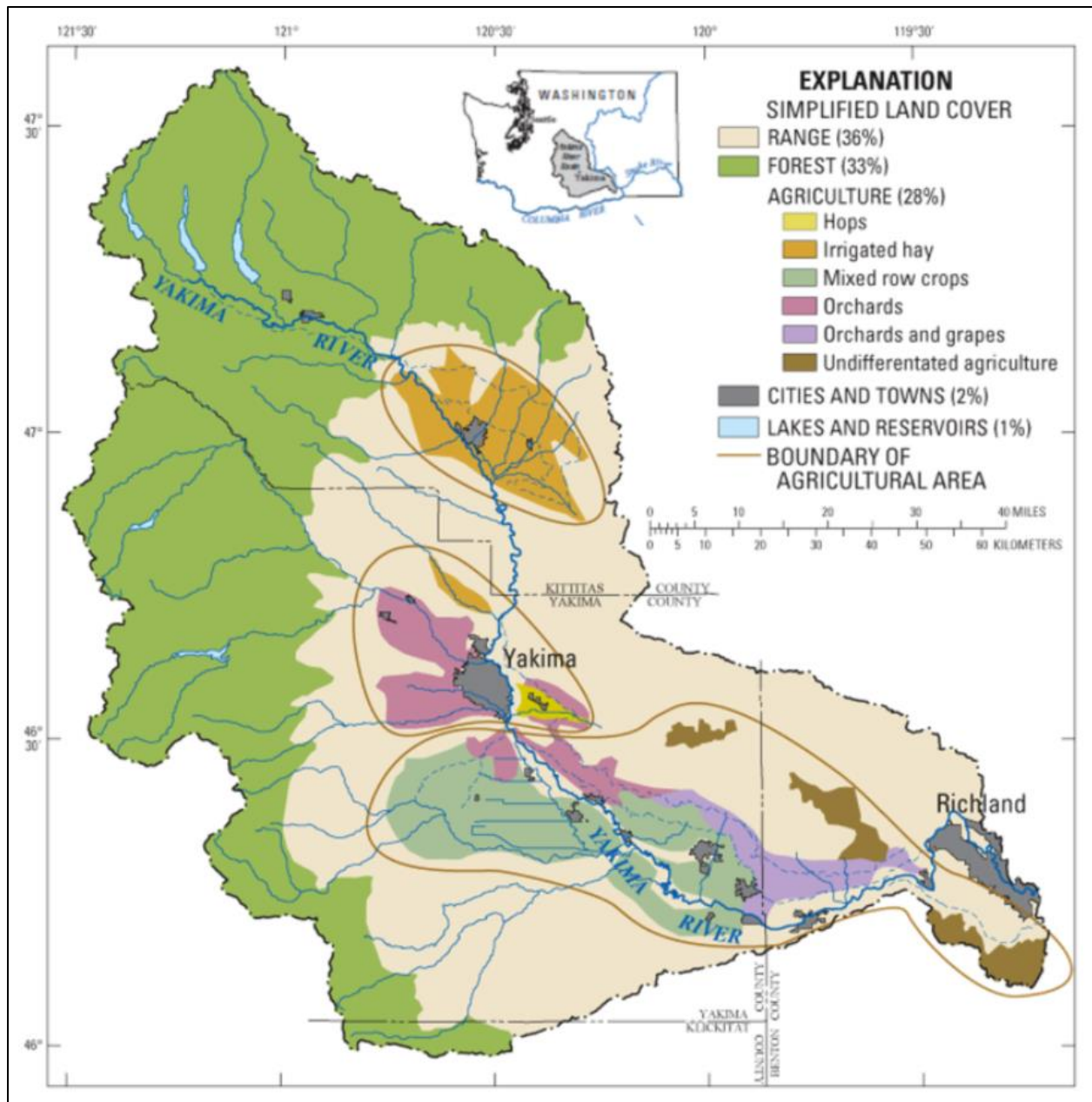


Figure 1. Yakima Basin land cover map. This map highlights the major crops that sustain the agricultural industry. As noted in the legend, agriculture alone makes up 28% of the land area in the watershed. (WSU, 2023)

The Upper Yakima River Basin

The headwater tributaries of the Yakima River flow down the east central slopes of the Cascade Mountain range and serve as an essential water resource to the mountain and downstream residents during the arid summer months. This area was utilized by the timber industry during the early 20th century, the old-growth coniferous forests supplied building materials for downstream settlers (Collins et al., 2016). The river systems served as a conduit for timber transportation downstream through the practice of splash damming. This destructive practice stripped tributaries, including the Teanaway, of their natural large wood (LW) accumulations causing rapid incision into the underlying sandstone bedrock (Figure 2). To restore these river systems to a more natural state and repair habitat for native fish species, numerous large wood restoration projects were enacted throughout the upper basin (Collins et al., 2016).

The main goals of LW restoration are to provide fish habitat, re-aggrade channel bed sediment, decrease bank erosion, and increase groundwater connectivity between the channel and adjacent floodplain (Roni et al., 2015; Collins et al., 2012). Studies suggest that large wood facilitates groundwater connectivity by diverting water onto the floodplain during high flow for infiltration into the subsurface (Collins et al., 2012). Groundwater connectivity between the channel and floodplain is necessary to support fish and other aquatic life cycles (U.S. Bureau of Reclamation and WA Department of Ecology, 2012). When groundwater connectivity is disrupted during the hot summer months, river water temperatures rise and disrupt the ecological balance (U.S. Bureau of Reclamation and WA Department of Ecology, 2012). The complex

glacial history of this area could potentially complicate the storage, flow, and transmission of water between the floodplain and channel due to the deposition of a gray silt layer.

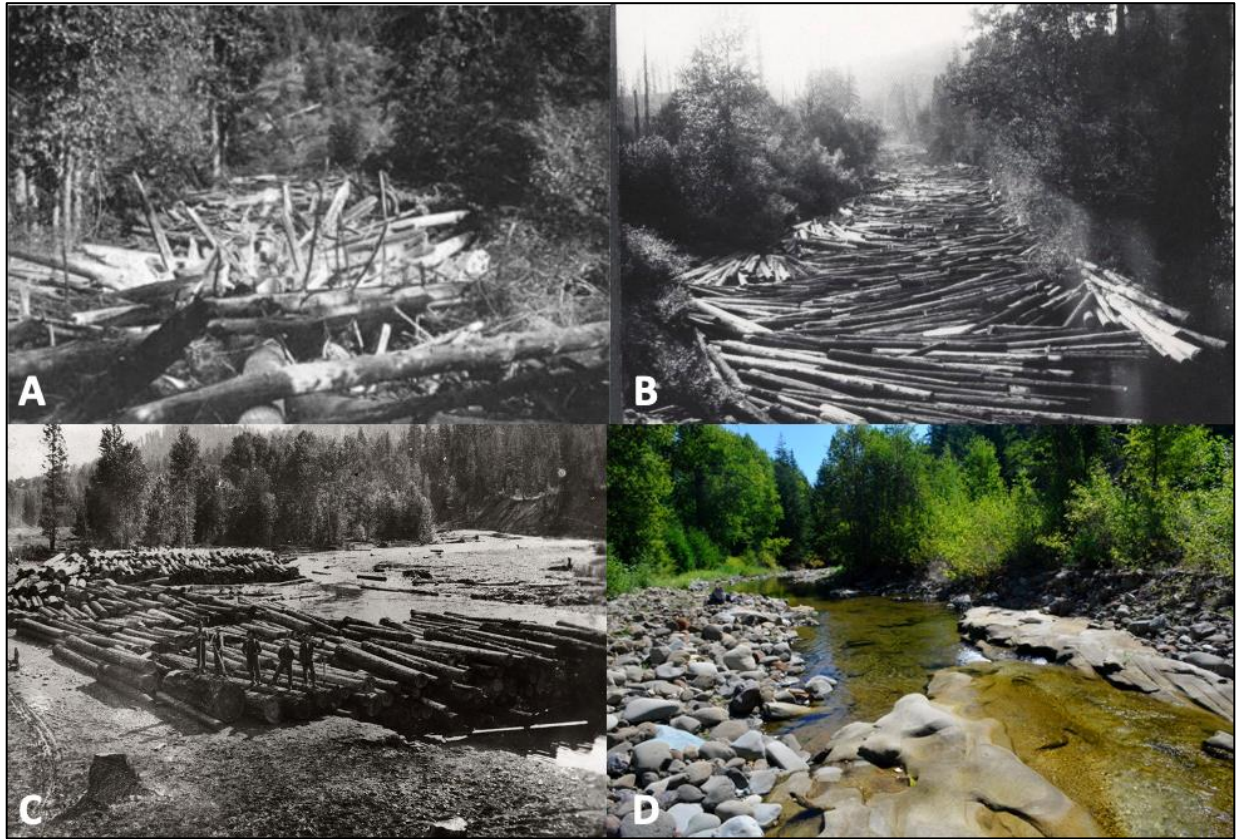


Figure 2. Historical logging in the Teanaway River. Photographs show the before, during, and results following logging practices. A) Natural in-stream wood prior to widespread logging practices across the Teanaway Watershed (Russell, 2016). B) Log drive in the Teanaway; logs were sent downstream to be processed at a mill using timed explosions. C) Decking logs on the Teanaway River; logs were loaded into the river behind a dam (The Frederick Krueger Collection, 1920). D) Modern day scoured bedrock channel in the Teanaway River (Schanz et al., 2019).

The gray silt could potentially be a lacustrine deposit from the last glacial period in the Pleistocene. Lacustrine units are fine-grained (clay and silt) sediment that slowly accumulate at the bottom of calm lake environments. They are sometimes reduced, due to anoxic conditions, giving them a gray color. A deposit of this origin was mapped in the Teanaway River watershed but not in the Taneum Creek watershed (Porter, 1976; Tabor et al., 1982). However, presence of this type of deposit in both the Taneum Creek and Teanaway watersheds and their proximity to

moraines suggests the rivers may have been dammed during the last glacial maximum, 20 thousand years ago (kya; Porter, 1976; Figure 3). The dammed river systems potentially caused the deposition of this gray silt seen in both watersheds. Presently, the gray silt has the potential to limit the volume available to water storage and the ability for water to transmit between the channel and floodplain.

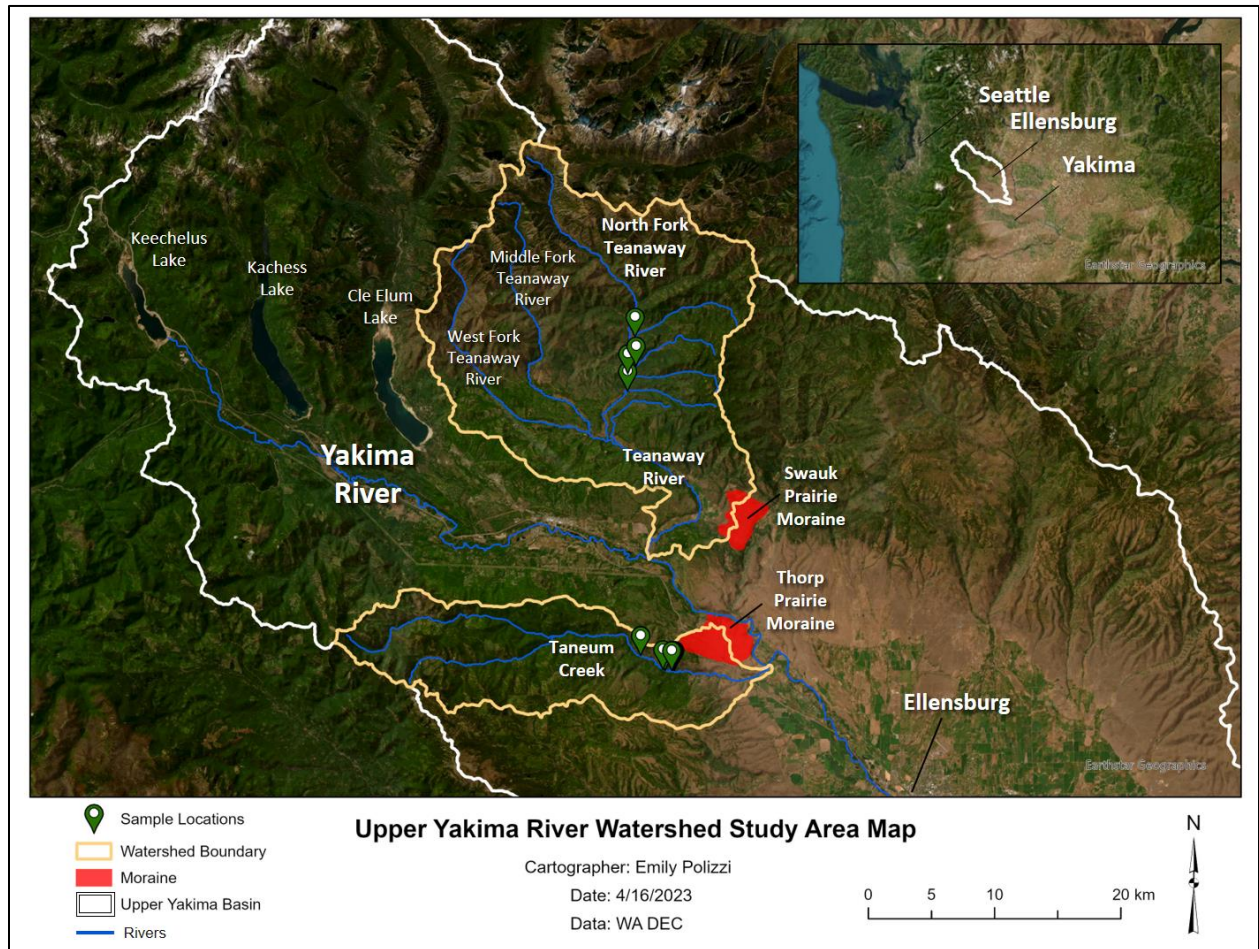


Figure 3. Upper Yakima River study area map. The two watersheds of interest are Taneum Creek to the south and the Teanaway River to the north. The moraines were traced using a map from Porter (1965). The proximity of the moraines to both rivers and the presence of the gray silt in both watersheds suggest the potential for a lacustrine depositional environment sometime in the recent glacial past. The three lakes in the NW corner are man-made reservoirs used to control flow to downstream irrigation canals.

Previous studies by Dickerson-Lange and Abbe (2019) quantified the floodplain storage available in the Teanaway River watershed, specifically, the main stem Teanaway, West Fork

Teaway (WFT), Middle Fork Teaway (MFT), and North Fork Teaway (NFT). Their models considered a uniform sandy loam floodplain aquifer under varying degrees of incision but did not include tributaries to these branches. While Taneum Creek is the subject of water storage research and well-established LW restoration, little research was done on the floodplain sediments. My research aims to better quantify the volume available for shallow floodplain aquifer water storage based on the stratigraphy and composition of the sediment in the NFT and Taneum Creek watersheds. These components are key in understanding the nuances of the system and hold valuable clues to water storage potential.

CHAPTER II

BACKGROUND

Yakima Basin Integrated Plan

The Yakima Basin Integrated Plan is a thirty-year plan with the goal of meeting the Basin's water needs in the years to come and ensuring healthy water sources for future generations of fish, families, farmers, and forests. The plan relies on stakeholders from a multitude of governmental agencies (local, state, federal, and tribal), non-governmental organizations, and irrigation districts (YBIP, 2021). The YBIP is centered on seven elements to achieve comprehensive watershed management and ecological restoration: (1) reservoir fish passage, (2) structural and operational changes, (3) surface water storage, (4) groundwater storage, (5) habitat/watershed protection, (6) enhanced water conservation, and (7) market reallocation (YBIP, 2021). Each element plays an important role in ensuring a functional and sustainable future for basin dwellers. More than 70 projects extend across the basin from headwaters to mouth, where the Yakima drains into the Columbia River (YBIP, 2021).

My research falls under the groundwater storage element, which aims to find additional water storage opportunities. More specifically, where water can be pumped out of the ground for irrigation in the lower basin or naturally stored in the floodplain for flow back into streams in the headwaters. Facilitating natural floodplain water storage through the summer months would improve flow regimes and lower instream water temperatures, benefitting aquatic life (U.S. Bureau of Reclamation and WA Department of Ecology, 2012). Identifying additional groundwater storage options is important because climate change is altering precipitation patterns in the Cascades. Changing patterns are leading to less snowpack in the Yakima basin

headwaters, more precipitation falling as rain rather than snow, and snowpack melting earlier in the spring. This is causing the peak river flow to come earlier in the year and lower baseflow in the summer months (U.S. Bureau of Reclamation and WA Department of Ecology, 2012).

Resident and Anadromous Fish

Changing precipitation patterns are also causing higher water temperatures in river systems which disrupt the water quality by reducing the amount of dissolved oxygen available to aquatic life (U.S. Bureau of Reclamation and WA Department of Ecology, 2012). In the late summer when water temperatures are rising, the lack of cooler groundwater contribution downstream puts increased stress on fish life cycles and other aquatic life. According to Mantua et al. (2010), climate projections suggest a significant increase in Upper Yakima basin air and water temperatures. For example, Mantua et al. (2010) found the number of weeks water temperatures rise above 21°C will increase from less than 5 weeks historically to 10 weeks by the 2040s. Two native species, the Middle Columbia River steelhead, and Columbia River bull trout are already federally listed as threatened species and could be at additional risk under future warming climates. Thermal stress results in an increase in mortality during all stages of salmonid life cycles and the offspring's inheritance of undesirable traits. Many restoration projects attempt to address these problems by adding instream large wood structures to encourage the formation of salmonid habitats. In-stream large wood promotes fish habitat via the increased frequency of pools, areas of refuge, cooler water temperatures, and retention of spawning-sized gravels (U.S. Bureau of Reclamation and WA Department of Ecology, 2012).

Climate

The water supplying the Yakima River Basin originates in the Cascade Mountain Range as snowpack that accumulates during the winter. The basin has a west-to-east precipitation gradient where the mountainous headwaters on the western margin receive over 100 inches of annual precipitation and the lower elevation eastern basin receives less than 10 inches per year (Gendaszek et al., 2014; Figure 4). In the spring when the snow melts, the water is transported downstream as surface runoff or caught in reservoirs. While some of this water is caught in the manmade reservoirs at the headwaters: Lake Cle Elum, Lake Keechelus, and Lake Kachess, a lot is lost as it flashes downstream during peak flow (Figure 3). The lakes are managed reservoirs that deliver water to irrigation canals through the hot summer months when precipitation decreases (Gendaszek et al., 2014). Construction of dams to create the reservoirs began as early as 1860 and led to the loss of spawning habitat for sockeye salmon, eventually decimating the run by 1910 (YBIP, 2021).

Large Wood

The significance of large wood (LW) in river systems became increasingly evident in the 21st century as climate change began to have noticeable effects on rivers around the world. The practice of splash damming caused major destruction of ecological habitats and resulted in rapid incision of channels into bedrock. Splash damming entailed loading timber into rivers behind temporary dams, and when the channels were filled with logs, they set off timed explosions in the dams to send it all downstream for processing at mills (Figure 2). With the logs, went all the alluvial sediment which facilitated rapid vertical incision and bedrock channel erosion (Collins et al., 2016). On the eastern slopes of the Cascades, these negative effects were particularly evident

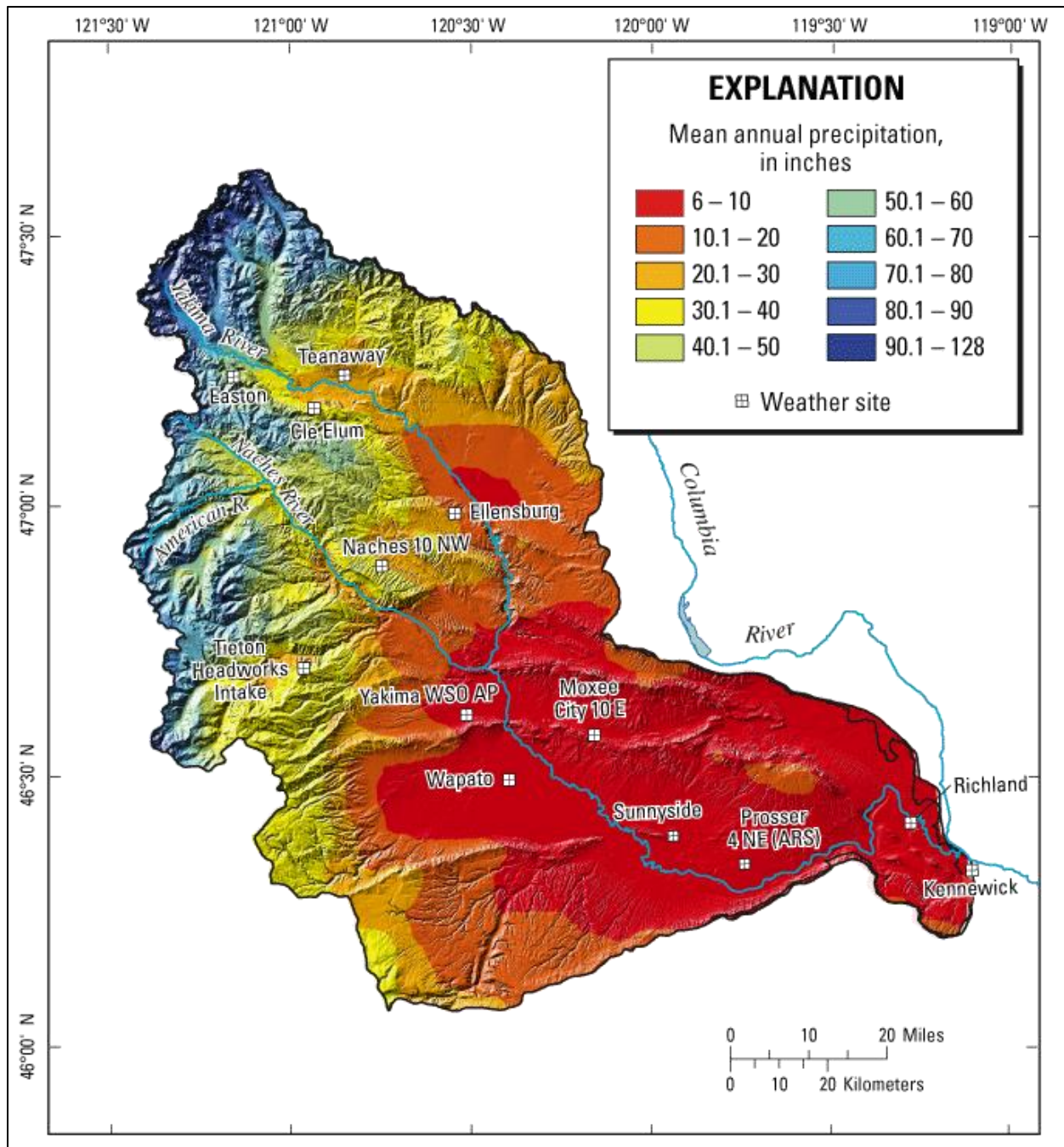


Figure 4. Yakima Basin mean annual precipitation map. The west-to-east gradient is accentuated by the topography of the region as the Cascade Mountains shift into the Yakima Fold and Thrust Belt, to the mouth of the Yakima River in the city of Kennewick (USGS, 2009).

on the Teanaway River. While there are numerous railroad beds throughout the watershed, splash damming was a more cost-effective practice than transporting timber downstream via train.

From a groundwater storage perspective, the down cutting and erosion of the channel bed alluvial deposits was detrimental to floodplain-channel groundwater connectivity. The channel bed alluvium serves as a groundwater aquifer unit that connects the channel and floodplain allowing water to transmit, but the removal triggered incision and disconnection (Dickerson-Lange and Abbe, 2019). The more incision there was, the more detached the floodplain became from the channel, and the less floodplain volume there was available for groundwater storage. Collins et al. (2016) and Schanz et al. (2019) found the incision rate of the Teanaway River to range from 1.3 to 23 mm/year with the highest incision rates and abandonment of the most recent strath coinciding with the onset of splash damming in 1891. The subsequent downcutting of 4 to 10 m resulted in a floodplain reduction on the Middle Fork of 20% and 53% on the West Fork (Schanz et al., 2019). In my research it was important to consider all branches of the Teanaway River when choosing locations for groundwater storage. Since there were varying degrees of incision and floodplain reduction in each branch, I chose the NFT and tributaries which had the most floodplain available.

My research in conjunction with LW restoration projects on the NFT aims to identify areas where LW structures would most effectively, increase floodplain and channel habitat; increase retention of alluvium and natural wood; and increase connectivity between channel and floodplain groundwater. The addition of LW structures would most immediately influence fish habitat complexity to support resident and anadromous fish life cycles. While the channel

alluvium retention and groundwater connectivity may take longer, the LW emplacement will act as a catalyst to guide the river back to a more natural state for future generations.

Tectonics and Lithology

The headwaters of the Yakima River Watershed lie on the southeastern margin of the northern Cascade Mountains in Lake Keechelus and drain to the southeast via tributary rivers and creeks (Waite, 1979). The Cascade Mountains are a product of a convergent margin from the denser oceanic Juan de Fuca Plate subducting beneath the less dense continental North American Plate. The Cascades give way to the Yakima Fold and Thrust Belt (YFTB) which is suggested to be actively deforming due to recent moderate earthquakes in the region (Blakely et al., 2011). The YFTB isolates the synclinal valleys of Central Washington via a series of NW-SE trending anticlinal ridges. The Yakima River crosscuts the ridges in a string of pearls fashion: narrowly through the ridges and widely through the synclinal valleys between. This creates a tight entrenched meandering pattern through the ridges and a wider floodplain area in the valleys.

The Yakima River Watershed has a wide range of lithologies, from volcanic and sedimentary rocks of the Tertiary to Quaternary alluvium deposits (Tabor et al., 1982). These lithological formations influence the geomorphology and floodplain aquifer capacity of the Yakima River and its tributaries. On the Teanaway River, the contact between the poorly indurated Roslyn and the Teanaway Basalt is a location of increased vertical incision due to the transition from stronger volcanic rocks to weakly lithified sandstone (Collins et al., 2016). On the NFT the major surficial geologic units are Roslyn Sandstone, Teanaway Basalt, Quaternary mass wasting/alluvial deposits, and Pleistocene alpine glacial drift (Figure 5). In a fluvial

environment that undergoes continuous wetting and drying cycles, units like the Roslyn become friable and erode easier than stronger units like the Teanaway Basalt (Collins et al., 2016).

Quaternary alluvial, glacial, and mass wasting deposits are very common throughout the Yakima River Watershed (Tabor et al., 1982). These units can greatly affect the floodplain storage potential of the Yakima River tributaries. As an example, a glacial outwash sand deposit would serve as a better aquifer than a mass wasted talus deposit or a lacustrine clay. Although the clay layer would have the potential to store water, it wouldn't allow water to effectively transmit through the unit, making it a poor aquifer. Understanding the stratigraphy of sites proposed for river restoration and groundwater storage is important for the success and efficiency of the project.

Taneum Creek is in a narrower canyon than the NFT and consequently has a narrower floodplain. While Taneum Creek may not be as wide as Teanaway, both rivers cut through similar lithologies. Taneum Creek primarily cuts through the Eocene arkosic sandstones of the Manastash Formation, and the Miocene age Grande Ronde basalt flows (Figure 6; Stearns et al., 1983). The confluence of Taneum Creek and the Yakima River is adjacent to the Pleistocene alpine till of the Thorp Prairie Moraine, signifying the furthest extent of alpine glaciers during the last glacial maximum (Stearns et al., 1983).

Hydrogeologic Setting

The Yakima River Watershed has numerous tributaries that could potentially serve as groundwater storage in the spring and early summer months. Tributaries currently being investigated for seasonal water storage are Indian Creek, North Fork Teanaway River, and Taneum Creek (Bartlett, 2022; Dickerson-Lange and Abbe 2019; Ely and Gazis, 2021). These

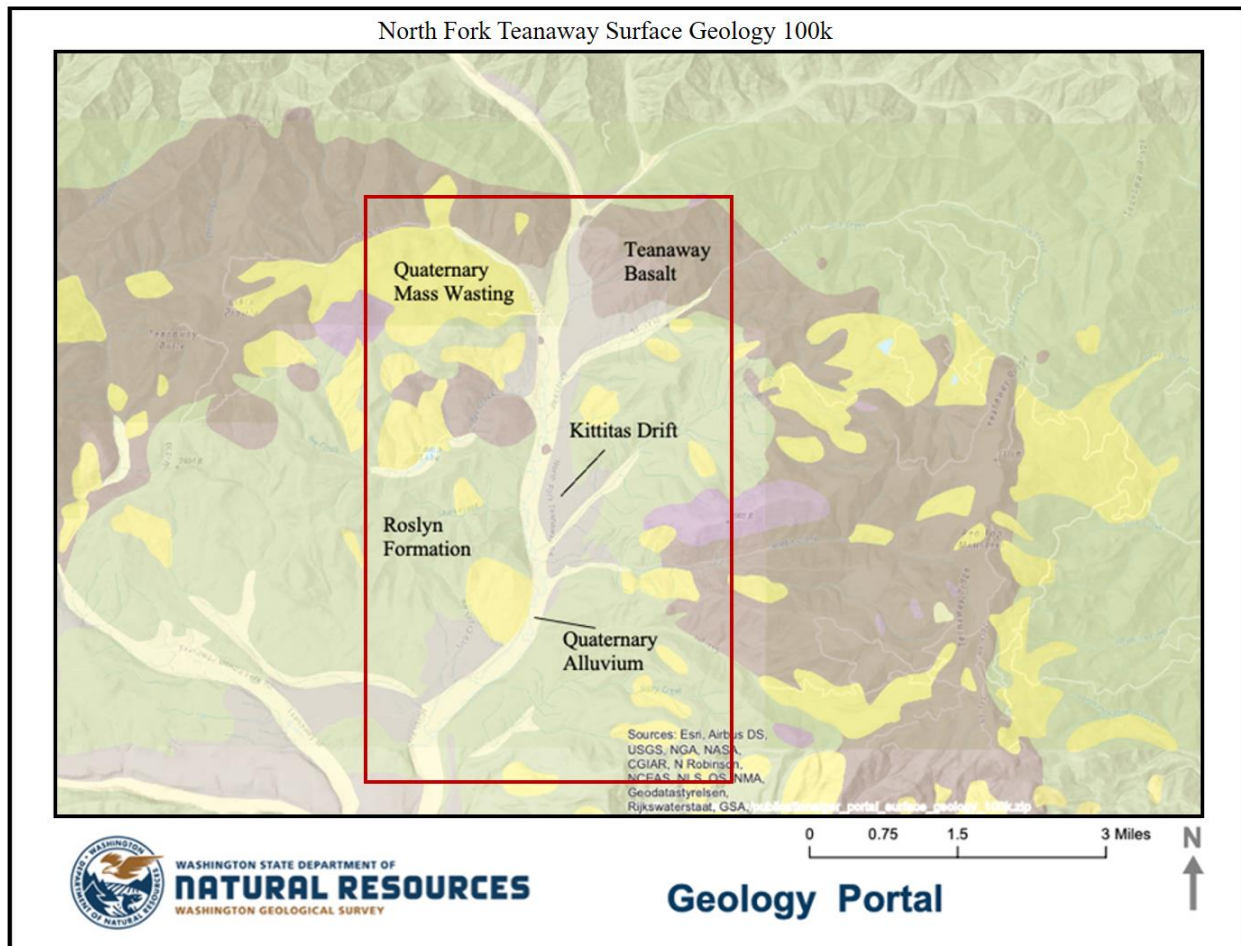


Figure 5. North Fork Teanaway River Watershed 100k surface geology map. Key units are annotated on the map in black font and the red box denotes the study area. Areas labeled Kittitas Drift include Quaternary till, outwash, and glaciolacustrine sediments.

tributaries are located upstream of the Kittitas Valley, on the eastern margin of the Cascade Mountains. The Teanaway River is glaciated terrain while Taneum Creek was previously determined to be unglaciated (Tabor et al., 1982; Waite 1979). A regional fine-grained gray unit found in both watersheds could have implications on groundwater storage and flow.

The North Fork Teanaway River flows through the Teanaway Community Forest; 50,000 acres of land purchased by the state in 2013 for recreational and conservational use. The community forest is now host to several conservation efforts including LW and floodplain restoration projects. The northern boundary of the community forest serves as a boundary for the study area

and also coincides with the transition into Teanaway Basalt bedrock canyon. Two sites are the subject of focused research on groundwater dynamics and storage. The Teanaway Valley Family Farm (TVFF) acquisition on the main stem of the Teanaway River serves as a project site to inform floodplain restoration based on hydrogeologic data from wells spanning across the valley (Figure 7; Petralia, 2022). Projects on Indian Creek investigated groundwater dynamics in relation to water storage in the floodplain aquifer (Figure 7; Boylan, 2019; Bartlett, 2022). In both projects a fine-grained gray deposit was observed and at the TVFF this layer was even confirmed to be a confining layer.

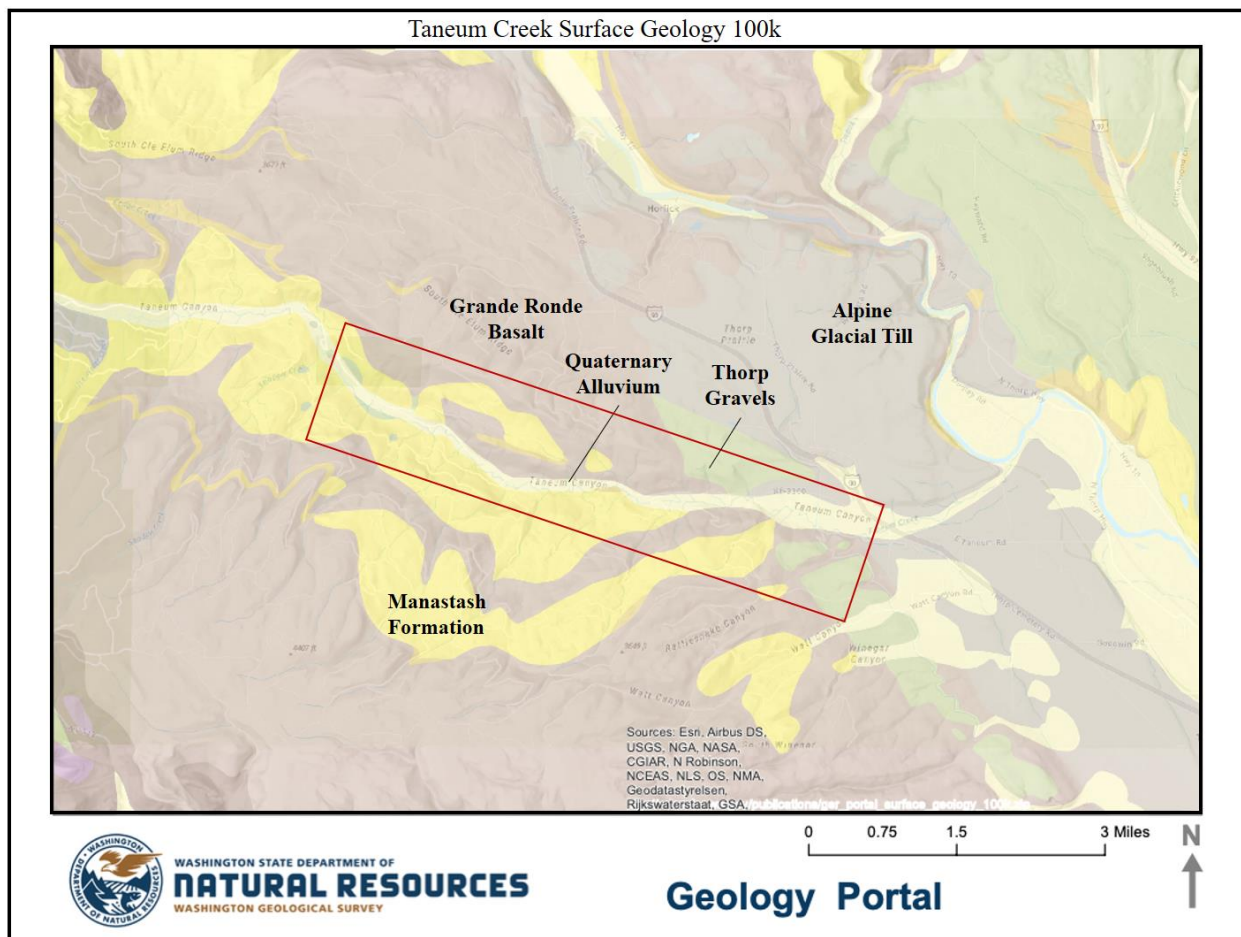


Figure 6. Taneum Creek 100k surface geology map. Key units are annotated on the map in black font and the red box denotes the study area.

Taneum Creek was a pilot site for the Kittitas Reclamation District floodplain inundation and aquifer project (Figure 8; Ely and Gazis, 2021). It was one of the first to install LW in 2008. This makes it an excellent site to monitor and analyze floodplain inundation and channel morphology in response to large wood emplacement after 15 years. In 2008 multiple LW structures were established at Taneum Creek and in 2011 a large flood with an estimated discharge of $69 \text{ m}^3/\text{s}$ (24,000-28,000 cfs) mobilized that LW and increased channel complexity (Fixler, 2022). In addition to the increased channel complexity there was an increase in the NDVI index, indicating more greenness and vegetation. Consequently, the growth of new vegetation could also increase evapotranspiration, removing water from the system (Ely and Gazis, 2021). CWU graduate student, Edward Vlasenko, seeks to quantify the amount of water being lost through evapotranspiration on the Taneum Creek floodplain to further evaluate the water storage potential of the floodplain. This evapotranspiration value in conjunction with my aquifer storage potential will constrain a water budget for Taneum Creek.

Beaver dam construction on the newly formed side channel near the large wood emplacement site has increased the wetland area, creating a more complex floodplain conducive to water infiltration (Figure 9). The beaver pond is now wet year-round and has a series of several dams that slows flow through the pond. The depth of the pond fluctuates through the year and is highest in the spring and lowest in the late summer. A more connected floodplain increases surface-water infiltration into the floodplain aquifer. Further downstream, the KRD plans on using their canal to supply a pilot groundwater storage project through infiltration on a field at the top of the Taneum Creek fan (Figure 8). They will monitor the water table response in wells installed in the corners of the field.

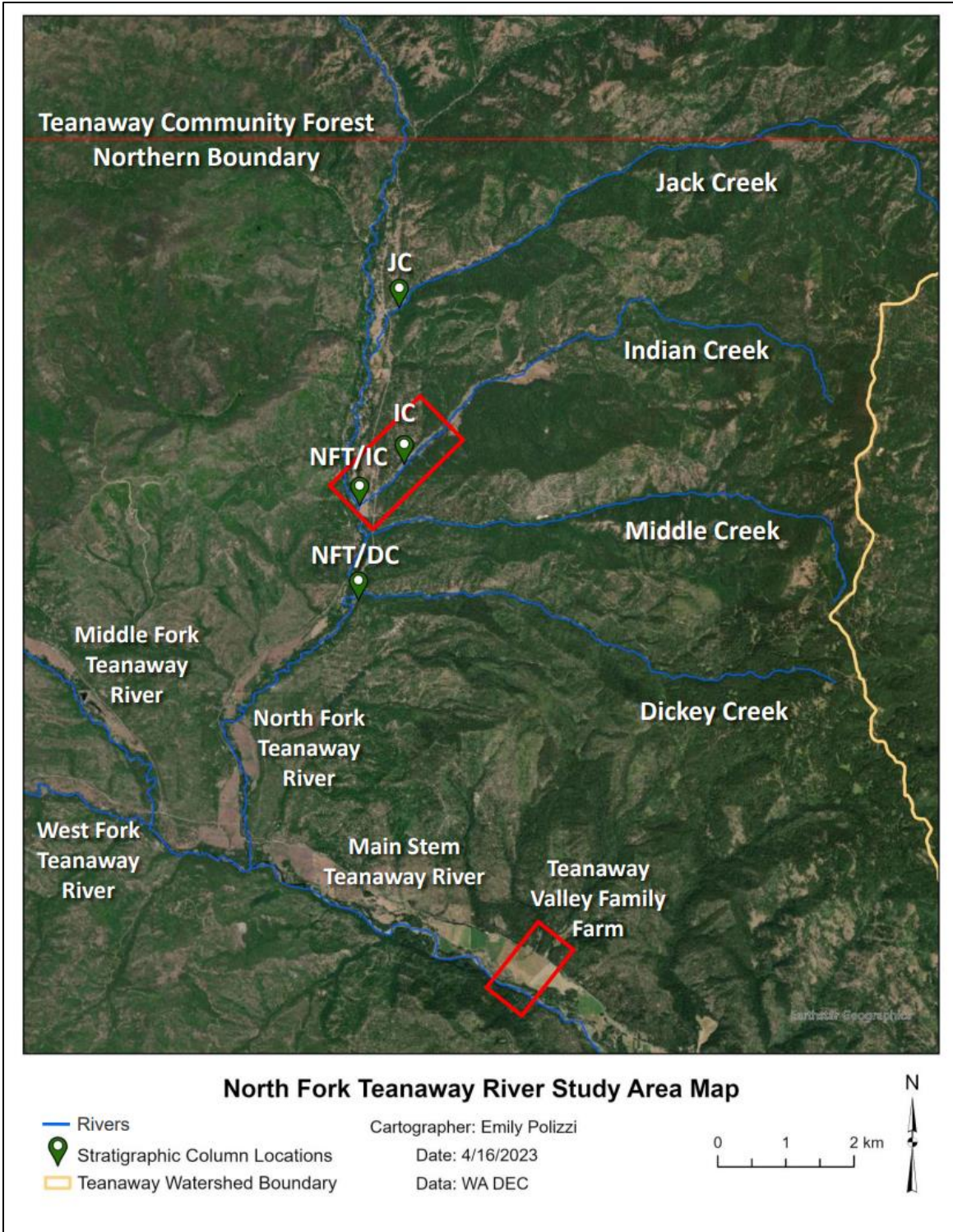


Figure 7. North Fork Teanaway River Watershed study area. Stratigraphic profile sites are denoted by the green markers and abbreviations. Tributaries and the Teanaway Valley Family Farm project site are labeled. The study area does not extend beyond the Teanaway Community Forest boundary.

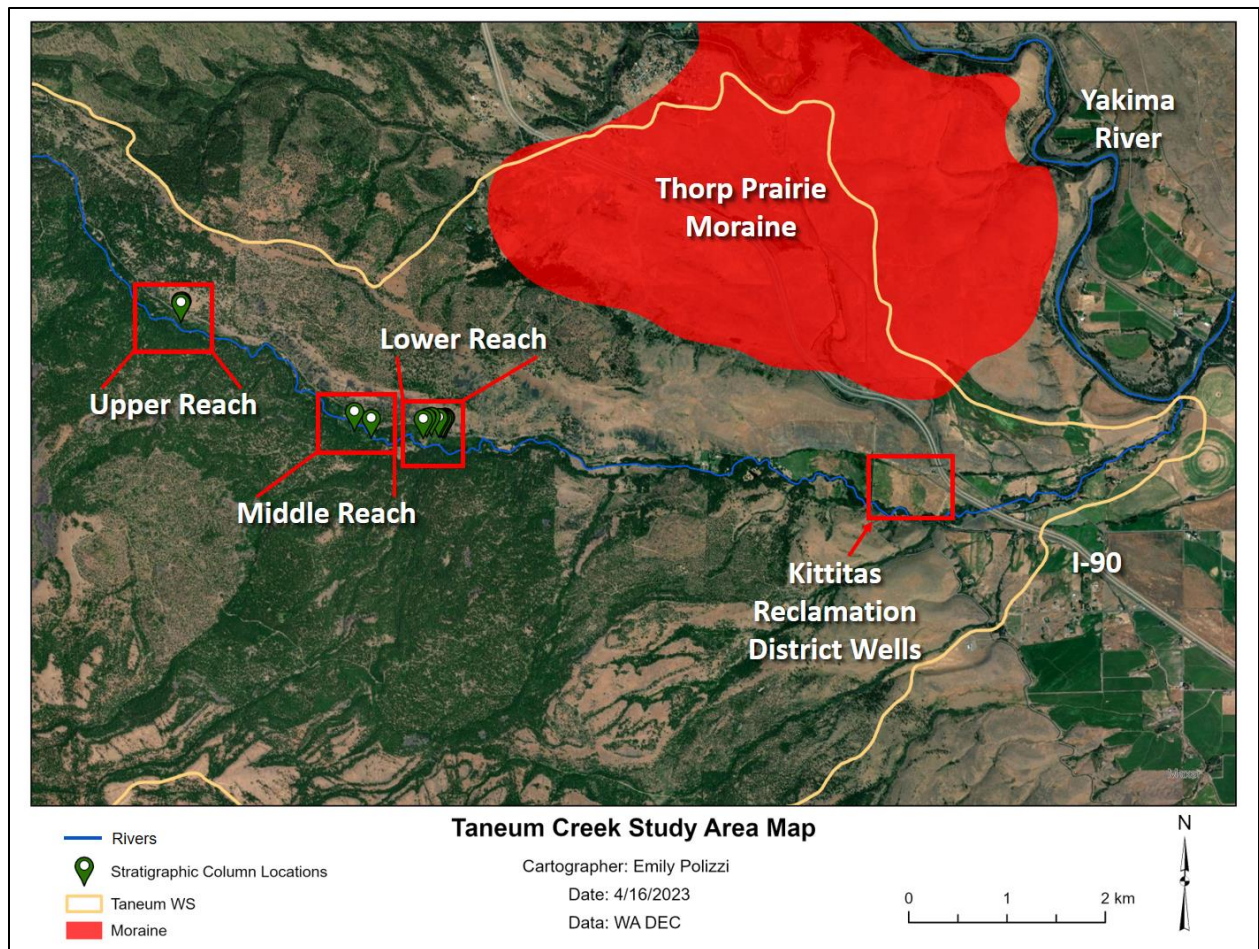


Figure 8. Taneum Creek study area map. Specific areas of interest are denoted with red boxes. Field work was conducted in the upper, middle, and lower reaches to analyze floodplain stratigraphy. The Kittitas Reclamation District plans to flood the field near I-90 to monitor groundwater levels in response to floodplain inundation. The Thorp Prairie Moraine lies to the north of the creek, still within the watershed.

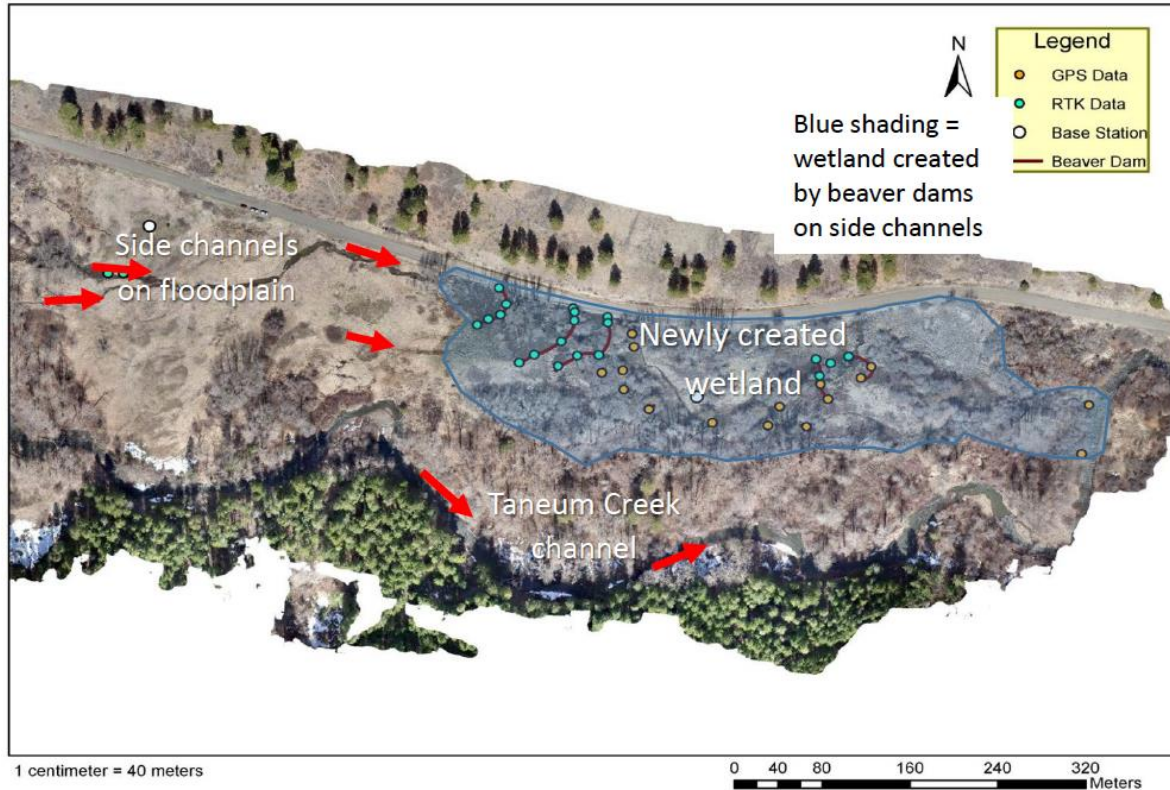


Figure 9. Taneum Creek lower reach beaver dam map. This area is downstream of an instream LW installation. Mobilization of the LW by the 2011 flood, caused the formation of the new side channel and allowed beavers to move in. Beavers built several dams causing newly created wetland to form on the floodplain (Ely and Gazis, 2021).

Glacial History

Porter (1976) did extensive research on the remaining glacial features and Pleistocene extent of alpine glaciers in the Central Cascades. Glacial lobes from alpine glaciation influenced the surface geology of the upper Yakima drainage basin. The three major Pleistocene drifts preserved in this area are from three separate glacial ages: the Thorp Drift (700 thousand years ago - kya), Kittitas Drift (120 kya) and Lakedale Drift (15-13.5 kya) (Porter, 1976).

Outwash from the oldest, Thorp Drift, was deeply incised by ~75 m and eroded leaving only ~25% of what was originally deposited (Porter, 1976). The outwash is composed mostly of Yakima basalt gravel that decreases in mean grain size up valley to Ellensburg from 10 cm to 3 cm. The Swauk Prairie Member of the Kittitas Drift extends to the north end of the Kittitas

Valley; the remnants are less eroded than the Thorp, leaving “subdued moraines and thick dissected outwash fills” down valley from Cle Elum. Till from the Swauk Prairie Member extends as far south as Swauk Prairie and Thorp Prairie. The Swauk Prairie till has stony cobbles and pebbles from Teanaway Basalt, Swauk Sandstone and Roslyn Sandstone mantled with loess. Thorp Prairie till is composed of angular Yakima Basalt boulders covered by a thin, discontinuous eolian mantle (Porter, 1976).

The Indian John Member of the Kittitas Drift represents a readvancement of the Yakima Valley glacier following the retreat after the Swauk Prairie advance (Porter, 1976). Subdued moraines indicate the Indian John advancement terminus lies in the lower Teanaway River where the till is underlain by deformed lacustrine rhythmites containing drop stones. Of particular interest to my thesis project is the gray silt that was deposited following the Indian John advancement of the Kittitas Drift. Porter, (1976), explains the bedrock valley floor between Lakedale and the mouth of the Teanaway River is overlain by more than 200 m of sedimentary fill which is overlain by “a thick body of bluish lacustrine silt, clay, and sand that thickens down valley from 60 m to 150 m.”. This clay unit is overlain by Lakedale Drift outwash and postglacial alluvium. Porter, (1976) explains the lake formed due to the glacial retreat from the Indian John terminal moraine. Outwash and till plugged the Yakima River to the south of Lookout Mountain and caused meltwater to pond 275 m up valley until breaching the drift dam and draining the water. The existence of this lake is hypothesized to have reduced deposition of the reddish-brown, oxidized Kittitas loess. At Indian Creek, the gray silt layer is overlain by a unit of this description which could indicate proximity to the edge of the lake possibly as it was draining to 20-40% of its original capacity (Porter, 1976).

CHAPTER III

METHODS

Stratigraphy

Field study sites were on Taneum Creek between the beaver pond at the lower reach and the log jam at the upper reach beaver pond. In the North Fork Teanaway watershed, study sites extended from Dickey Creek in the south to Jack Creek in the north and on the North Fork Teanaway River (Figure 7). Field data were collected from July 2022 to October 2022. Field reconnaissance was performed to find the best locations to collect samples and record stratigraphic profiles. Ideal sites displayed two to three meters of vertically incised floodplain. These sites were exposed by river erosion and allowed easy access to the stratigraphy with minimal floodplain disruption (Figure 10). Field sites chosen displayed consistent incised floodplain stratigraphy 25 m upstream and downstream of the profile location. The presence and absence of the gray silt was noted at potential sites, to inform the floodplain aquifer capacity calculation. Coordinates of potential sites were recorded using a handheld GPS unit.

Sites were chosen in the NFT watershed to establish a broad understanding of the stratigraphy. Sites within the Middle Fork and West Fork Teanaway were considered but ultimately eliminated due to a lack of floodplain available. In the lower WFT watershed strath terraces eliminated connectivity of channel and floodplain and on the MFT there was a lack of floodplain available before the river ran through bedrock canyon upstream.

At Taneum Creek I selected more sites in a smaller area to establish a more thorough understanding of the watershed. Several factors make Taneum Creek a great comparison for the NFT watershed: the established LW structures that were mobilized by the 2011 flood, less



Figure 10. North Fork Teanaway River and Dickey Creek confluence. A) This site has a well-exposed riverbank where the floodplain is incised, revealing the stratigraphy. The gray silt unit forms a resistant bench on the edge of the channel, protecting the floodplain from further erosion. B) A close up photograph of the mottled material in the lower part of the bench. C and D) Looking upstream and downstream the incised floodplain extends well beyond the profile location. The red lines bound the laterally continuous stratigraphy of the incised floodplain.

channel scouring, and more shallowly exposed floodplain. Taneum serves as a model for what the NFT could potentially become if successfully restored.

Upon finding a site, I cleared off the side of the channel bank to expose a fresh profile of sediment. I identified the geomorphic context of the location in relation to the river morphology and how it could potentially impact the stratigraphy. From there I divided the profile into distinct layers and described the qualitative and quantitative characteristics of each unit: depth, color, texture, porosity, vegetative composition, structure, and grain size. I took samples from each layer, noting the depth from which I extracted the sample. I took multiple samples from layers where one sample was not enough to capture the vertical diversity of the entire layer. I later used the samples to evaluate the grain-size distribution using the Mastersizer 3000 and Hydro LV Cell in the Murdock Research Laboratory in Discovery Hall on the Central Washington University campus (Figure 11).

To constrain the age of the gray silt and attempt to correlate it with glacial origins, additional field investigations were required. A wood sample was collected from the unit at the NFT River and Indian Creek confluence for radiocarbon dating. Knowing a date for the unit could help gauge the time of deposition or most recent time of interaction and mixing in the unit. To gain a better understanding of maximum Pleistocene lake levels in the Teanaway watershed, I recorded the highest point on the Swauk Prairie Moraine with a handheld GPS units. Matching the moraine elevation with the elevation of the gray silt unit higher in the watershed could shed light on whether a moraine dam could have created a setting in which the gray silt layer accumulated.

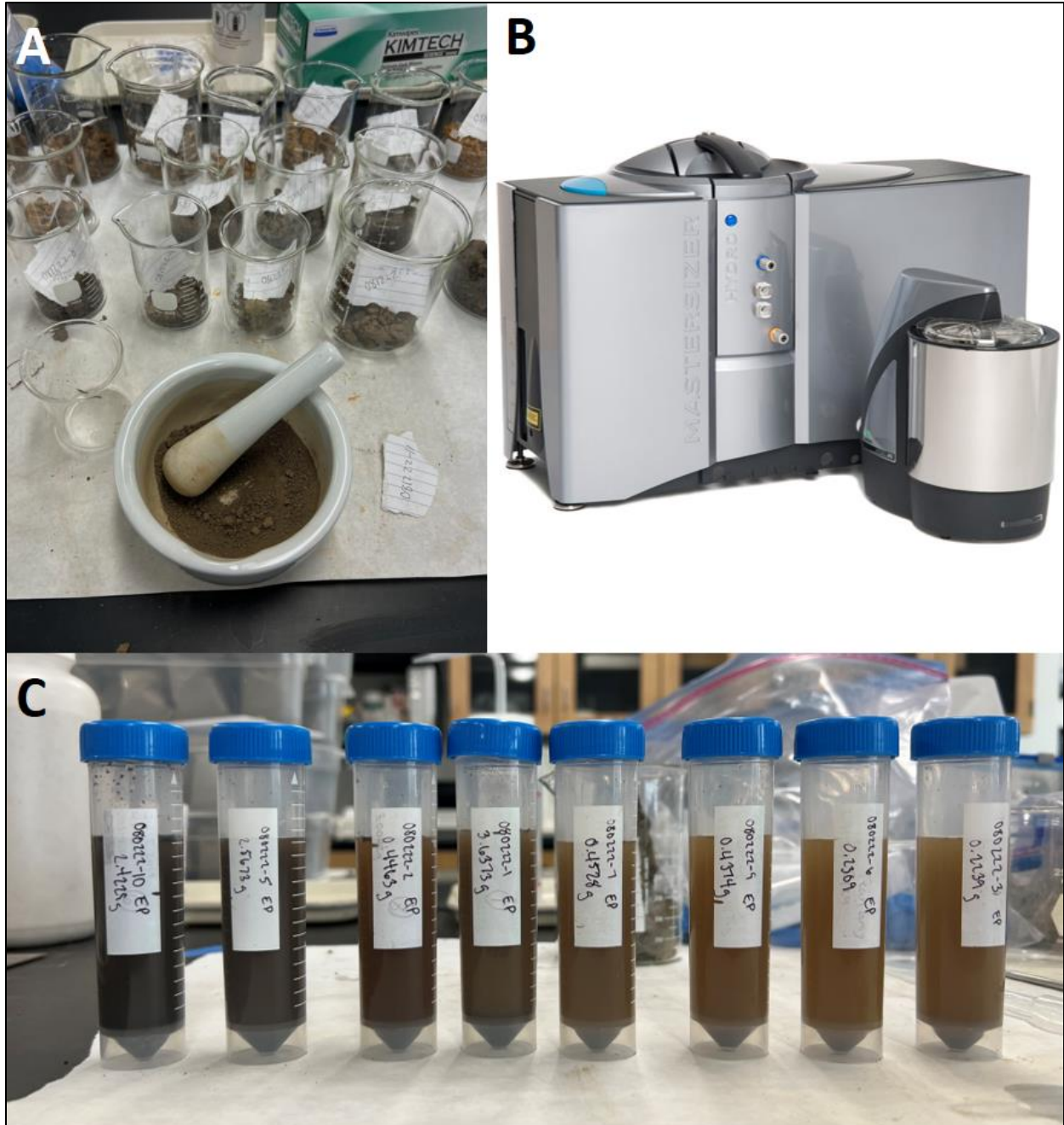


Figure 11. Grain-size analysis process. Photographs of the lab process to determine the grain-size distribution of samples from the field. A) Samples were dried in an oven and crushed using a mortar and pestle to ensure there were no sediment conglomerates. B) The Malvern Mastersizer 3000 with the accompanying Hydro LV cell were used to analyze the sediment size distribution. C) The solution prepared using different weights of sample based on the grain size and mixed with sodium hexametaphosphate to deflocculate the clay particles.

Piezometer Analysis

A piezometer analysis was conducted at Taneum Creek and the Dickey Creek NF Teanaway confluence to evaluate the transmissivity of the gray silt in each watershed (Figure 3). The purpose of the pump test was to measure the rate at which water moved into the unit and the gravel unit below. Pump tests at Taneum Creek and Dickey Creek were performed where the gray silt was the surficial unit. Measurements were taken in the stream to be able to record the water level inside the piezometer and outside at the river water surface. First, a soil probe was used nearby to gage the depth of the unit in relation to the gravel. The piezometer was then pounded into the unit to an appropriate depth using a rubber mallet. For the clay unit the piezometer was placed approximately at the middle depth of the unit. For the gravel below, the piezometer was pounded as deep as it could go below the fine-grained layer, enough so that the holes were completely submerged in the gravel.

Once the piezometer was placed in the unit with no gaps to let surface water in, an initial water level measurement was taken inside and outside the piezometer. Then, a bailer was used to purge the water from inside the piezometer. As soon as the bailer was pulling clear water or no water, we took the first measurement and started the clock. The water level measurements for the inside and outside of the piezometer were recorded at the 0, 2, 4, 6, 10, 30, and 60 minute marks. Each pump test was run for a minimum of 60 minutes to allow maximum infiltration of water. The first test was run for 80 minutes to confirm that 60 minutes was the optimal amount of time to see the most change in water level. After 60 minutes there was no significant change in the water levels of the piezometer. At the Taneum Creek site, the gray silt and the gravel unit below were tested to observe if the gray silt acted as a confining layer. This could not be accomplished

at Dickey Creek because the gray silt was underlain by Roslyn Sandstone bedrock which could not be penetrated by the piezometer.

Sediment Size Analysis

Sediment size data was measured using a Malvern Mastersizer 3000 and Hydro LV attachment (Figure 11B). Samples most representative of the grain-size diversity within the stratigraphic profile were then dried in the laboratory oven for 48 hours at 95°F. Once they were thoroughly dried, a mortar and pestle were used to separate the hardened clumps of sediment (Figure 11A). The samples were run through a 1 mm sieve and the coarse fraction was weighed. Most samples had some portion of clay, so to be consistent, all samples were deflocculated to ensure accurate testing of clay content. Samples were prepared for Mastersizer analysis using the methods developed by Trent Adams and the CWU Sample Prep Laboratory. Samples were weighed out based on observed texture. The optimal masses of sediment were then mixed with 30 ml solution of sodium hexametaphosphate (5.5g/L). Each specimen was shaken with a vortex mixer for 60 seconds and allowed to rest for 24 hours before a final round of shaking immediately before Mastersizer analysis (Figure 11C). Once samples were analyzed, they were normalized by dividing the volume percent for each grainsize class by the maximum. The normalized volume percent data were then plotted against grain-size (μm) to display the grain-size distribution from 0.06 μm to 1 mm (clay-sand).

Floodplain Mapping

ArcGIS Pro 3.0 software was used to evaluate the dimensional parameters of the floodplain and calculate potential aquifer capacities. Relative Elevation Model (REM) generation and geomorphic mapping of the active floodplain, incised floodplain, and terrace were the two

GIS methods accomplished using LiDAR (Light Detection and Ranging) data from the Washington State Department of Natural Resources LiDAR portal. The publicly accessible portal offers LiDAR data in a variety of formats: Digital Surface Models (DSMs), which include the vegetation and other surface features of the earth; Digital Terrain Models (DTMs) which strip away the surface features leaving the bare ground; and DTM hillshade models which allow users to see a shaded relief surface of the earth that is more easily interpreted than a regular DTM. Digital Terrain Models (DTMs), alternatively known as Digital Elevation Models (DEMs), were used as inputs for the analysis portion while DTM hillshades were used for visualizing purposes only.

Table 1. LiDAR metadata. The metadata for LiDAR files used in GIS Analysis and Visualization. All files are from the Washington State Department of Natural Resources LiDAR Portal.

| WA DNR LiDAR File Names | Resolution | DTM Hillshade | DTM | Geotiff File Numbers | Imagery Location |
|--------------------------------|-------------------|----------------------|------------|-----------------------------|-----------------------------|
| Teaway 2015 | 1.5 feet | X | X | 7, 8 | North Fork Teaway Watershed |
| Teaway Bathy 2015 | 1.5 feet | X | | 7, 8 | North Fork Teaway Watershed |
| Kittitas FEMA 2011 | 1.5 feet | X | X | 11 | Lower Taneum Creek |
| Yakima Basin 2018 | 1.5 feet | X | X | 85, 86, 87 | Taneum Creek Canyon |

North Fork Teaway Watershed

The geomorphic mapping process used aerial imagery provided by ESRI with an overlain DTM hillshade layer to better evaluate the difference between active floodplain, incised floodplain, and terrace. During this process, the terrace was the most visually prominent and served as an outer boundary for the digitization of the floodplain. The abandoned terraces

indicate the past channel elevation relative to the modern channel and can be used in the relative age dating of the landscape. The incised floodplain was digitized next followed by the active floodplain. The difference in sediment composition between the incised floodplain (silt dominated) and the active floodplain (boulder dominated) lead to a separation of them for water storage calculation reason. While the active floodplain is the most likely to be inundated due to its proximity to the active channel, it is not the ideal floodplain to be used as seasonal water storage. All features were digitized at a 1:1,300-foot scale on the east side of the river since the west side is bordered by shallow gravel bars and cliff.

While geomorphic mapping a strict process was followed to prevent gaps and misalignment of features. To align each polygon perfectly they were first roughly digitized, leaving a 30-70 foot buffer between the two features. Once finished, the Align Features tool was used to automatically build one polygon onto the border of the other. This step ensured there were no gaps between polygon features and that adjacent polygons shared a border. Once all polygons were digitized, the floodplain area was calculated using the calculate geometry tool in the attribute table and manually summed to calculate a total area value.

As an alternative to the geomorphic mapping method, a relative elevation model (REM) was created to compare the final results with Dickerson-Lange and Abbe (2019). REM generation methods from Olson et al. (2014) and Dilts et al. (2010) were adopted to create REMs for the NF Teanaway River, Dickey, Middle, Indian, Jack, and Taneum Creeks. The first step in this process required digitization of the channel thalweg. The NFT, Jack Creek, and Indian Creek had bathymetric data collected in 2015 that was used as a hillshade layer to more accurately digitize the channel bed.

To extract an area value from the REM, the layer was transformed from raster to vector. This involved making the numeric values integers, using the raster to polygon tool, turning the integer values back to decimals, then selecting elevation data that represented floodplain elevations likely to be inundated based on the height above the digitized channel. This method allowed for a finer resolution area designated as floodplain but lost the context gained with the geomorphic mapping method. REMs are inherently skewed at the upstream and downstream end so that introduced a source of error to consider in the accuracy of the final area value. The final polygon product of the REM method was more like a fishnet than a traditional vector polygon. The data was unable to be manipulated or manually edited to exclude artifacts like the skewed floodplain where the tributaries meet the NFT.

Taneum Creek Watershed

The lower section of Taneum Creek has a lot more infrastructure obstacles than the upper section. There is private land, buildings, agricultural fields, irrigation canals, interstates, and roads. While digitizing at a 1:2,000 scale I did my best to avoid interstates since they are raised impervious surfaces that would not allow infiltration water storage. Once up in the canyon, the floodplain becomes significantly narrower and more dissected than the Teanaway watershed floodplain. While this makes Taneum a more desirable site for water storage due to the existing increased interaction between groundwater and surface water, it makes geomorphic mapping of the river more complicated. Given the multi-channel nature of Taneum Creek, I digitized more separate polygons than I did for the Teanaway.

Since the reach of Taneum Creek I am looking at is composed of several different DEM files, some of the floodplain was cut off in my REM creation. An additional complication with

this is the skewing of the values at the upstream and downstream ends of where two REMs meet. This occurred at the KRD well site where they are testing groundwater infiltration by diverting excess irrigation water onto a field. The downstream end of the upstream REM represents the floodplain as being lower whereas the upstream end of the downstream REM represents the floodplain as being higher than its immediate upstream counterparts. This unfortunately is unavoidable and a byproduct of working with REMs. Creating another REM using the adjacent LiDAR file would yield useless results since there is no intersection of the river with that DEM and there is not enough area to create a REM that would not further misrepresent the elevation differences.

Aquifer Storage Capacity Calculation

The mapped area values, depth values from stratigraphic profiles, and grain size interpretations were used to calculate the aquifer storage capacities based on the varying scenarios of the unit's ability to store and transmit water. The formula used to calculate the volume was $\text{Volume} = \text{Area} * \text{Height}$. The area is the quantity calculated based on the geomorphic mapping and the height above the channel in the REM. The volume calculation follows the methods set by Petralia (2022) in their volume of a saturated aquifer calculation. Their equation used $\frac{1}{2}$ area to better represent the wedge shaped alluvial fan geometry. I used a rectangular volume calculation to represent the u-shaped glacial valley floor. The depths for this calculation were specifically chosen for each individual tributary based on the incision observed in the field and the elevation range chosen during the REM-derived floodplain process.

Three depths were chosen to simulate different inundation possibilities. The absolute minimum volume considers the inability for water to inundate the incised floodplain and only

accounts for the area of the active floodplain mapped during the geomorphic mapping process on the North Fork Teanaway River. The depth chosen for this calculation was 3 feet as this is well below the incised floodplain but high enough to inundate the boulder bars. This is also the same value used by Dickerson-Lange and Abbe (2019) in their minimum volume calculation. The minimum and maximum depths for the incised floodplain area were chosen based on the stratigraphy at each tributary considering the silt-dominated layers. The minimum volume, excluded the silt-dominated layers, while the maximum volume includes the entire stratigraphic profile from the surface to the channel bed. All data collected in the field and lab were recorded using the metric system. For consistency with GIS and the use of results by watershed management in the United States, the remainder of the project was completed using the imperial system.

CHAPTER IV

RESULTS

Stratigraphy

The North Fork Teanaway watershed had generally consistent stratigraphy across the incised floodplain of the main river and the tributaries. The grain-size distribution varied with depth oscillating between silt and sand-dominated zones. The NFT and Indian Creek confluence serves as a representative example of the watershed in describing the basic units and grain-size distribution (Figure 12). The major stratigraphic zones were traced and determined to be laterally continuous for at least 100 m along the exposed cut bank at the NFT and Dickey Creek sites (Figure 10). A correlation of all stratigraphic profiles in the NFT watershed indicates that the stratigraphy of the incised floodplain and where the gray silt layer lies in relation to the other units is similar in the incised floodplain of the tributaries and main river (Figure 13). The majority composition of the floodplain was clayey silt with about 15% clay. Generally, the farther down in the profile, the sandier the units became and the less clay there was. The gray silt layer had the second lowest percentage of clay (7.4%) but the highest percentage of silt (61.2%) in the profile. While this layer did not have as much clay as originally thought, it should be noted that it behaved like clay in the field. It was sticky and cohesive both in hand sample and as resistant benches in the channel. The clay found at TVFF behaved in a similar manner but did not have the gray color observed in the NFT watershed. I hypothesize that even though these units vary spatially, they are from the same facies. For the remainder of the document, this reoccurring unit will be referred to as gray silt.

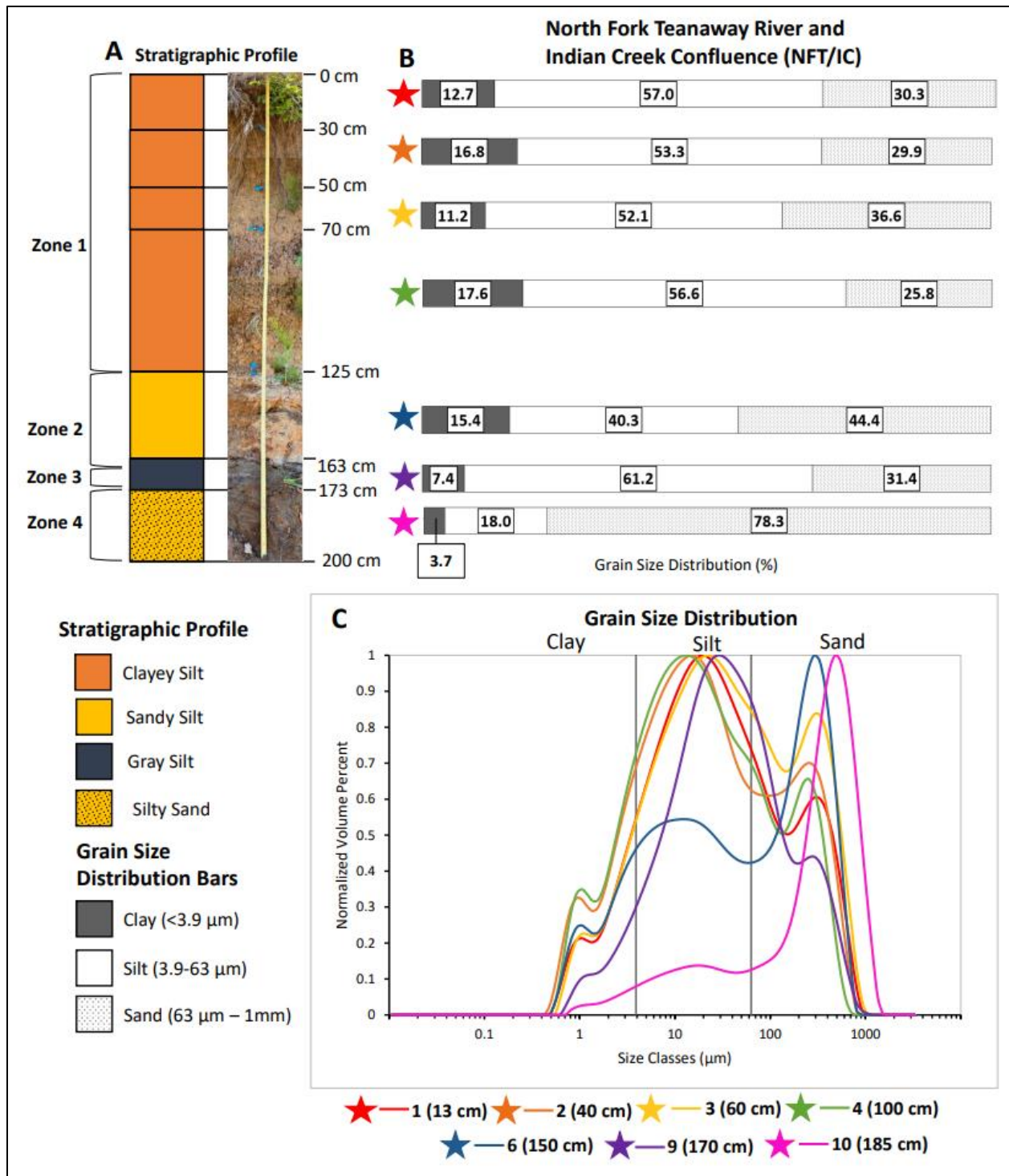


Figure 12. Stratigraphy and grain-size distribution from the North Fork Teanaway and Indian Creek confluence. A) Stratigraphic profile displaying the different units and zones observed in the field. B) Grain-size distribution bars with colored stars indicating the corresponding grain-size distribution curve. C) Grain-size distribution curve with samples plotted in corresponding colors. The first number is the sample number and the second is the depth where the sample was collected.

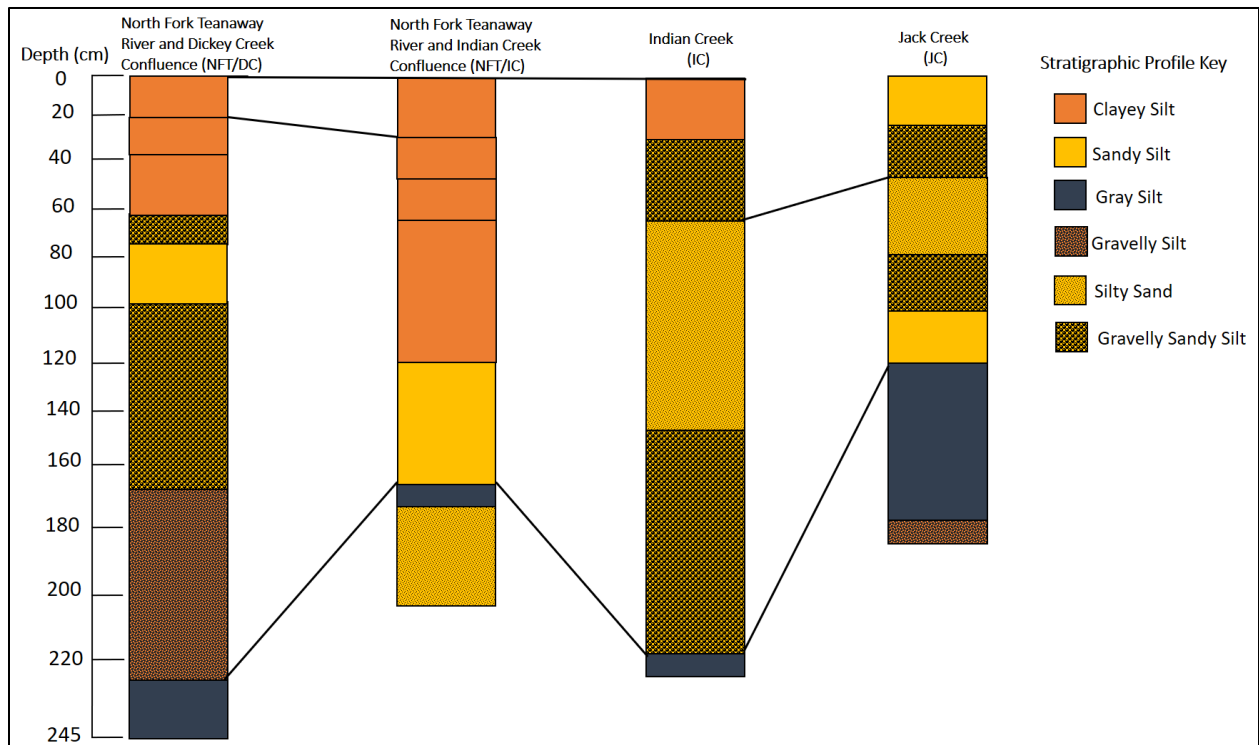


Figure 13. North Fork Teanaway watershed stratigraphic correlation (Figure 7). The profiles display the distinct layers observed during fieldwork. The gray silt layer is found at all four locations at variable depths and thicknesses.

Middle Reach Taneum Creek #2 was chosen as a representative location to expand on grain-size distribution (Figure 14). Middle Reach Taneum Creek #1 was used in a stratigraphic profiles correlation (Figure 15). The map shows the location of the two profiles in the middle reach of Taneum Creek (Figure 16). Transect samples from across the meadow at the lower reach of Taneum Creek were analyzed to visualize and quantify spatial variation across different sections of the floodplain (Figure 17). Since Taneum Creek was not flowing over bedrock, the stratigraphic profile often bottomed out at a sandy gravel unit just below the water table.

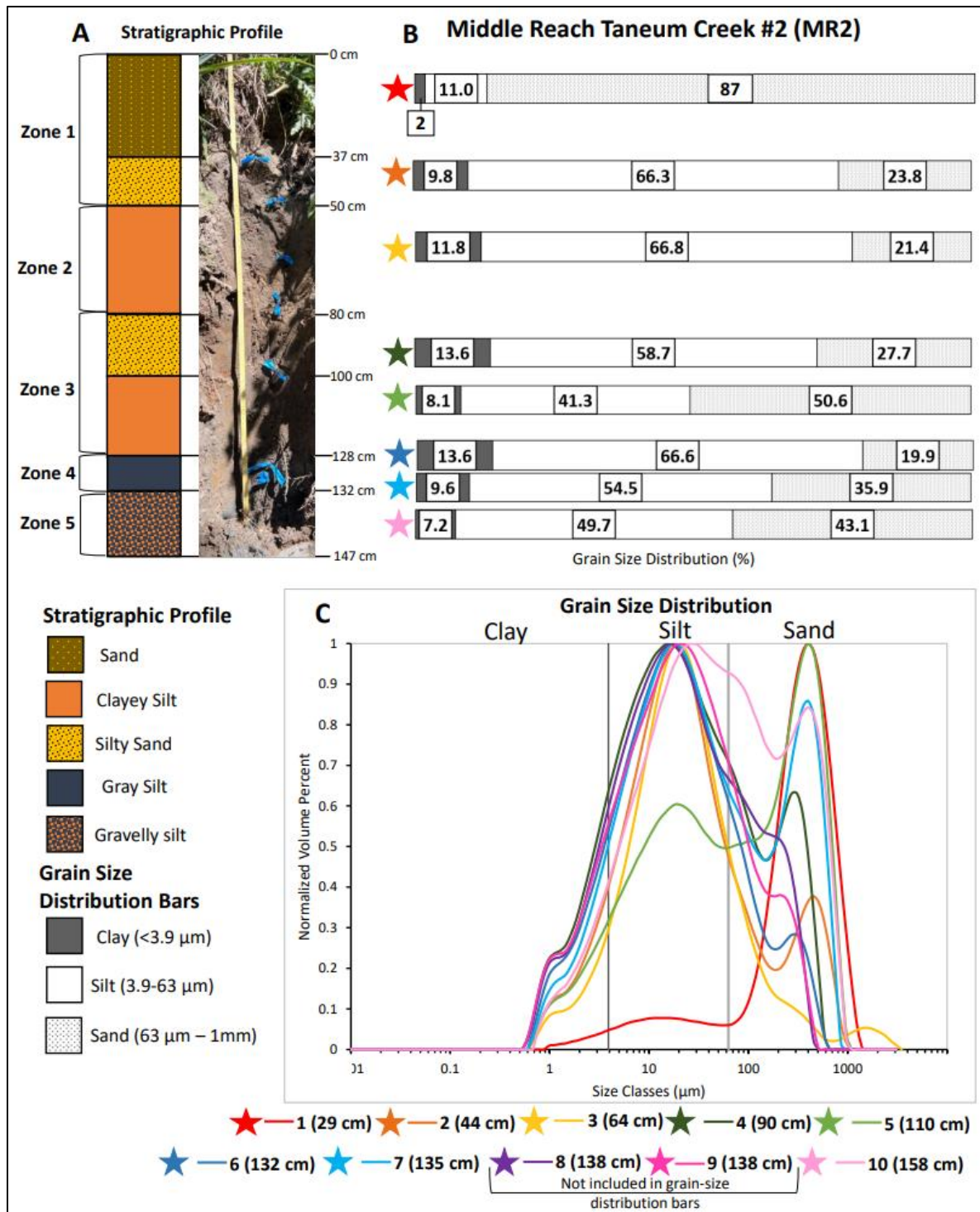


Figure 14. Stratigraphy and grain-size distribution from the Middle Reach Taneum Creek #2 site. A) Stratigraphic profile displaying the different units and zones observed in the field. B) Grain-size distribution bars with colored stars indicating the corresponding grain-size distribution curve. C) Grain-size distribution curve with samples plotted in corresponding colors. The first number is the sample number and the second is the depth where the sample was collected.

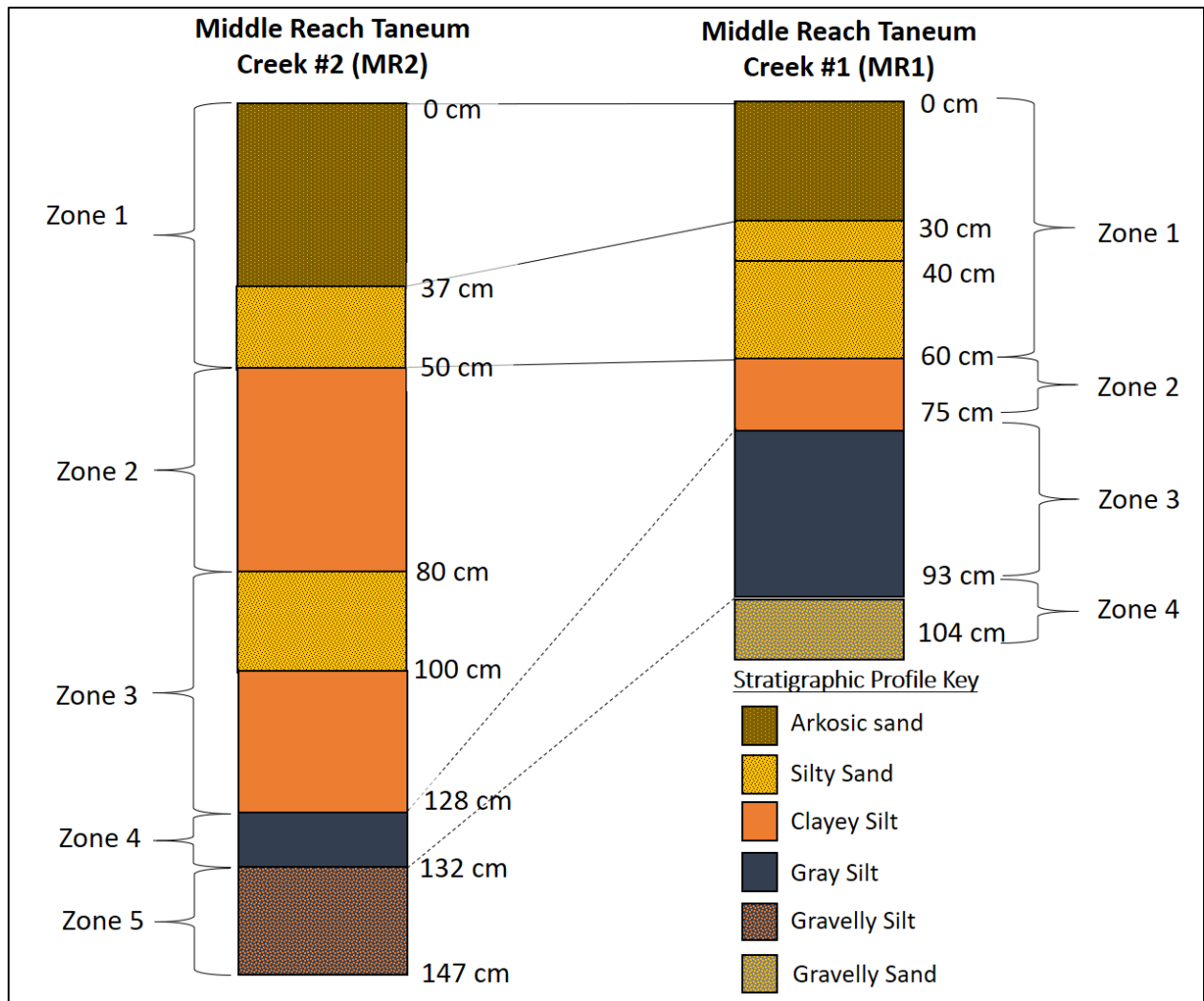


Figure 15. Taneum Creek stratigraphic correlation. Figure 16 shows in more detail the stratigraphic profile locations in relation to the old bridge. Middle Reach Taneum Creek #2 is slightly upstream of the old bridge (left) and Middle Reach Taneum Creek #1 is slightly downstream of the bridge (right).

The grain-size analysis yielded one challenge; each sample displayed the same plateau of clay content at the 1 μ m mark across all samples. To further investigate, CWU undergraduate students were enlisted to rerun the samples with the old window and different settings in the Mastersizer. Samples run by Stephen Bartlett (2022) also display this peculiar plateau and were run with the older window. There could be slight changes in sediment size data for the clay and

silt based on settings in the Mastersizer set during analysis. Further investigation into the Mastersizer and standard operating procedure for sample preparation may be required for future analyses.

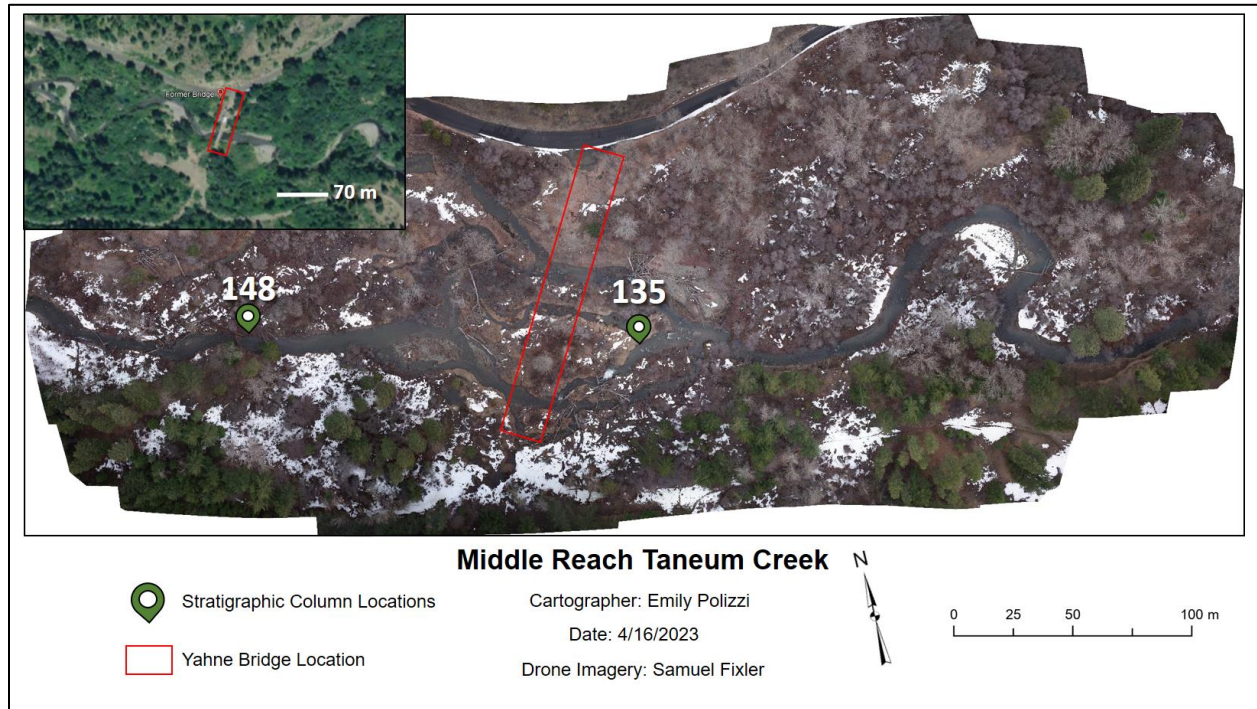


Figure 16. Taneum Creek middle reach map. The red box shows the area where the Yahne Bridge was removed in 2010. Prior to bridge removal, there was only one channel, now there are six threaded channels. Creek flows from left to right.

Gray Silt

All gray silt samples were plotted together to make comparisons between watersheds and locations within each watershed (Figure 18). Samples were plotted in descending order on the grain-size distribution bar chart with the most upstream locations listed at the top and the most downstream location at the bottom. The gray silt samples were also further broken down into very fine to fine silt (3.9 - 15.6 μm) and medium to coarse silt (15.6 - 63 μm) categories to better depict the finer grain-size distribution. The gray silt was observed at each stratigraphic profile location with varying degrees of mottling (Figure 19).

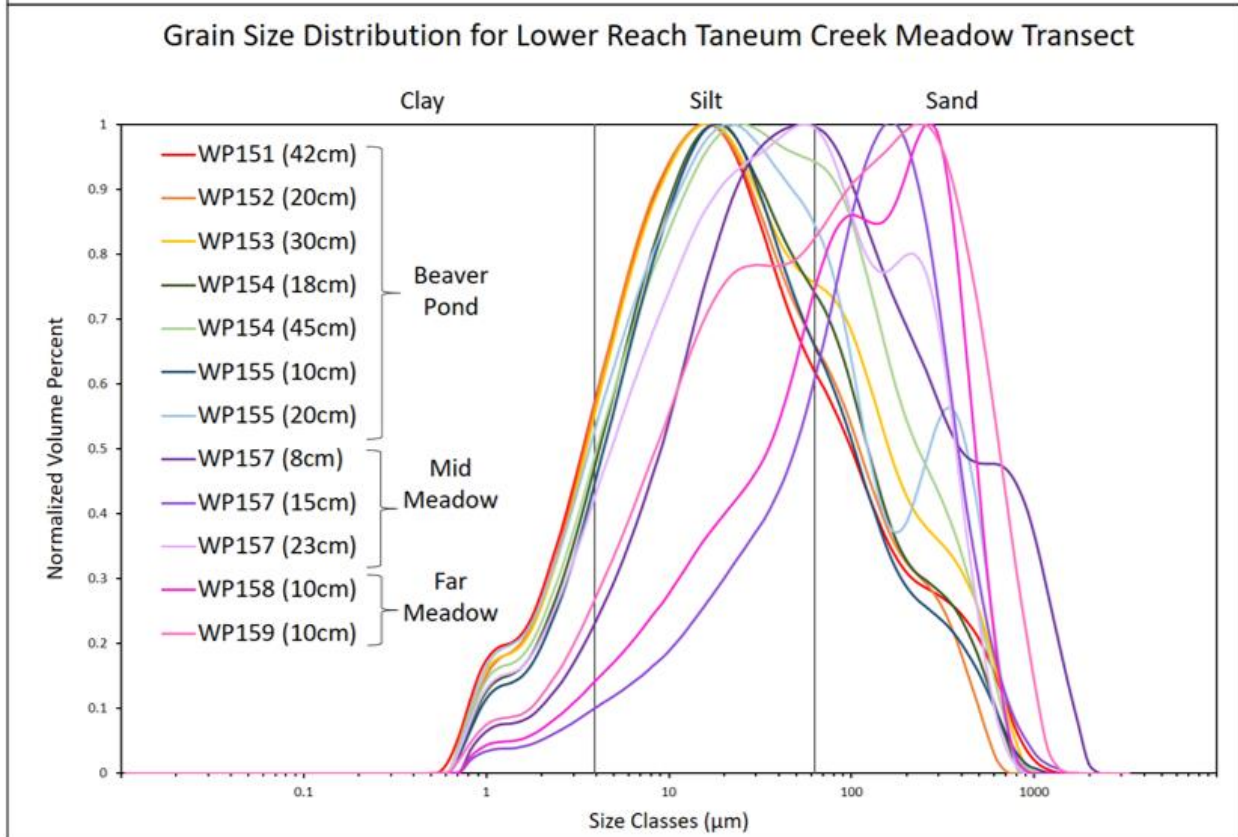
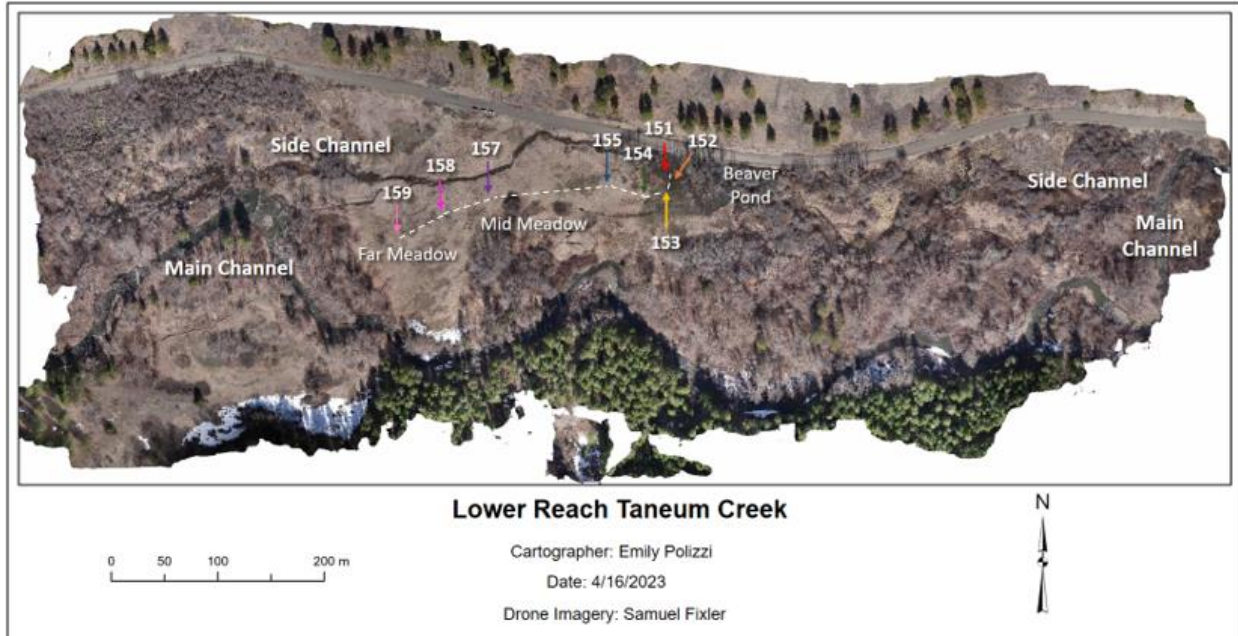


Figure 17. Taneum Creek lower reach meadow transect. The aerial imagery map shows sample locations marked with a waypoint number and color arrow along a floodplain transect (white dashed line) at the lower reach of Taneum Creek (top). The corresponding grain-size distribution graph depicts samples with color-coordinated map locations (bottom). Samples closest to the beaver pond had more silt while samples further from the pond had more sand.

Radiocarbon ages from the NFT River/Indian Creek Confluence location and Indian Creek tributary are displayed in Table 2. Samples from Indian Creek were collected by Stephen Bartlett for his thesis (Bartlett, 2022)

Piezometer Analysis

At the upper reach of Taneum Creek, the gray silt layer is exposed as the surface unit that the channel runs over. Pump tests were conducted in this area to evaluate the transmissivity of the gray silt layer and the underlying gravel unit (Figure 20). The same test was conducted at the North Fork Teanaway and Dickey Creek confluence on the bench pictured in (Figure 10). The water levels in the piezometer stabilized immediately at this location and with a difference of 0.05 (no change).

The clay layer at TVFF was determined to be a 2 - 4-meter-thick confining layer to the sandstone bedrock aquifer below (Figure 21; Petralia, 2022). The confining nature of this aquifer was verified through isotopic testing of water and groundwater levels monitored over time. Wells 1-3 were installed into the clay layer and wells 4-8 into the coarser-grained alluvial aquifer. When river water levels rose, wells 4-8 responded but wells 1-3 did not. The primary water level changes in wells 1-3 were in response to winter snow melt and local tributary creek levels. While the groundwater elevation in well 1 was consistently higher than in the others pointing towards confining behavior of the TVFF clay, it should be noted that the surface elevation was also higher (Figure 22; Petralia, 2022). It was interpreted that the water in well 1 was under the confining pressure of the clay causing the groundwater to rise higher than all the other wells. While the unit could transmit water it was not on a timescale appropriate for the seasonal storage

purpose of the project. This consequentially limited the floodplain storage capacity available to store seasonal groundwater on the TVFF (Petralia, 2022).

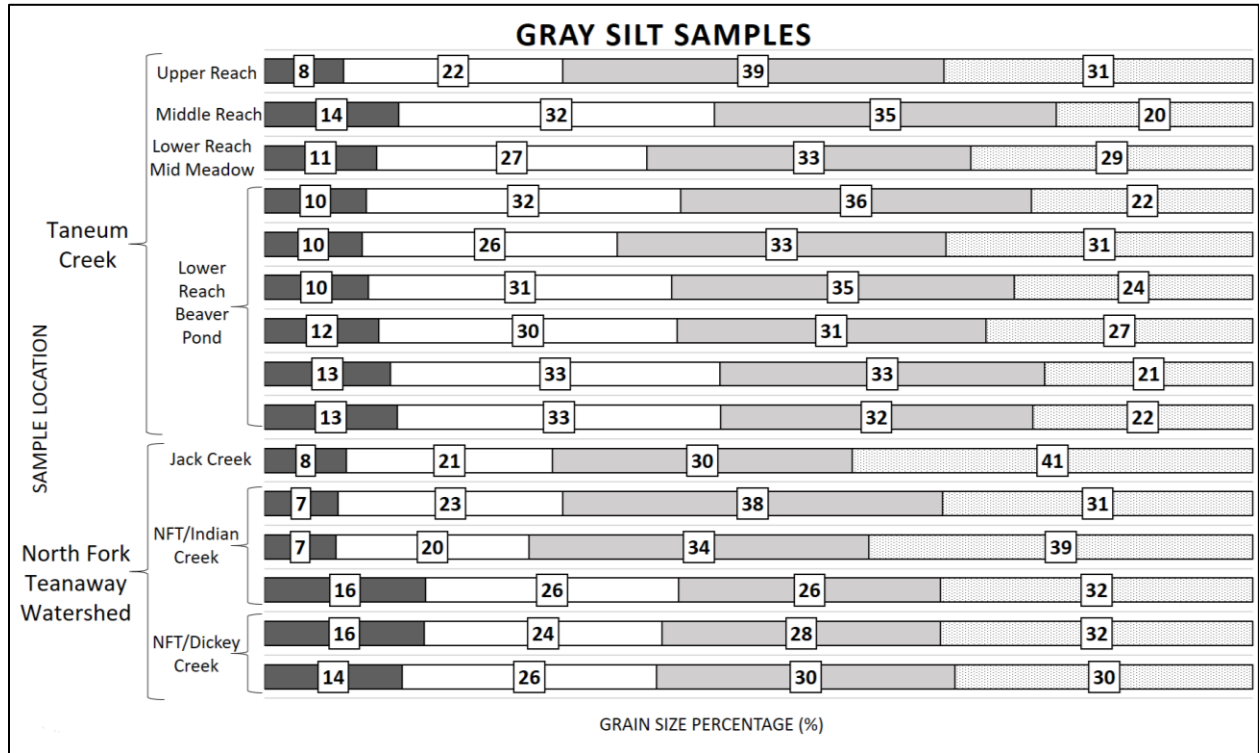


Figure 18. Gray silt grain-size distribution. Grain-size distribution bars for every sample taken from the gray silt units across the Taneum and NFT watersheds. From left to right on the chart, grain sizes are as follows: clay (<3.9 μm), very fine to fine silt (3.9 - 15.6 μm), medium to coarse silt (15.6 - 63 μm), and sand (63 μm - 1 mm).



Figure 19. Photographs of the gray silt. Photographs were taken at each stratigraphic profile in the North Fork Teanaway Watershed and at Taneum Creek. The gray silt varies spatially in grain-size distribution, mottling, and degree of mixing with surrounding units.

Table 2. North Fork Teanaway Watershed radiocarbon ages. The radiocarbon ages for wood/charcoal from the gray silt layer in the NFT watershed.

| Submitter | Location | Sample Type | Fraction of modern | | Radiocarbon age | | |
|---------------|-------------------|-------------|--------------------|------------------|-----------------|------------------|--------------------------------------|
| | | | pMC | 1 σ error | BP | 1 σ error | Calibrated Age BP (2 σ error) |
| Bartlett 2022 | Indian Creek | charcoal | 62.98 | 0.19 | 3714 | 24 | 3981-4149 |
| Bartlett 2022 | Indian Creek | charcoal | 62.13 | 0.18 | 3823 | 23 | 4099-4351 |
| Polizzi 2023 | NFT/IC Confluence | wood | 81.95 | 0.23 | 1599 | 23 | 1410-1530 |

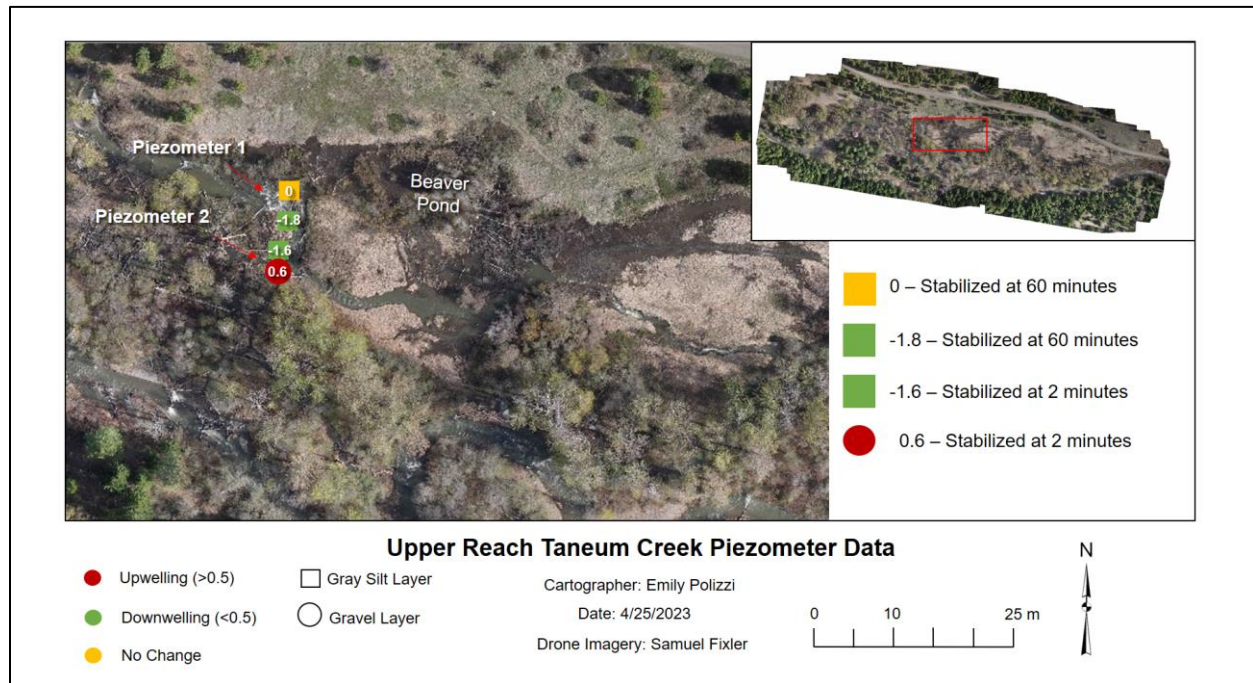


Figure 20. Taneum Creek upper reach piezometer map. Map displaying the pump test data from the upper reach of Taneum Creek. The squares represent measurements taken in the gray silt layer and the circles are measurements taken in the underlying gravel layer. Red indicates upwelling, green indicates downwelling, and yellow indicates no significant difference in the water level.

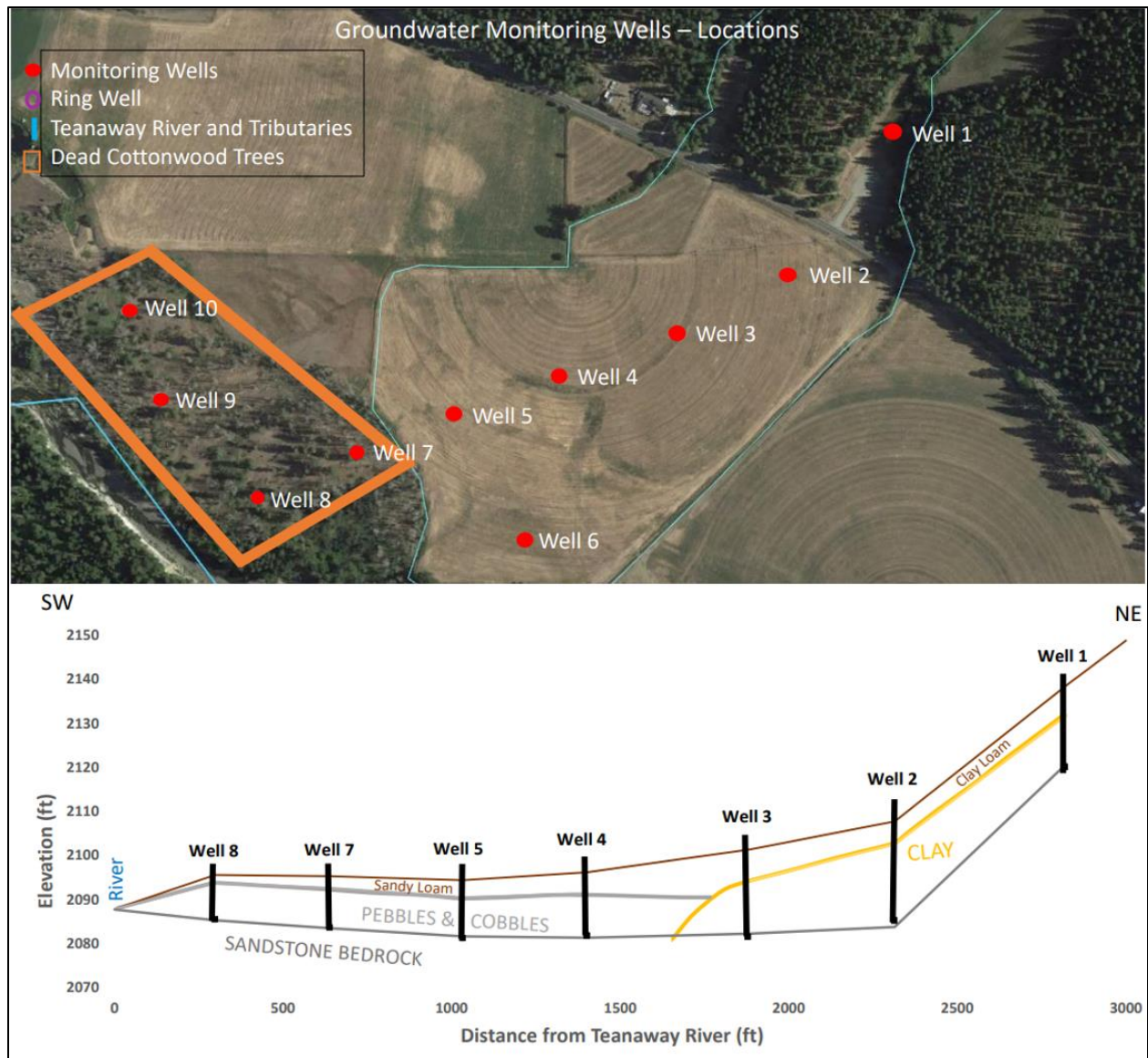


Figure 21. Teanaway Valley Family Farm well cross-section. Aerial view of the valley at the Teanaway Valley Family Farm site on the main stem of the Teanaway River. Wells were installed across the valley to monitor groundwater levels, stratigraphy, and isotopic signatures of water in different aquifers (above). The valley cross section shows the resulting stratigraphy observed when installing the wells. A confining clay layer present on the valley wall impeded the exchange of groundwater between the down-gradient units limiting the floodplain aquifer storage capacity (Petralia, 2022).

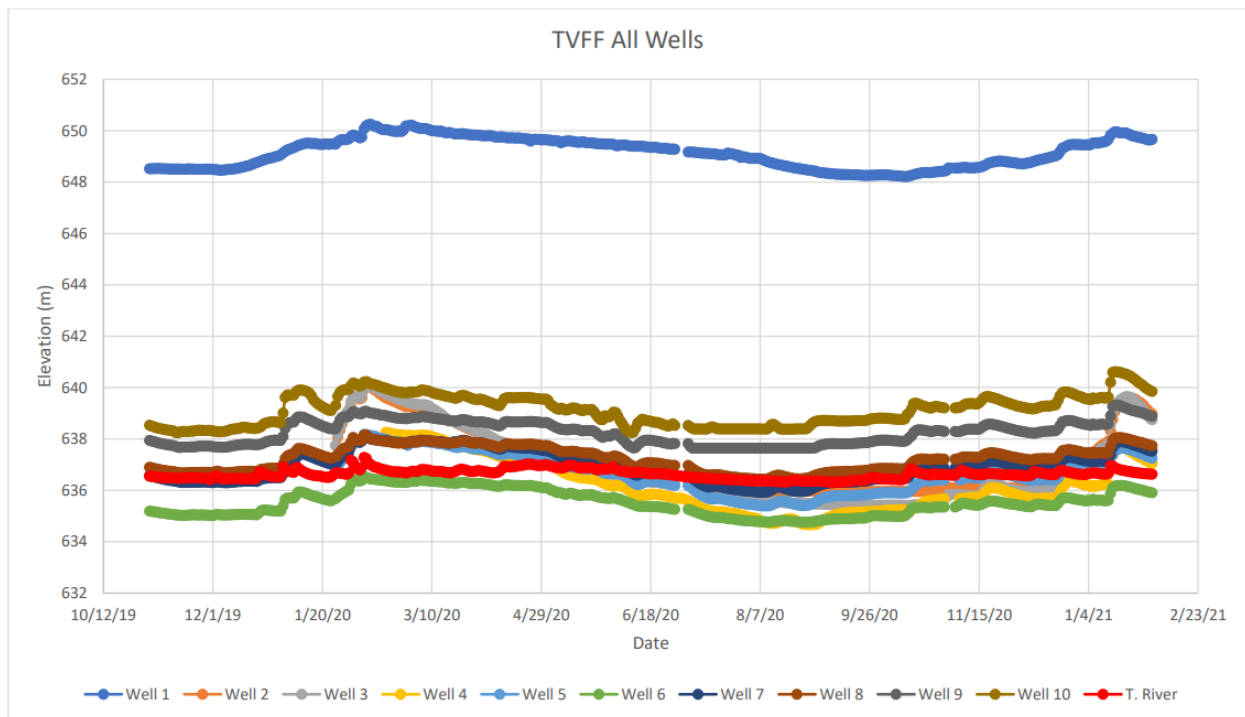


Figure 22. TVFF groundwater elevation. Groundwater elevation for all wells at Teanaway Valley Family Farm on the main stem Teanaway River (Figure 7). Groundwater elevation in well 1 is consistently 10 m higher than the second-highest elevation in well 10 (Petralia, 2022).

North Fork Teanaway Watershed Floodplain Mapping

The mapping portion of this project yielded several deliverables. The first was a geomorphic map, where all units were digitized by hand using hillshade imagery derived from DEMs (Figure 23). The geomorphic units delineated were the river Thalweg, active floodplain, incised floodplain, and terrace. The REM generation process yielded the actual relative elevation model and the incised floodplain extracted from the REM (Figures 24 and 25). The final deliverable was an overlay to compare the geomorphic map incised floodplain to the REM-extracted floodplain (Figure 26).

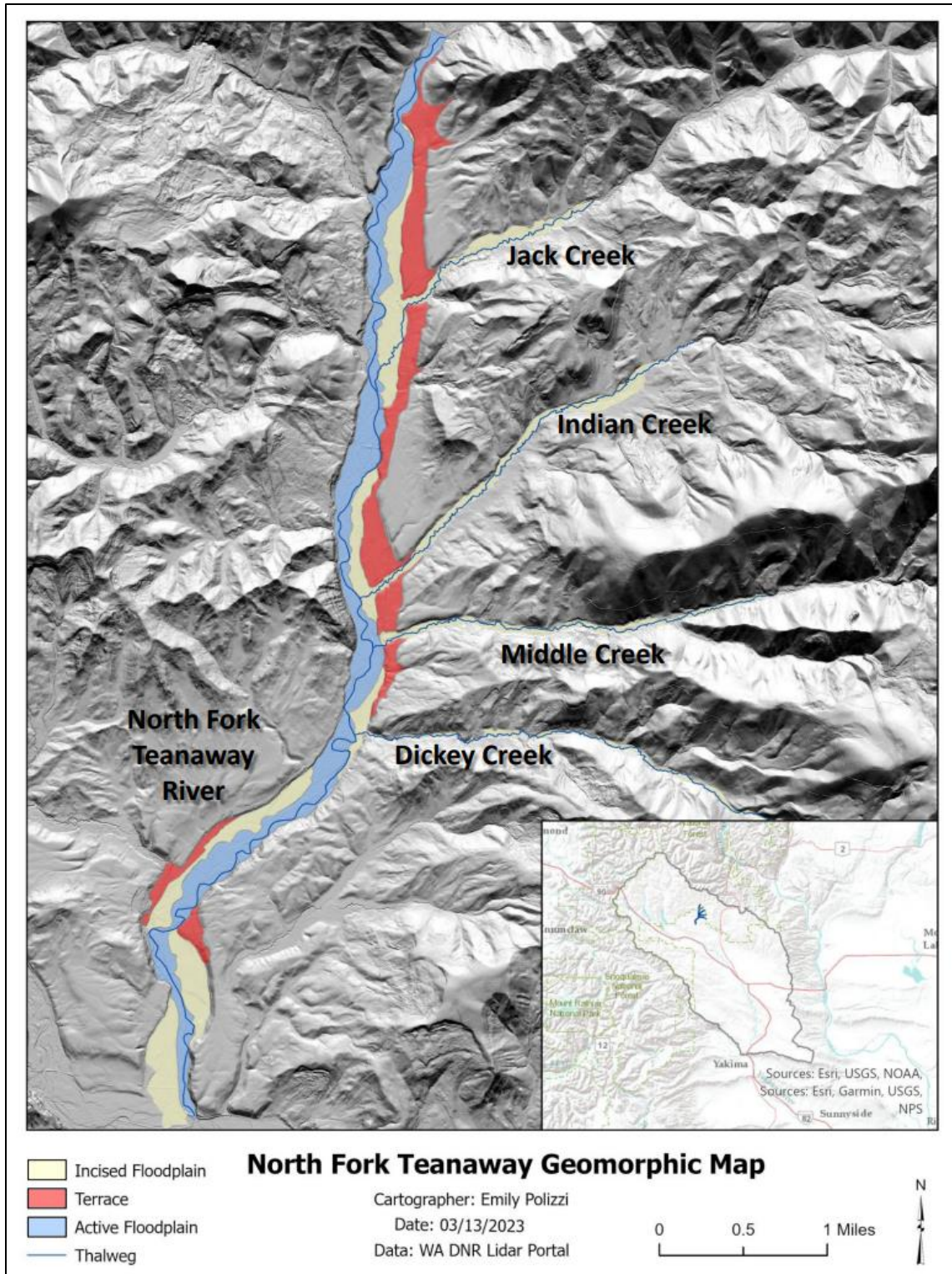


Figure 23. NFT watershed geomorphic map. This map displays the difference between active floodplain, incised floodplain, and terrace across the NFT watershed. The terrace lies outside of the current floodplain and was not used in the aquifer capacity calculation.

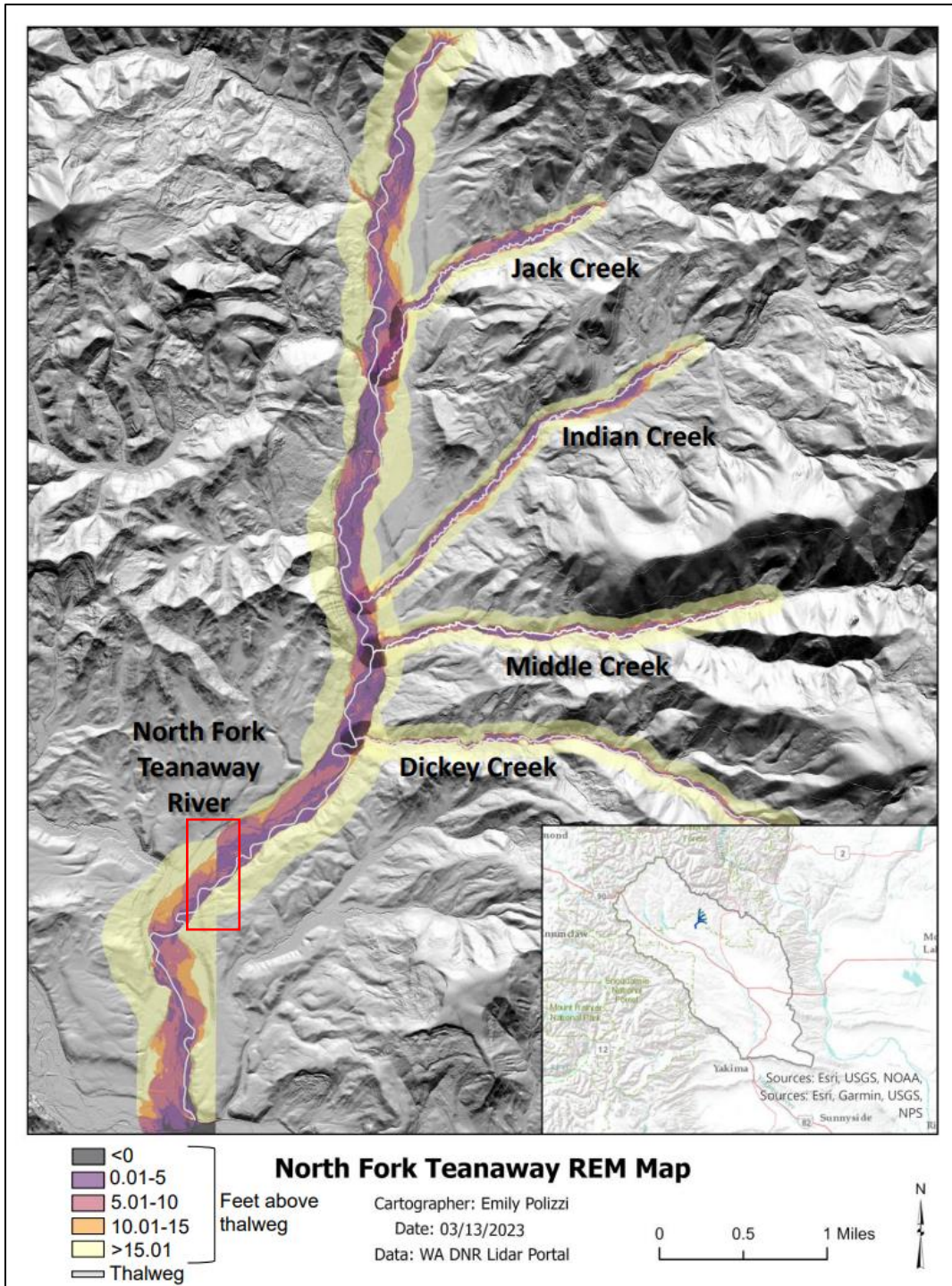


Figure 24. NFT watershed REM map. The colors indicate the different elevations given to each pixel based on their elevation in feet above or below the water surface in the river. The seam between DEM files is present downstream of Dickey Creek and is highlighted by a red box.

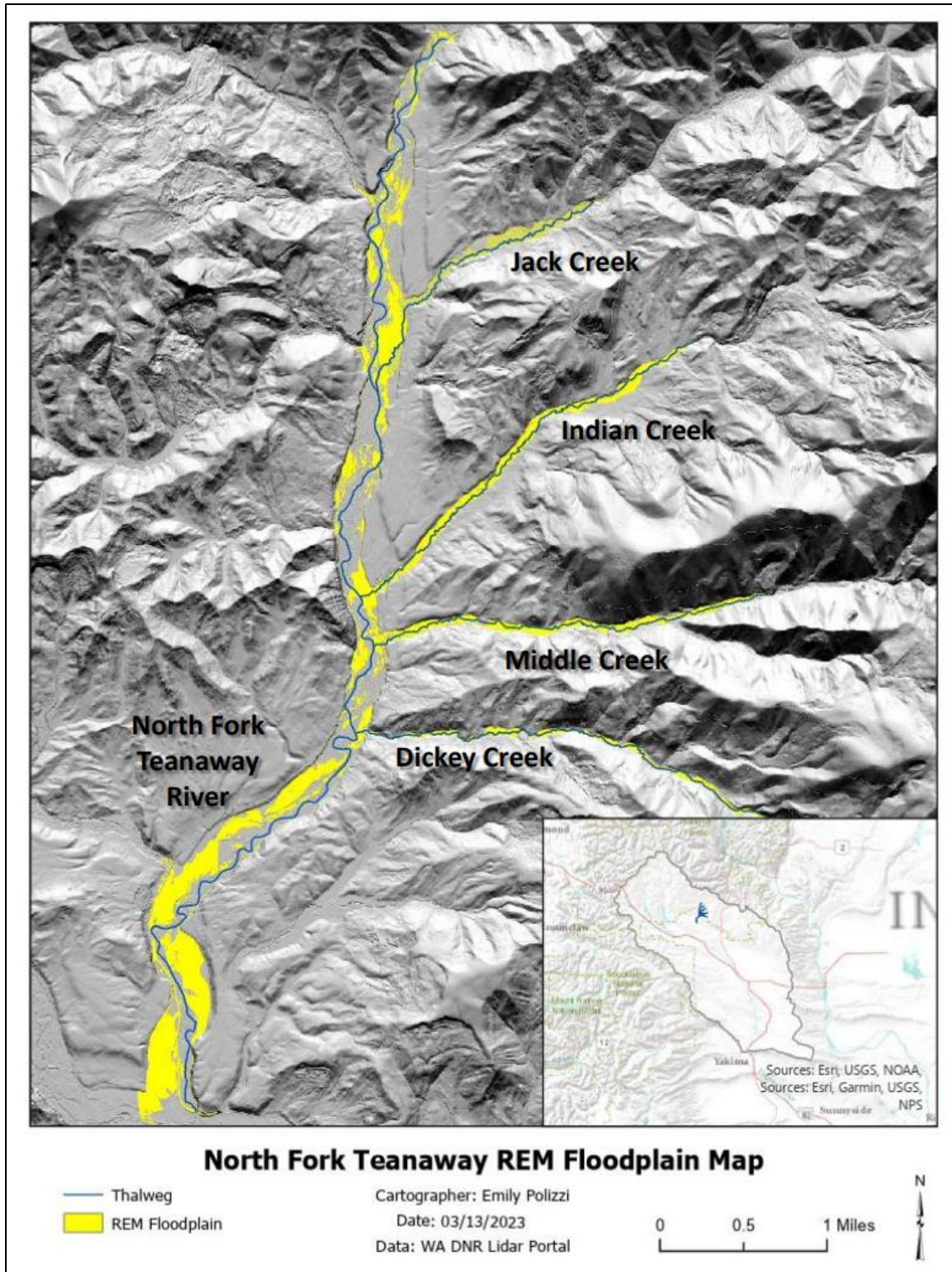


Figure 25. NFT watershed REM extracted floodplain map. Varying elevation ranges were chosen for each tributary to account for differences in incision across the watershed.

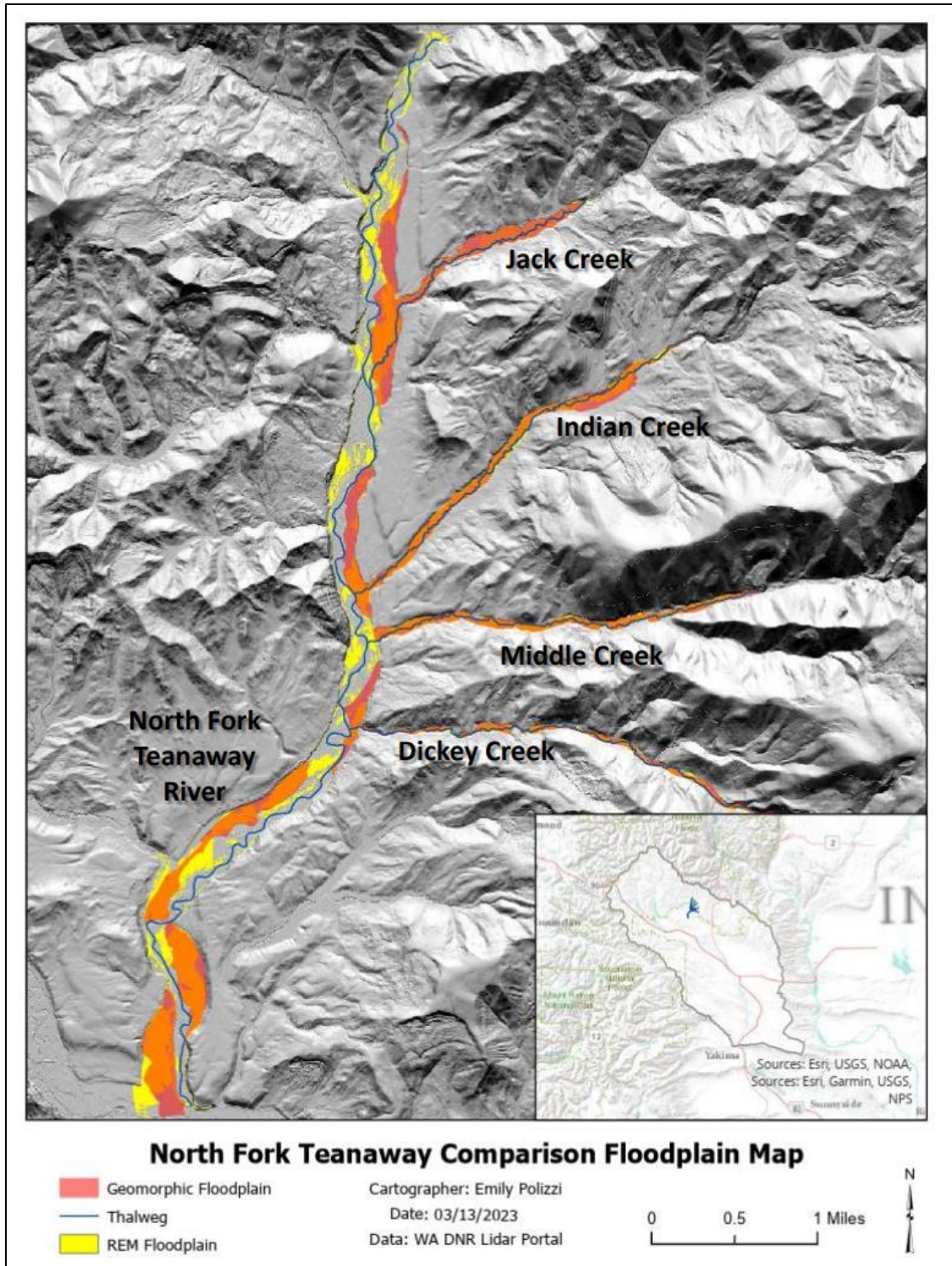


Figure 26. NFT watershed floodplain comparison map. This map compares the geomorphic mapped incised floodplain (red) and REM extracted incised floodplain (yellow). The orange depicts where the two floodplain methods overlapped.

The calculate geometry tool was used in both approaches to quantify the area covered by the floodplain. The REM tended to have larger values than the geomorphic mapping with the largest percent difference at Dickey Creek (Table 3). This demonstrated the difference between these methods and provided reassurance that they achieved similar results.

Table 3. North Fork Teanaway Watershed incised floodplain area. A comparison between the REM and geomorphic mapping areas in the North Fork Teanaway Watershed (Figure 26).

| Tributary | REM Area (Acres) | Geomorphic Area (Acres) | % Difference |
|---------------------------|-------------------------|--------------------------------|---------------------|
| North Fork Teanaway River | 363 | 298 | 19.6 |
| Dickey Creek | 51.0 | 36.3 | 33.6 |
| Middle Creek | 58.6 | 55.8 | 5.0 |
| Indian Creek | 77.4 | 81.9 | 5.6 |
| Jack Creek | 71.3 | 75.0 | 5.0 |
| Totals | 622 | 548 | 12.7 |

Taneum Creek Floodplain Mapping

The mapping at Taneum Creek yielded the same deliverables as the NFT watershed. The first was a geomorphic map, where all units were digitized by hand using hillshade imagery derived from DEMs (Figure 27). Different geomorphic designations were used on Taneum Creek because the floodplain incision was not to the degree of the NFT watershed. The geomorphic designations chosen were the river thalweg, multi-threaded channel bed, floodplain, and terrace. The REM generation process yielded the relative elevation model and the incised floodplain extracted from the REM (Figures 28 and 29). The final deliverable was an overlay to compare the geomorphic map floodplain to the REM-extracted floodplain (Figure 30). Floodplain areas for both methods are displayed in Table 4. The REM-derived area was slightly larger than the geomorphic mapped area with a percent difference of 11.8%.

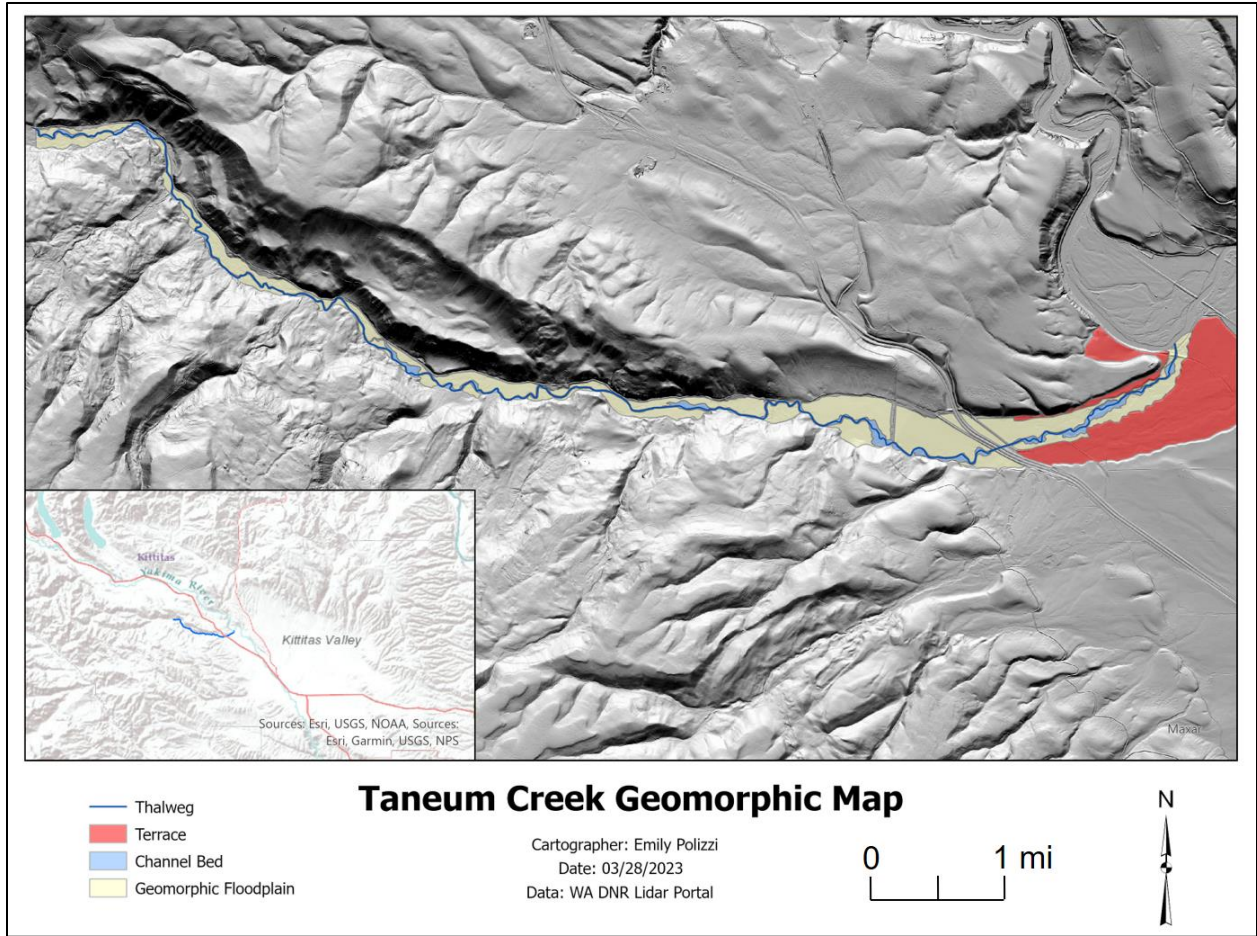


Figure 27. Taneum Creek geomorphic map. Map displaying the different geomorphic units: floodplain, channel bed, and the lowest river terrace.

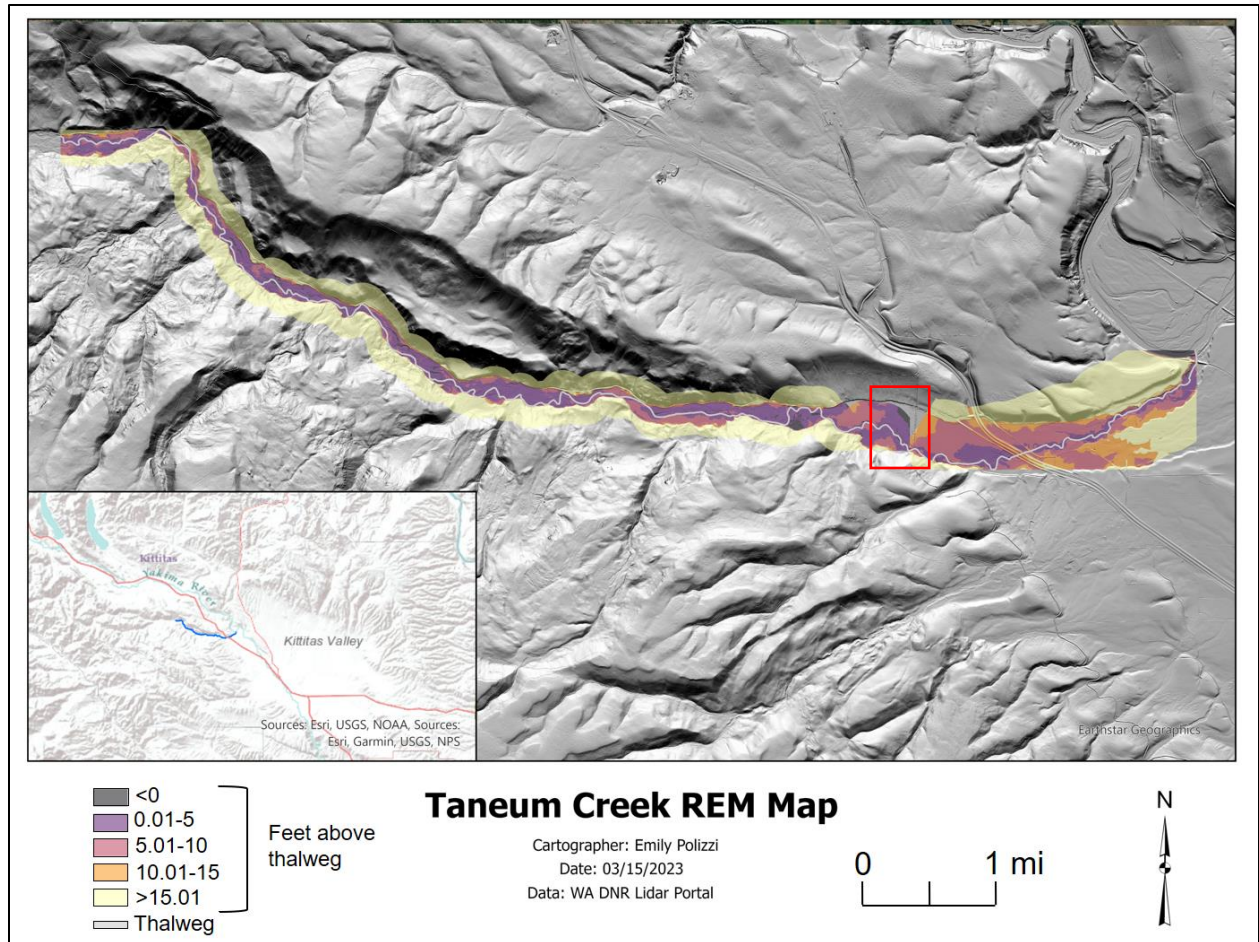


Figure 28. Taneum Creek REM map. The colors indicate the different elevations given to each pixel based on their elevation in feet above or below the water surface in the river. The two DEM files used to generate the REM meet at the KRD well site, just upstream of 1-90. It should be noted that the REM was unable to account for a portion of the floodplain (red box).

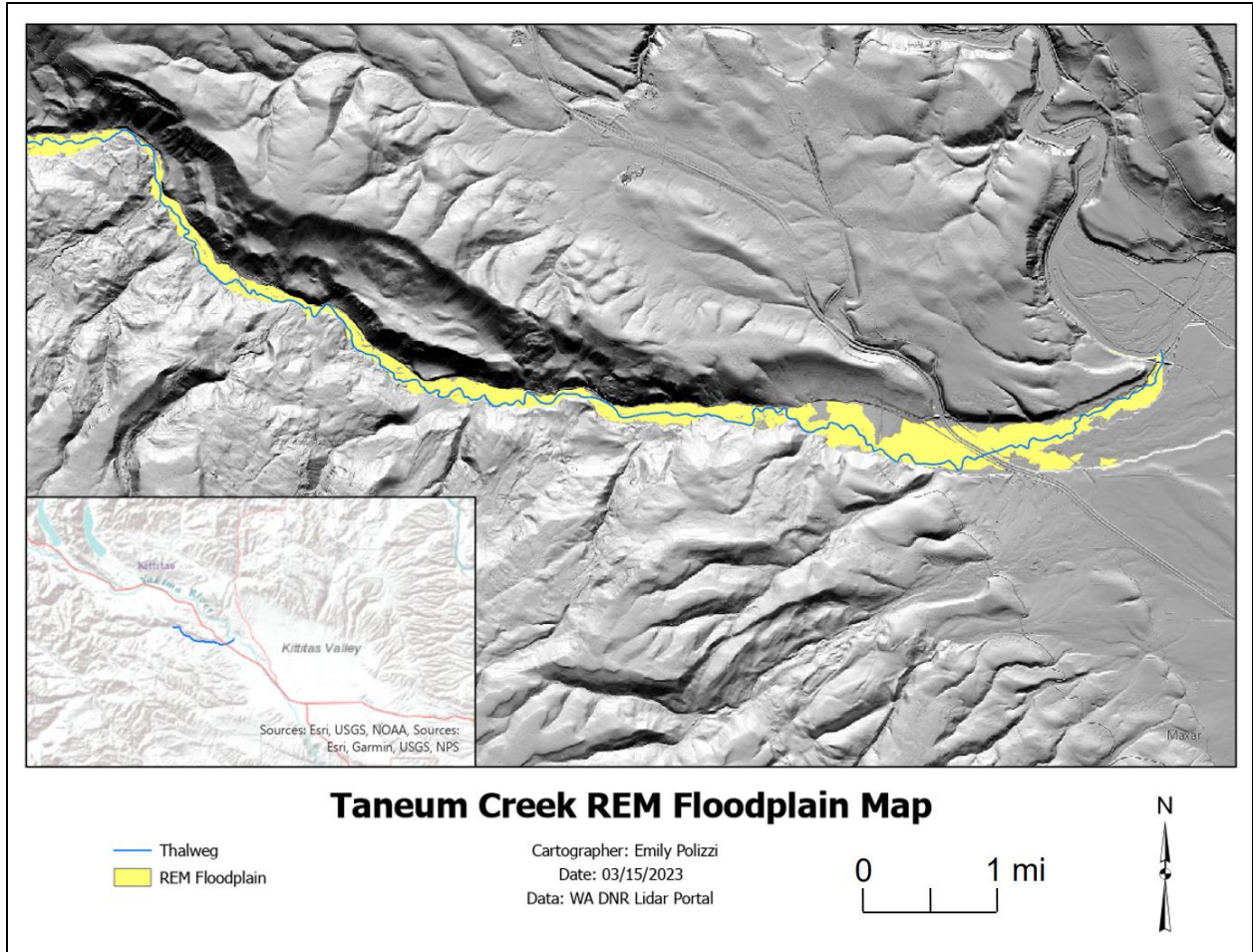


Figure 29. Taneum Creek REM extracted floodplain map. Varying elevation ranges were chosen for each DEM file area to account for skewing.

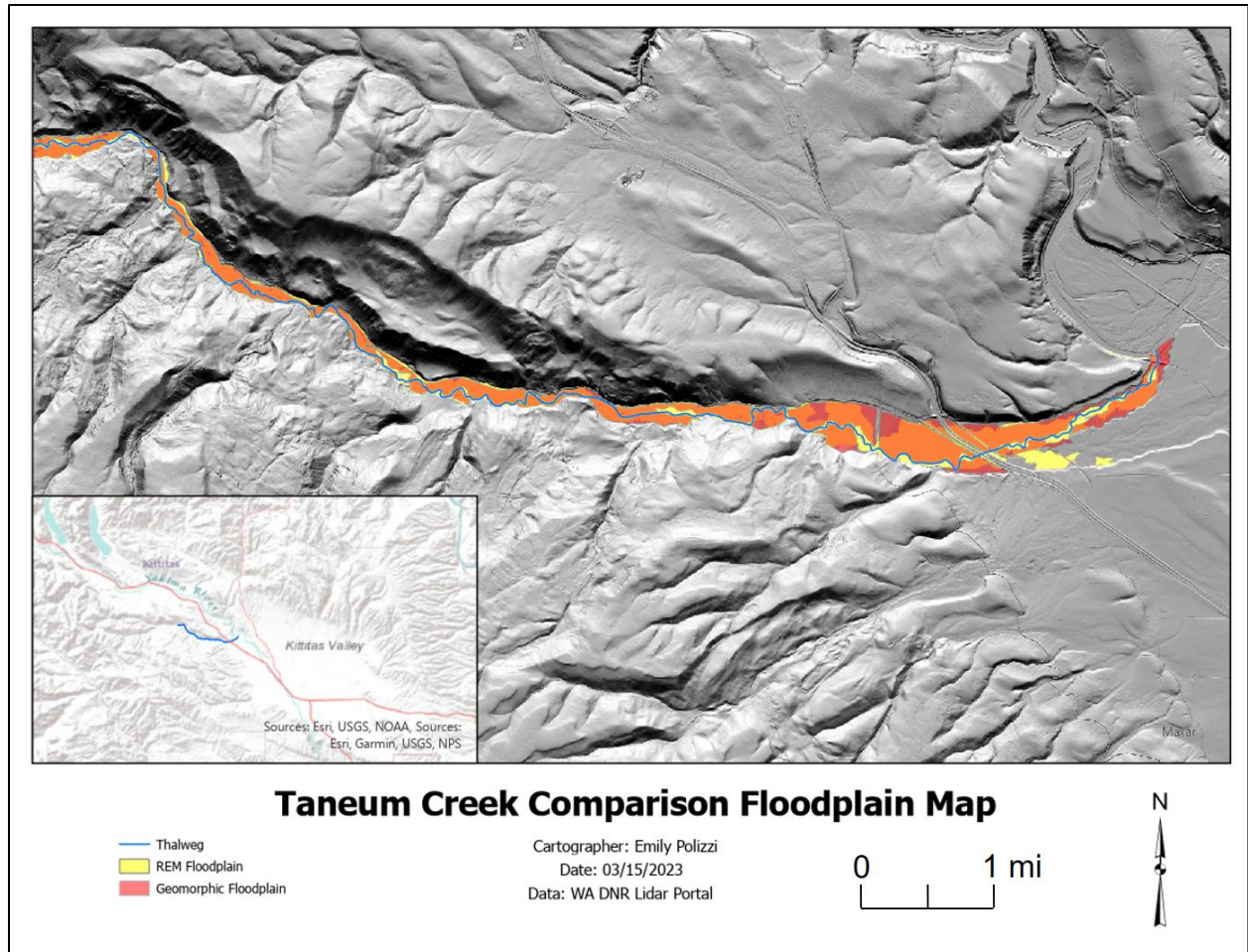


Figure 30. Taneum Creek floodplain comparison map. Compares the geomorphic mapped floodplain (red) and REM extracted floodplain (yellow). The orange depicts where the two floodplain methods overlapped.

Table 4. Taneum Creek floodplain area. A comparison between the REM and geomorphic mapping areas at Taneum Creek (Figure 30).

| Tributary | REM Area (Acres) | Geomorphic Area (Acres) | % Difference |
|--------------|------------------|-------------------------|--------------|
| Taneum Creek | 693 | 616 | 11.8 |

Floodplain Aquifer Volume

To determine the depth to use in the volume calculation, a minimum and maximum range of depths were chosen based on profiles in each tributary. The total areas calculated for each watershed were similar but, the volumes were different (Table 5). The active floodplain volume uses the geomorphic mapping active floodplain area multiplied by a depth of 3 feet. The active floodplain is separate from the incised floodplain and represents what is currently inundated at peak flow. The incised minimum volume uses the incised floodplain area multiplied by a depth of 2.1 feet to represent the stratigraphic profile from channel bed to surface but excluding the silty units inferred to be less permeable (Zones 1 and 3; Figure 31). The incised maximum volume used the incised floodplain area multiplied by the entire stratigraphic profile depth from the channel bed to the surface, not excluding any units. The volumes were multiplied by a minimum and maximum porosity to better estimate the storage capacity of the incised floodplain considering the sediment composition. The minimum porosity (0.3) was used by Dickerson-Lange and Abbe (2019) in their potential volume calculations of the Teanaway River watershed and represents a sandy loam. The maximum porosity (0.38) was used by Bartlett (2022) in the Indian Creek floodplain volume calculation and represents a silt/clay floodplain.

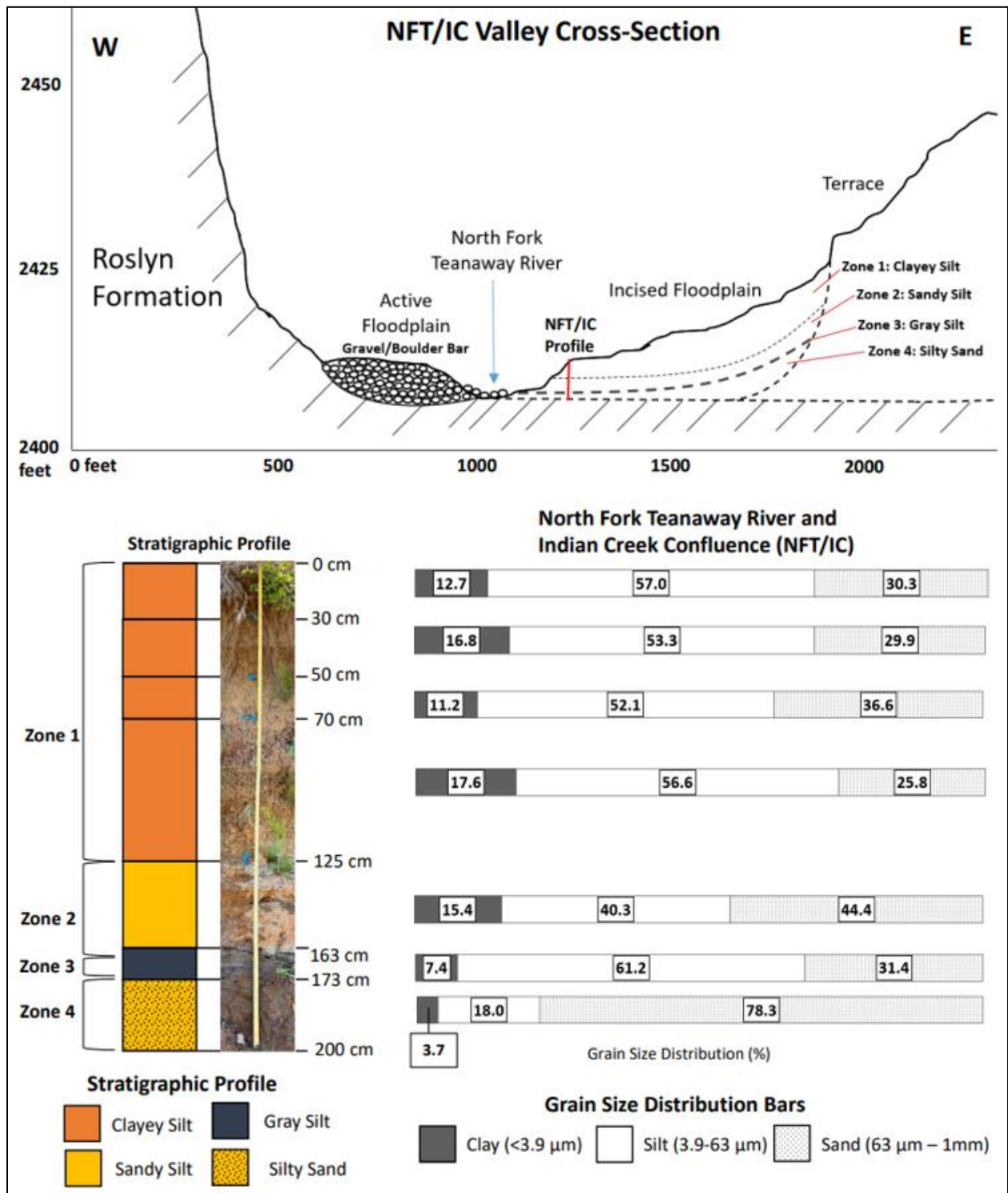


Figure 31. North Fork Teanaway River and Indian Creek Confluence Cross-Section. The above cross-section shows the incised floodplain stratigraphy in the greater context of the North Fork Teanaway River Valley. The zones delineated in the cross-section are expanded upon in the stratigraphic profile below.

Table 5. Potential aquifer storage capacity in the North Fork Teanaway Watershed. Volume estimates under varying scenarios of aquifer thickness and porosity. All areas used in this table are from the geomorphic mapping method (Figure 23).

| Tributary | Floodplain Description | Thickness (feet) | Area (acres) | Volume ac-ft (m³) 0.3 Porosity | Volume ac-ft (m³) 0.38 Porosity |
|-------------------------------|-------------------------------|-------------------------|---------------------|--|---|
| North Fork Teanaway River | A | 3 | 506 | 455 (561,000) | 576 (710,000) |
| | B | 2.1 | 298 | 188 (232,000) | 238 (294,000) |
| | C | 6.6 | 298 | 591 (729,000) | 749 (924,000) |
| Dickey Creek | B | 5.4 | 36 | 59 (73,000) | 75 (93,000) |
| | C | 8 | 36 | 88 (109,000) | 111 (137,000) |
| Middle Creek | B | 5.4 | 56 | 91 (112,000) | 115 (142,000) |
| | C | 8 | 56 | 134 (165,000) | 170 (210,000) |
| Indian Creek | B | 6.2 | 82 | 153 (189,000) | 194 (239,000) |
| | C | 7.5 | 82 | 185 (228,000) | 235 (290,000) |
| Jack Creek | B | 4.1 | 75 | 92 (113,000) | 117 (144,000) |
| | C | 5.2 | 75 | 118 (146,000) | 150 (185,000) |
| Total (min. thickness) | A + B | - | - | 1040 (1,290,000) | 1320 (1,630,000) |
| Total (max. thickness) | A + C | - | - | 1570 (1,930,000) | 1990 (2,450,000) |

A = Active floodplain area, B = Incised floodplain area (excluding stratigraphic profile zones 1 & 3), C = Incised floodplain area (entire stratigraphic profile thickness). All values are rounded to three significant figures and represent the maximum amount of storage in the floodplain aquifer if it were completely void of water.

Table 6. Potential aquifer storage capacity in the Taneum Creek Watershed. Volume estimates under varying scenarios of aquifer thickness and porosity. The geomorphic mapping and REM method areas are both used in this table to compare volumes (Figure 30).

| River | Thickness (feet) | Area (acres) | Volume ac-ft (m³) 0.3 Porosity | Volume ac-ft (m³) 0.38 Porosity |
|--------------------|-------------------------|---------------------|--|---|
| Taneum Creek | 2 | 587 | 352 (434,000) | 446 (550,000) |
| Geomorphic Mapping | 5 | 587 | 880 (1,090,000) | 1,120 (1,380,000) |
| Taneum Creek | 2 | 693 | 416 (513,000) | 527 (650,000) |
| REM method | 5 | 693 | 1,040 (1,280,000) | 1,320 (1,620,000) |

2 feet stratigraphic profile thickness excludes stratigraphic profile zones 2 & 4, 5 feet stratigraphic profile thickness includes the entire stratigraphic profile thickness. All values are rounded to three significant figures and represent the maximum amount of storage in the floodplain aquifer if it were completely void of water.

CHAPTER V

DISCUSSION

North Fork Teanaway Watershed Stratigraphy

Previous research on the floodplain storage of the North Fork Teanaway River by, Dickerson-Lange and Abbe (2019) investigated the floodplain aquifer capacity under varying scenarios of incision and assumed a sandy loam aquifer. Studies on Indian Creek, by Boylan (2020) and Bartlett (2022) further investigated the effects LW restoration had on groundwater recharge, storage, and flow and found no significant difference in seasonal or long-term groundwater levels after LW emplacement in 2016-2018. Wells were installed in the floodplain along Indian Creek, down to the mouth where it joins the NFT River. Across this 2 km distance, the well water levels followed the same trend in response to precipitation (Figure 32). This could indicate consistency in floodplain stratigraphy and groundwater behavior across both the Indian Creek and NFT River floodplain (Figure 31). Investigation into the stratigraphy of the NFT watershed helps further assess the efficacy of LW restoration on groundwater recharge, storage, and flow and better estimate the conditions under which natural floodplain-channel interaction may resume.

Overall, the floodplain stratigraphy in the NFT watershed had a slightly higher distribution of sand and lower distribution of silt compared to Taneum Creek. This could be attributed to the most abundant surface bedrock in the study area being the Roslyn Formation. This continental sedimentary formation is commonly found throughout this watershed as a friable sandstone bedrock (Collins et al., 2016). A friable sandstone as the dominant surface bedrock unit could have resulted in a more continuous distribution of sand throughout the

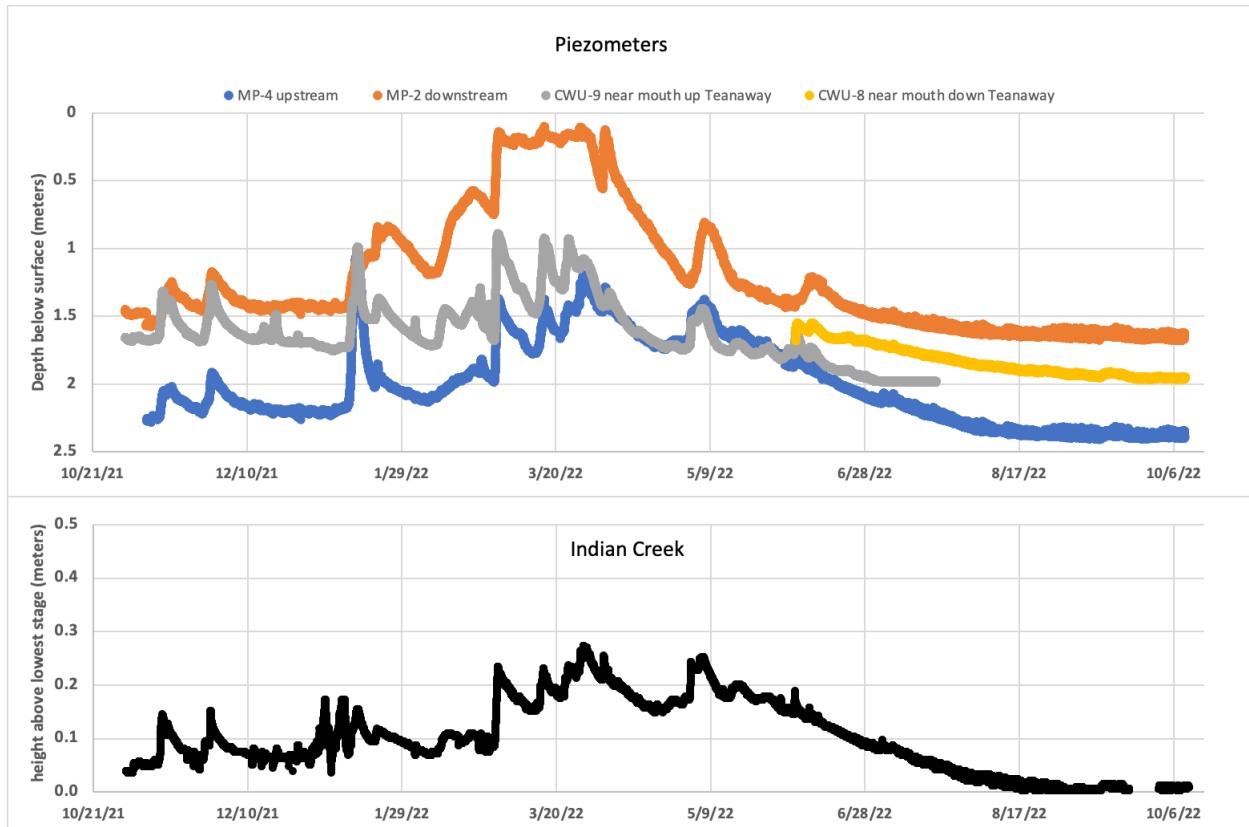


Figure 32 Indian Creek piezometer data. The top graph shows the water levels in wells installed along Indian Creek. MP-2 and MP-4 are approximately 1 and 2 km upstream along Indian Creek (Bartlett, 2022), and CWU-8 and CWU-9 are at the confluence of Indian Creek and the NFT River. The bottom graph shows Indian Creek water height above the lowest stage. Both display data from October 2021-October 2022. C. Gazis, Central Washington University, unpublished data 2023.

deposition of incised floodplain stratigraphy. Grain-size analysis displayed a bimodal distribution in most layers, indicating that both sand and silt dominate the NFT watershed (Figure 31). This could be a positive sign for water storage in the NFT watershed, as sand generally has a higher permeability than silt and clay. Consequently, sand is more effective at temporarily storing water than silt and clay. It is worth noting the stratigraphic profiles were recorded along riverbanks. So, sediment farther into the floodplain could potentially vary in sand composition from the river margins.

The stratigraphic correlation displayed the spatial variation in stratigraphy and grain-size distribution upstream in the NFT watershed (Figure 13). The farther upstream and higher in elevation, the more sand-dominated the units became, including the gray silt layer. Downstream in the main stem Teanaway River at the TVFF site, a gray layer was observed as a confining clay unit (Figures 20 and 21; Petralia, 2022). Upstream at the Dickey Creek and NFT River confluence the dominant grain size was silt (clay: 14%, silt: 56%, sand: 30%), and at Jack Creek, there was slightly less clay and silt and more sand (clay: 8%, silt: 51%, sand: 41%; see appendix for grain size distribution). It is worth noting that the Jack Creek floodplain was recently restored and there is a possibility that the floodplain surface sediment was altered due to that project. Regardless, the increase in sand higher in elevation is good for the aquifer storage capacity.

Taneum Creek Stratigraphy

Compared to the bimodal distribution in the NFT watershed, Taneum Creek had more unimodal distributions of sand and silt in the lower reach and bimodal distribution in the middle reach (Figure 33). This variation could have implication on floodplain water infiltration and storage within the different reaches of Taneum Creek. The lower reach of Taneum Creek provided an excellent opportunity to evaluate the grain-size distribution variability across the floodplain by comparing the beaver pond and dry meadow (Figure 33). The formation of the beaver pond on the side channel coincides with a silty deposit overlying a gravelly unit. The silty unit promotes the retention of the water in the pond in conjunction with the upkeep of the dams by the beavers. Water is retained but still able to flow through the pond. Without this silty unit, the beaver pond area would likely not hold water through the summer. While the pond shrinks in the later summer, it does not go completely dry. Just upstream of the beaver pond, the grain-size

distribution of the floodplain sediment begins to shift to coarser sediment sizes, straddling the silt and sand boundary (Figure 33). In the far meadow, the floodplain sediment is slightly bimodal with a more dominant sand signal. This was consistent in the abandoned channel location (WP 158) and the farthest meadow location (WP 159). The mid-meadow samples had the most variation in grain-size distribution as the floodplain transitioned from silt to sand dominated (WP 157).

At the Middle Reach of Taneum Creek, the Yahne Bridge was removed in 2010 (Figure 16). The bridge removal in conjunction with the instream LW installations and the 2011 flood, catalyzed the formation of multi-threaded channels, which rapidly increased channel complexity (Fixler, 2022). In terms of geomorphology, the LW restoration and flood at Taneum Creek resulted in the formation of side channels, sediment aggradation, and increased inundation of the floodplain. Fixler (2022) found higher NDVI values (an indicator of vegetation greenness) following the 2011 flood with larger increases in reaches where there were established LW installations. The increased channel complexity led to multi-threaded channels, floodplain inundation in the spring, and the formation of side channels.

The correlation at the middle reach of Taneum Creek displayed slightly different stratigraphy, with a more incised, siltier floodplain just upstream of the bridge (Figure 15). Even though the two stratigraphic profiles are only ~150 m apart they varied in sediment composition (Figures 15 and 16). Generally, the downstream MR#1 was sandier than and not as incised as the upstream siltier MR #2. The MR#1 profile is on the incised island which formed following the bridge removal. The MR#2 profile is part of the main riverbank and likely had more time to incise than the downstream island. Given the bridge removal construction, the downstream

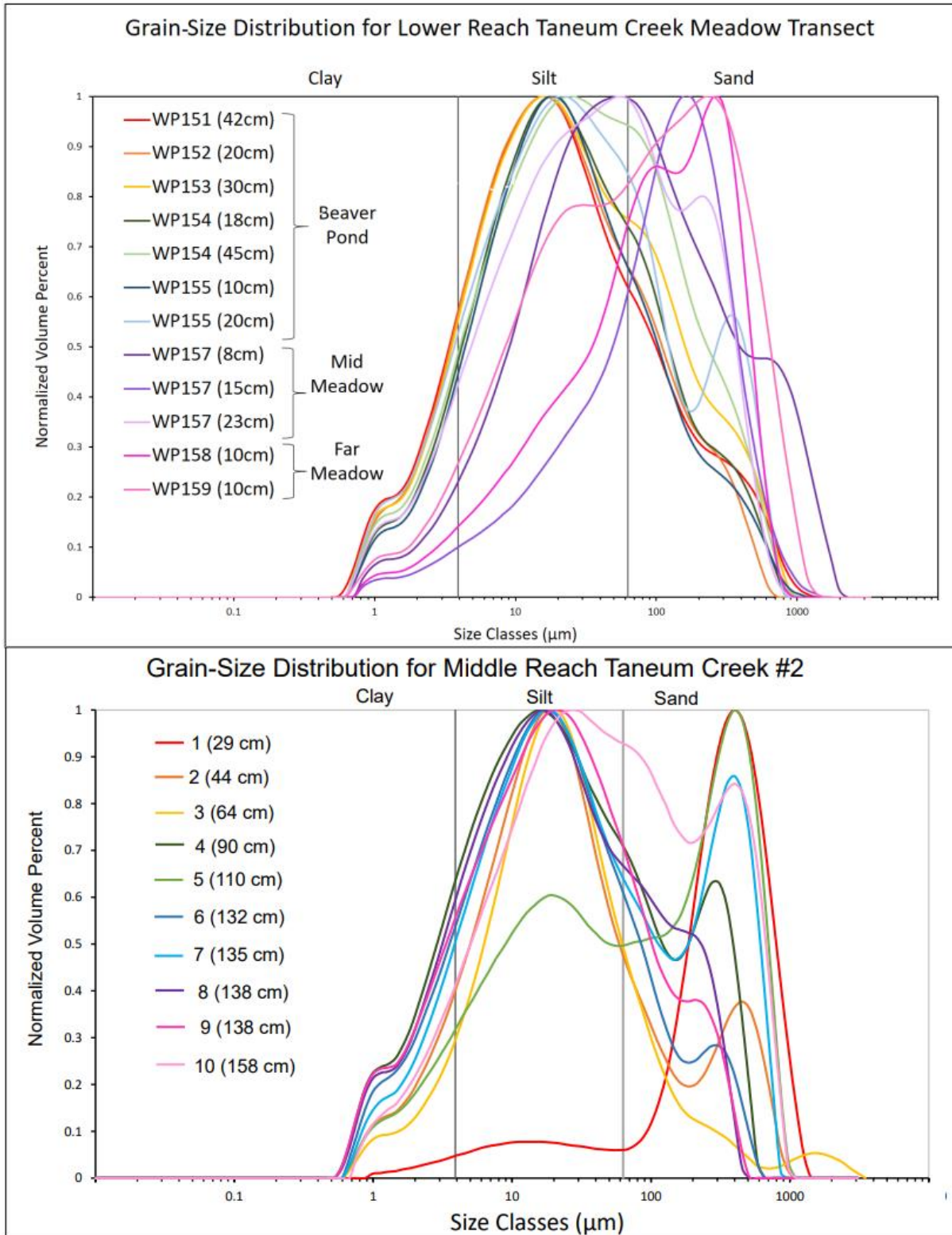


Figure 33. Taneum Creek grain-size distribution comparison. Comparison between the more unimodal lower reach (above) and bimodal middle reach (below).

stratigraphic profile could be altered but while working at this location in the field, it did not appear to be altered or mixed in any obvious way.

The bedrock at Taneum Creek is dominantly the Grande Ronde Basalt and Manastash Formation arkosic sandstone (Stearns et al., 1989; Figure 6). This is somewhat comparable to the NFT watershed Roslyn Formation sandstone and Teanaway Basalt. While the bedrock types are similar in both watersheds, the basalt at Taneum Creek is more exposed than the sandstone. Exposures of the Manastash Formation on Taneum Creek are much less frequent compared to the NFT River exposures of the Roslyn Formation sandstone where the river is actively incising into the bedrock. This could indicate less influence of the Manastash Formation sandstone on Taneum Creek floodplain sediment and more Grande Ronde Basalt influence on the floodplain sediments. While in the field for reconnaissance, I only found one exposure of the Manastash Formation sandstone (Figure 34D). The Manastash Formation borders Taneum Creek as the surface geologic unit but is covered in soil and vegetation.

Overall, the floodplain stratigraphic profiles at Taneum Creek were more variable in composition, less incised, and more heavily vegetated than the NFT watershed. This could possibly be due to the longer-established LW restoration at Taneum Creek and a slightly lower elevation than the NFT watershed. This stratigraphic investigation was conducted 15 years following the LW restoration and 12 years following the large flood that mobilized the LW. While the NFT watershed units had a strongly bimodal distribution of sand, Taneum Creek had a more variable unimodal and bimodal distribution of sediment (Figures 12 and 14). The unimodal distribution was extremely evident in the sand-dominated units and was more easily tied to

geomorphic signatures in the lower reach. An example in the Taneum Creek transect is where the samples with high percentages of sand were in dry abandoned side channels.

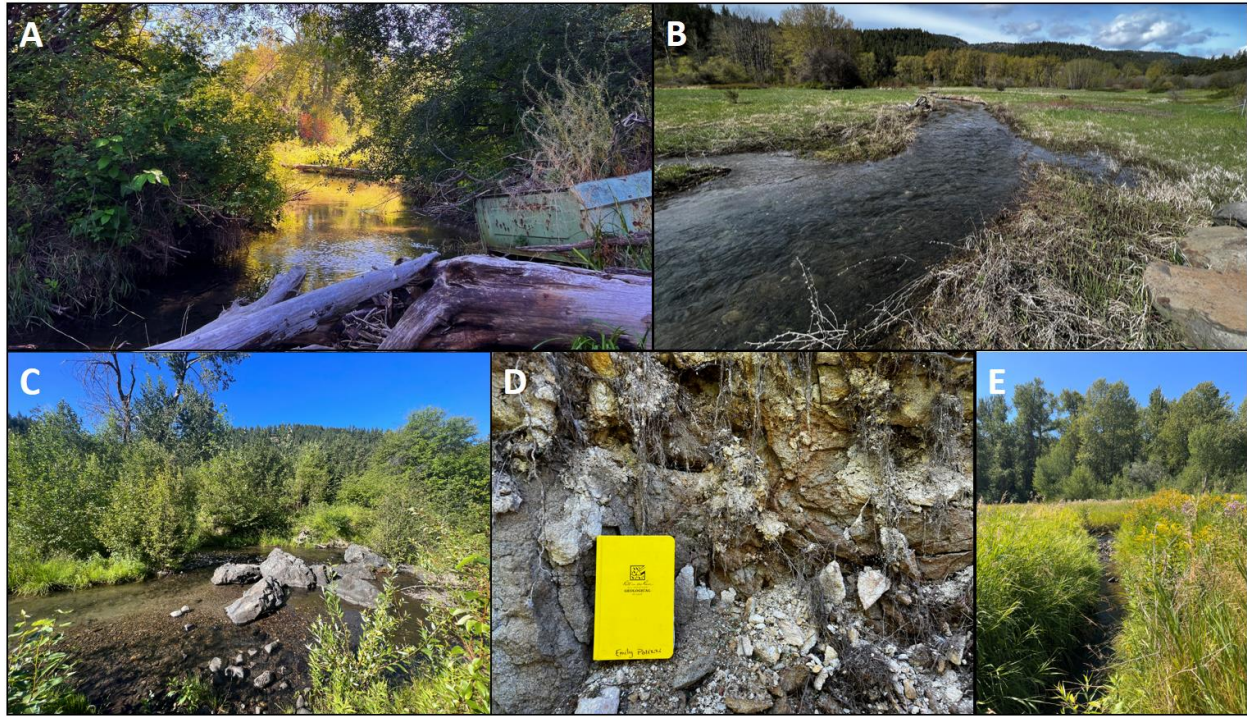


Figure 34. Taneum Creek photographs. The active side channels formed following the LW restoration in 2008 and the large flood in 2011. A) Middle reach channel with thick brush and natural LW accumulations B) lower reach flooded side channel during peak spring flow C) middle reach channel with a lush, vegetated island in background D) exposure of the Manastash Formation in the upper reach study area E) active side channel that flows through the summer.

Gray Silt

In the field, the gray silt layer behaved like clay, it was very sticky and plastic. While the gray silt was distinctive in texture and appearance in the field, it was not as distinctive in grain-size distribution (Figures 12 and 14). The gray silt blended in with surrounded silty units when plotted on a grain-size distribution graph. While it did not stand out in any obvious way, it did vary spatially in grain-size distribution and thickness across the watershed. For example, gray silt samples from the NFT watershed had a higher distribution of clay in the lower watershed samples but also a higher distribution of sand consistently. Samples from Taneum Creek had

approximately the same distribution of clay everywhere but had more silt and less sand than the NFT watershed (Figure 18). This difference in grain-size distribution between watersheds could cause a difference in the hydraulic properties of the unit and varying implications on water storage and flow.

The results of the pump tests in Taneum Creek point towards a variation in the transmissivity of the gray silt layer (Figure 20). At all four locations, the piezometer was placed ~2 m downstream of a LW accumulation knick point pool on the edge of the channel. At the three locations where the unit was more confining, the piezometer was placed on the edge of the channel. This interpretation was based on downwelling when placed in the gray silt or upwelling when placed in the gravel unit below. At one location conditions were more neutral as the water levels eventually reached equilibrium after 60 minutes. There were no geomorphic differences in the neutral vs downwelling vs upwelling locations besides their locations along the transect. The neutral location was the furthest north with the downwelling and upwelling locations slightly to the south. The lack of incision into the gray silt unit at the upper reach and the depth at which the gray silt lies across the watershed could ultimately influence the floodplain aquifer storage capacity across the reaches of Taneum Creek.

At the North Fork Teanaway River and Dickey Creek Confluence, the piezometer was placed into the downstream edge of the silt bench at the depth of the gray silt unit. The water levels stabilized immediately, indicating no significant effect on transmissivity during the pump test. This could mean the gray silt in the bench has more gravel than anticipated or we were in the wrong unit. The gray silt unit was better exposed on the channel bank slightly downstream but was in a vertical orientation, so a pump test was impossible. Another explanation for the

difference in transmissivity between the NFT River and Taneum Creek gray silts could be the higher distribution of sand in the NFT watershed and the more exposed bench morphology of the gray silt layer, especially in the lower watershed. Therefore, the gray silt is probably less likely to impede groundwater storage moving progressively upstream in the Teanaway study area.

The three samples collected from the gray silt unit on the NFT River and Indian Creek were sent for radiocarbon dating. They yielded ages ranging from 1400-4500 cal BP (Table 2), which were much younger than expected. The age of the samples was anticipated to be closer to the last glacial maximum, less than 20,000 years BP but greater than ~10,000 years BP to align with the glacial lake hypothesis (Porter, 1976). The lake would need to be present long enough to deposit a clay/silt layer ≥ 10 cm thick at Indian Creek and 90 cm thick farther downstream in the main stem Teanaway River. The lake would then need to drain, revert to a river system, and allow the deposition of 1.5 - 2 meters of floodplain sediment and the reduction of the gray silt layer. While the radiocarbon age did not come back as expected, additional testing of samples from further into the floodplain could yield an older age.

The Kittitas Drift (120 kya) is the warm period responsible for the deposition of the Swauk Prairie Moraine, hypothesized to dam the Teanaway glacial lake, and the Thorp Prairie Moraine hypothesized to dam Taneum Creek (Porter, 1976; Tabor et al., 1982). The deposition of both moraines provides the absolute maximum age for glacial lake deposition of the gray layer. In the Teanaway River watershed, Porter (1976) also found the “thick body of bluish lacustrine silt, clay, and sand” to be overlain by Lakedale Drift outwash which establishes an absolute minimum age for deposition at ~15-13.5 kya. This does not align with the 1400-4500 years BP range established through radiocarbon dating.

Several alternative scenarios could explain the relatively young radiocarbon ages in the gray silt layer. (1) The layer deposition was related to another instance of damming, higher up in the watershed. However, there was no evidence of a landslide dam found in either watershed as another, more localized possibility for the deposition of the gray silt layer. (2) The organic material found within the pre-existing gray silt layer could have possibly been reworked during a period of exposure 1400-4500 years BP via river incision. Using an auger to locate additional organic samples from the gray silt layer further into the floodplain could yield older dates. (3) It is possible that the moraine dam lasted well after the retreat of the ice, long enough to deposit the gray silt 1400-4500 years BP followed by the overlying floodplain sediment.

The modern base and peak elevations of the Swauk Prairie Moraine are 2050 and 2414 feet respectively. The gray silt layer is consistently found at an elevation of 2380-2610 feet in the NFT watershed which lies above the moraine elevation range. At the TVFF, the gray clay was recorded between 2085 ft near the channel and 2125 ft up the valley wall. While the TVFF clay does not exceed the peak moraine elevation, the Indian and Jack Creek gray silt does. It is unclear if the reduced gray silt layer is the same as the TVFF clay and if it could be from a glacial ice or moraine-dammed lake. If it were an ice dam, the elevation could have been higher than the modern moraine. If it were a moraine-dammed lake, the elevation during the Pleistocene could have been higher as well. The history of this lake could be more complex than just a layer of silt/clay depositing and then the lake draining. There could have been intermittent periods of water being released, draining, reverting to a river to rework sediment, and the cycle repeating. The radiocarbon ages determined do not necessarily make sense as a depositional age since there are 1.5-2 meters of silt and sand above the gray silt layer across the watershed. The range of

1400-4500 years BP may not be enough time to deposit this much sediment on top of the reduced gray silt layer.

In the NFT watershed, the mottling consistent through the bottom half of each stratigraphic profile and particularly in the gray silt layer indicates periodic wetting and drying (Figure 19). The splotchy pattern of the mottling highlights the difference between the coarser pockets of sediment which are orange from oxidation and the finer pockets which are gray from reduction. This means that as the water table level fluctuates, there is preferential flow of the groundwater through these coarser sediment conduits. The water moves through the unit then, during the period of drying the coarser conduits lose water and dry out more quickly than the finer material which hold on to the water and continues reducing. This implies the unit is transmitting groundwater, however ineffective it may be. One potential explanation for this mottled layer could be the erosion and mixing of the “original” gray silt layer with other inflowing stream sediments as the glacial lake water levels declined.

The relatively small percentage of clay to silt and sand means the gray silt layer may not impede the flow of water as much as previously hypothesized. If this layer did happen to operate as a confining layer it might be beneficial from a water storage perspective. If the water being diverted onto the floodplain by LW slowly infiltrates, it may be slowed down by the fine layers and released more slowly during the rest of the year. However, where sand increases with stratigraphic depth, it may mean more rapid water transmission. While the gray silt layer has more sand than originally thought, it is resistant and sticky enough to form benches as seen in the North Fork Teanaway River at the Dickey Creek and Indian Creek confluences. Along parts of Indian Creek, it forms the stream bed and there is a small knick point where water falls over the

unit, incising into it. This resistance to erosion is unique in this layer and present across the North Fork Teanaway River watershed.

Floodplain Area

Overall, both the geomorphic mapping and REM methods were successful in isolating the floodplain area in the watersheds. I anticipated that the REM-derived floodplain would be larger than the geomorphic mapped floodplain, due to the nature of the tools used to construct the model and the contextual limitations of the process. The geomorphic mapping allowed more control over the delineation of active floodplain vs incised floodplain based on the geomorphic context of the area (Figure 23). As an example, in the NFT watershed, I was able to manually make the distinction between the active floodplain consisting of boulder bars and the incised floodplain using satellite imagery. This could not be as accurately distinguished in the REM, because the only factor considered by the software is the elevation of a specific pixel, not what part of the river that pixel represents. There was also some unavoidable overlap of the separate REMS created for each tributary where they flowed into the main stem (Figure 24). This overlap was minimal and while I did my best to adjust the geomorphic map accordingly, it could account for some of the difference in my final area values.

Another REM limitation was the seam between DEM files used to construct the REMs. In the process of generating the REM the upstream and downstream ends of the river become skewed. When there are multiple DEM files next to each other this creates an obvious seam between the two adjacent files (Figure 25). In the generation of the REM, no matter the number of DEM files in the area you must create the REMs separately. As a result, the seam between the two files was obvious due to the skewing and they do not match well. One way to

make them appear to match is to change the symbology and break up colors based on elevations that depict continuity between the two files. This however would vastly change the floodplain area values generated by the REM when extracting specific elevation ranges.

The selection of the elevation range to depict the REM incised floodplain was based on how well a chosen range fits within the incised floodplain unit that was created during the geomorphic mapping. This involved trial and error to find the elevation range above the thalweg that best matched the geomorphic incised floodplain. This trial and error also considered the geomorphic context of the river. For example, the elevation range for the upper NFT River was 1.5 – 3 meters above the channel. Starting the range at 1.5 meters instead of 0 meters ensured the boulder-dominated active floodplain was not being added to the incised floodplain area. When choosing an elevation range for Indian Creek, 0 - 1.8 meters was most successful in capturing the incised floodplain. To compare the results of both methods, the geomorphic incised floodplain was overlain on the REM-derived incised floodplain to better visualize the similarities and differences (Figure 26). While the two methods do not match perfectly, they are displaying the same general areas designated as incised floodplains by the geomorphic map. The tributaries were better suited for this method because there was no active floodplain to consider when choosing elevation ranges.

At Taneum Creek the canyon narrows, eliminating the geomorphic signature of the terrace and leaving only the floodplain adjacent to the channel sandwiched between the valley walls (Figure 27). At Taneum Creek, because there were no tributaries to create REMs for, there was also no overlap to account for (Figure 28). However, due to where the DEM files meet near the KRD irrigation canal, there were areas of the floodplain that could not be included in the

REM map (Figure 28). At this location, the same issue with upstream and downstream skewing existed. The floodplain was extracted from the REM based on how well the chosen elevation matched the mapped geomorphic floodplain (Figure 29). An elevation range of 0 – 8 feet was chosen for Taneum Creek upstream of the KRD irrigation canal, and 0 – 10 feet downstream of the KRD irrigation canal. The overlap at Taneum Creek visually appeared to be a better match than in the NFT River but the percent difference between the REM and mapped floodplain areas for the two watersheds was very close (NFT Watershed 12.7%; Taneum Creek 11.8%; Figure 30).

Overall, the REM method produced better results in the smaller tributaries than on the main channel of the NFT River. This could be due to the increased complexity of the main channel and the much wider floodplain than in the tributaries. The REM method performed well at Taneum Creek possibly because it was a narrower channel and more comparable to the NFT tributaries proportionally. The only complication on Taneum Creek was the floodplain area excluded due to no DEM coverage. However, this did not result in a significant difference in the final area values. Considering the two methods, I think the geomorphic mapping yielded more accurate values for floodplain area and subsequent volume. While the values yielded by both methods were relatively similar, the REM values were usually higher, except in the case of Jack Creek and Indian Creek. The floodplain area results at Taneum Creek yielded a similar total acreage value to the combined NFT River and tributaries (Tables 3 and 4). The REM value for Taneum Creek also followed the same tendency in the NFT watershed of being slightly larger than the geomorphic mapping area. The contextual explanation for this in the NFT holds true for Taneum.

Floodplain Aquifer Volume

Previous studies by Dickerson-Lange and Abbe (2019) calculated floodplain aquifer volume for the lower North Fork Teanaway River under varying scenarios of incision and a sandy loam subsurface. Their total subsurface storage values for the lower NFT River did not include the tributaries so they were excluded from the comparison (Table 7). In this study, the volume for the North Fork Teanaway Watershed, was calculated using the area from the geomorphic mapping method, a minimum and maximum thickness and a minimum and maximum porosity. It should be noted that while a higher porosity results in a higher volume, the permeability of the floodplain will be lower. More void space is available to water but that void space is harder to fill. These calculations serve as endmember estimates for storage under varying conditions.

Table 7. Potential aquifer storage capacity comparison. Comparison between Polizzi (2023) methods and Dickerson-Lange and Abbe (2019) calculated estimates of potential storage capacity in the North Fork Teanaway River floodplain aquifer.

| Study | Floodplain Description | Thickness (feet) | Area (acres) | Volume ac-ft (m³) Minimum Porosity (0.3) | Volume ac-ft (m³) Maximum Porosity (0.38) |
|---|-------------------------------|-------------------------|---------------------|--|---|
| Polizzi, 2023 Geomorphic Mapping Method | A | 3 | 506 | 455 (561,000) | 576 (710,000) |
| | B | 2.1 | 298 | 188 (232,000) | 238 (294,000) |
| | C | 6.6 | 298 | 591 (729,000) | 749 (924,000) |
| Polizzi, 2023 REM Method | B | 2.1 | 363 | 229 (282,000) | 290 (358,000) |
| | C | 6.6 | 363 | 720 (888,000) | 911 (1,120,000) |
| Dickerson-Lange & Abbe, 2019 Model | minimum | 3 | - | 368 (454,000) | - |
| | median | 6 | - | 919 (1,130,000) | - |
| | maximum | 9 | - | 1470 (1,810,000) | - |

A = Active floodplain area, B = Incised floodplain area (excluding stratigraphic profile zones 1 & 3), C = Incised floodplain area (entire stratigraphic profile thickness). All values are rounded to three significant figures. Total volume is not included in this table.

The active floodplain area is regularly inundated today compared to the incised floodplain which is too high above the channel bed to be inundated. The active floodplain volumes serve as an absolute minimum and represent the capacity of the active floodplain as delineated during geomorphic mapping with a depth of 3 ft. These values are likely larger than the real active floodplain storage capacity. The topography of the active floodplain varies and the grain-size distribution ranges from boulders to fine sand and silt. As a result, the stratigraphy and depth of the active floodplain varies greatly across the watershed and the large distribution of grain sizes likely fills in a lot of the void space making it unavailable to water storage. Regardless, the active floodplain volume is included in the total volume for the NFT watershed in Table 5. It is important to include active floodplain volume because that is the area currently being inundated at peak flow.

In this study, NFT River volumes for the incised floodplain, were less than the estimates of Dickerson-Lange and Abbe (2019). Some difference in estimates between studies can be attributed to different methods of volume calculation. The volume calculation for this study was determined with a simplified equation of

$$V = A \times h \times \phi$$

where V is volume, A is area of the floodplain, h is the height/thickness of the floodplain, and ϕ is the porosity. Dickerson-Lange and Abbe (2019) used a more extensive model which incorporated different geometric and hydraulic parameters including valley bottom delineation, width, depth, gradient, incision depth, specific yield, and saturated hydraulic conductivity of the alluvial aquifer. Future research could involve refining the model by Dickerson-Lange and Abbe

(2019) with new specific yield values based on the stratigraphic profiles collected during this study.

Dickerson-Lange and Abbe (2019) did not elaborate on their floodplain area designations and calculation methods in their publication. Some potential difference in the active floodplain volumes could stem from different geomorphic designations and area calculation methods. In my methods the active floodplain area was specifically delineated using geomorphic mapping and did not include the incised floodplain area. Their methods may have used the same area in the incised floodplain model just with a 3 feet depth instead of 6 or 9 feet. So, instead of calculating the volume of the active floodplain, they calculated the volume of whatever terrain was 3 feet above the channel.

In my calculation of the incised floodplain minimum and maximum volumes, I based the thickness on what I observed in the field and in my grain-size distribution results. Instead of a 9 ft maximum, I used a 6.6 ft maximum because I found it best represented the stratigraphic profile depths I observed in the field (from channel bed to incised floodplain surface). When calculating the incised floodplain minimum volume, I found a 2.1 ft thickness was the most representative. To come to this conclusion, I compared the grain-size distribution results from each unit. The gray silt found in Zone 3 and the clayey silt found in Zone 1 were very similar in grain-size distribution so they both needed to be excluded to calculate a consistent volume based on the incised floodplain stratigraphy (Figure 31). This minimum volume calculation assumes storage of water in Zones 2 & 4 only. Due to the separation of the excluded zones (1 & 3) within the stratigraphic profile, further research is needed to evaluate the effects of each zone on

transmissivity. If water cannot move through Zones 1&3 from the surface, then it cannot be stored in Zones 2 &4.

When the NFT tributaries were added to the NFT River volume, the total volume nearly doubled (Table 5). The tributaries are as deeply incised as the NFT River but not as wide, so a lot of floodplain area is available for water storage. Whether or not the entire floodplain area could be inundated is uncertain. More channel aggradation is needed to raise the river water level and inundate all portions of the floodplain. Once this area is inundated, the permeability of the units should be considered to determine how easily water can transmit through the floodplain. The units closer to the surface of the floodplain have less sand than the underlying units making them less permeable. Spatial variation of these units is common and water could potentially travel through sand lenses as conduits to more effectively transmit through the floodplain.

Taneum Creek did not have any previous floodplain aquifer volume studies to compare to, but there is less storage available than in the NFT watershed. While there may be less volume available for water storage, less incision, increased channel complexity, and the existence of active side channels could mean a higher likelihood of floodplain inundation. One potential disruption to this storage is the increased vegetation due to the floodplain inundation. The healthier and more abundant the vegetation is, the more groundwater the plants will require. This means the permeability of surface floodplain units is an important consideration in terms of evapotranspiration. Sandy units at the top of the floodplain would be more conducive to groundwater infiltration than fine-grained silt which would impede surface water infiltration. At the Middle Reach of Taneum Creek, the top stratigraphic units are higher in sand content than the underlying units. This means the surface water will have a much easier time infiltrating the

floodplain (Figure 15). At the lower reach of Taneum Creek, the shallow floodplain stratigraphy varies across the floodplain with the beaver pond area having more silt near the surface and the mid and far meadow having more sand near the surface (Figure 17). As demonstrated by the beavers, the silty surface layers are less permeable and do not allow water to transmit through into the subsurface for storage. A calculation of evapotranspiration rates could contribute to a more complete water budget for this area.

While Taneum Creek and the North Fork Teanaway Watershed yield similar area values, the floodplain aquifer storage potentials are different (Tables 5 and 6). This is likely due to the deeper incision of the floodplain in the NFT watershed than at Taneum Creek. The 15-year established LW restoration and mobilization from the flood differentiates Taneum Creek from the more incised NFT watershed and leaves less floodplain depth available for potential water storage. Even though the NFT watershed has a higher potential aquifer storage capacity, it requires time and an increased sediment supply to aggrade the channel bed and inundate the incised floodplain to utilize the storage. Incised channels have increased hydraulic gradients between the floodplain and the channel because they are so disconnected. This means any water that inundates the floodplain now, will quickly flow into the channel instead of being stored seasonally.

To accomplish the floodplain water storage goal associated with the LW restoration in the NFT watershed, additional sediment is required to accumulate in the channel to reconnect it to the incised floodplain. The question to ask is where will this sediment come from? Some of the sediment that was occupying the channel beds prior to logging practices was transported downstream long ago (Collins et al., 2016; Schanz et al., 2019). The headwaters of the NFT

River, immediately upstream of the study area, flow through the more deeply incised Teanaway basalt bedrock canyon. The current degree to which the NFT River and tributaries are incised, led to a reasonable estimation that anywhere between 1.5 to 2 meters of aggradation may be required to reconnect the floodplain and channel enough to allow inundation during peak flow and seasonal water storage in the shallow floodplain aquifers.

One source of this sediment could be from an increase in mass wasting in post-wildfire environments. A study by Halofsky et al. (2020), projected longer fire seasons due to warmer and drier condition in the eastern Cascades which will likely increase frequency and extent of fires compared to the 20th Century. With shifting precipitation patterns on the eastern slopes of the Cascades and increased frequency and intensity of forest fires it is possible that post wildfire mass wasting events could contribute to the North Fork Teanaway River watershed.

Large wood is recognized to have geomorphological effects on river channels by decreasing river velocity, thereby decreasing energy available to transport sediment and increasing sediment storage (Montgomery et al., 2003). Some studies that investigated sediment storage in association with large wood found a significant increase in annual sediment yield (Megahan and Nowlin, 1976; Swanson et al., 1976; Mosley, 1981; Hogan, 1986). The caveat associated with LW decreasing sediment transport is the width of the channel. The LW is most successful in small channels (<15 m wide) and less successful in larger channels (>30 m wide) because the wood does not span enough of the channel width to slow water velocity (Keller and Swanson, 1979; Abbe and Montgomery, 1996). The North Fork Teanaway River lies within the intermediate range (15-30 m) therefore, the LW has an intermediate effect on sediment storage. The NFT tributaries are much narrower than the NFT River so LW restoration will likely have a

more significant impact on those streams. It should be considered, that if the NFT River cannot keep up with the aggradation in the tributaries, the difference in base level could trigger tributary incision and consequentially decrease sediment storage. So, LW restoration can aid in the aggradation process but probably not on a timescale that is conducive to promoting immediate floodplain aquifer storage solutions. Regardless of the amount of storage available in the NFT watershed and how available it is for immediate use, this research can be applied in other watersheds that may be more conducive to seasonal floodplain aquifer storage.

CHAPTER VI

CONCLUSION

When calculating the aquifer capacity of a river floodplain, the stratigraphy is an important aspect to consider. The floodplain sediment composition plays a key role in how water will be transmitted and stored in the aquifer. A range of possible storage capacity estimates were calculated based on the stratigraphy at individual locations in the watershed and the interpretation of the porosity and permeability of the different stratigraphic units. The thickness, arrangement, and grain-size distribution in stratigraphic units, aid in calculating floodplain aquifer storage capacity by setting minimum and maximum endmembers for storage conditions.

In the NFT watershed the thickness of the clayey silt zone and gray silt zone (1&3) were excluded from the minimum storage capacity calculations for the incised floodplain to account for the probability that these layers would limit the aquifer storage capacity (Figure 31; Table 7). The maximum endmember does not exclude any zones from aquifer volume and represents the entire depth of the incised floodplain from surface to channel bed (Table 7). The location of the clayey silt zone at the top of the stratigraphic profiles may impede surface infiltration in some areas. The active floodplain on the NFT River, represents the area that is regularly inundated compared to the disconnected incised floodplain (Table 7). The real capacity is likely smaller due to the unsorted nature of sediments that comprise the active floodplain and variability in topography. The disparity between the Dickerson-Lange and Abbe (2019) minimum volume and my active floodplain minimum volume is likely attributed to different methods for area delineation and calculation and volume calculation (Table 7). The difference in volumes for the

Dickerson-Lange and Abbe (2019) median and my incised floodplain maximum are likely attributed to difference in area used to calculate the volume (Table 7).

Regarding the gray silt layer in the North Fork Teanaway watershed, it may not impede groundwater storage and flow due to the low clay content. Pump tests found the layer is not confining at the North Fork Teanaway River and Dickey Creek confluence where the gray silt layer is the most clay rich. Radiocarbon dates from the gray silt layer in the NFT watershed do not align with a glacial lake deposition hypothesis but the existence of the gray silt in both watersheds, suggests a more regional cause for the deposition like glaciation. More sampling and age dating from the gray silt in the NFT watershed, main stem Teanaway River and Taneum Creek is needed to link the deposition of all three gray silt/clay layers. Regardless of the origin, the gray silt in the NFT watershed and Taneum Creek may not impede groundwater storage and flow. The presence of coarser grained lenses and the relatively high sand and low clay content of the silt do not make it a completely confining unit.

While the potential aquifer storage capacity at Taneum Creek is lower than the NFT watershed, the channel is less incised making it more likely to be inundated. Taneum Creek has more channel complexity to increase interaction with the floodplain. Considering the pump tests pointed towards the gray silt being confining to the underlying gravel, it may be more of a barrier to flow in Taneum Creek than in the NFT watershed. This could have implications for water storage and flow whether they be beneficial or detrimental. It could help store water more effectively while river levels are high and slowly release it as the summer water levels fall. Water is moving faster through the gray silt in some locations and the spatial variability could

allow transmission through the coarser grained pockets. Regardless, modern Taneum Creek is much more conducive to seasonal groundwater storage than modern NFT watershed.

While LW restoration is very important in terms of ecosystem health, it is not always the immediate solution for seasonal floodplain aquifer storage. In the NFT watershed, the anthropogenic incision of the channel will require more time and sediment to bring this watershed back to natural floodplain connectivity. Though we may not see a fully restored NFT River in our lifetimes we can have hope that future inhabitants of the Upper Yakima River Basin will share our dedication in promoting the health of this resource and protecting the natural beauty of the area. Future endeavors to increase shallow floodplain aquifer storage capacity look to manually inundate river floodplains in the Yakima River Basin in efforts to increase seasonal storage of water, lower instream temperatures, and increase instream flow in the late summer for aquatic life.

REFERENCES

- Abbe, T., Dickerson-Lange, S., and French, D., Natural Systems Design, 2021, Geomorphic Assessment & Restoration Prioritization Report Middle & West Fork Teanaway Rivers in areas within the Teanaway Community Forest, p. 91.
- Abbe, T. B., and Montgomery, D. R., 1996, Large woody debris jams, channel hydraulics and habitat formation in large rivers. *Regulated Rivers: research & management*, v. 12, p. 201-221.
- Bartlett, S., 2022, Assessing the effects of instream large wood on floodplain aquifer recharge and storage at Indian Creek, Kittitas County, Washington, USA [M.S. thesis]: Central Washington University.
- Blakely, R. J., Sherrod, B. L., Weaver, C. S., Wells, R. E., Rohay, A. C., Barnett, E. A., and Knepprath, N. E., 2011, Connecting the Yakima fold and thrust belt to active faults in the Puget Lowland, Washington. *Journal of Geophysical Research: Solid Earth*, 116(B7).
- Boylan, N. C., 2019, Assessing the link between large wood restoration and groundwater recharge and storage: an investigation of Indian Creek in Washington State [M.S. thesis]: Oregon State University.
- Collins, B. D., Montgomery, D. R., Fetherston, K. L., and Abbe, T. B., 2012, The floodplain large-wood cycle hypothesis: A mechanism for the physical and biotic structuring of temperate forested alluvial valleys in the North Pacific coastal ecoregion. *Geomorphology*, v. 139, p. 460-470.
- Collins, B. D., Montgomery, D. R., Schanz, S. A., and Larsen, I. J., 2016, Rates and mechanisms of bedrock incision and Strath Terrace Formation in a forested catchment, Cascade Range, Washington. *Geological Society of America Bulletin*, 128(5-6), 926–943. <https://doi.org/10.1130/b31340.1>
- Dickerson-Lange, S., and Abbe, T., Natural Systems Design, 2019, Potential for Restoration of Alluvial Water Storage in the Teanaway River Watershed, The Nature Conservancy, p. 1-40.
- Dilts, T. E., Yang, J., and Weisberg, P. J., 2010, Mapping riparian vegetation with lidar data predicting plant community distribution using height above river and flood height: ArcUser Online.
- Fixler, S. A., 2022, Decadal-scale effects of large wood restoration on channel morphology and groundwater connectivity, Taneum Creek, WA [M.S. thesis]: Central Washington University.
- The Frederick Krueger Collection, 1920, Central Washington University Library Archives, <https://digitalcommons.cwu.edu/frederickkrueger/>.

- Gendaszek, A.S., Ely, D.M., Hinkle, S.R., Kahle, S.C., and Welch, W.B., 2014, Hydrogeologic framework and groundwater/surface-water interactions of the upper Yakima River Basin, Kittitas County, central Washington: U.S. Geological Survey Scientific Investigations Report 2014 5119, 66 p., <http://dx.doi.org/10.3133/sir20145119>.
- Halofsky, J. E., Peterson, D. L., and Harvey, B. J., 2020, Changing wildfire, changing forests: the effects of climate change on fire regimes and vegetation in the Pacific Northwest, USA, *Fire Ecology*, v. 16, p. 1-26.
- Hogan, D. L., 1986, Channel morphology of unlogged, logged, and debris torrented streams in the Queen Charlotte Islands. Ministry of Forests and Lands.
- Keller, E. A., and Swanson, F. J., 1979, Effects of large organic material on channel form and fluvial processes, *Earth surface processes*, v. 4, p. 361-380.
- Mantua, N., Tohver, I., and Hamlet, A., 2010, Climate change impacts on streamflow extremes and summertime stream temperature and their possible consequences for freshwater salmon habitat in Washington State: *Climatic Change*, v. 102, p. 187–223, doi: 10.1007/s10584-010-9845-2.
- Megahan, W. F., & Nowlin, R. A., 1976, Sediment storage in channels draining small forested watersheds in the mountains of central Idaho, *PB US Natl Tech Inf Serv*.
- Montgomery, D. R., Collins, B. D., Buffington, J. M., and Abbe, T. B., 2003, Geomorphic effects of wood in rivers. In *American Fisheries Society Symposium*, v. 37, p. 21-47.
- Mosley, M. P. (1981). The influence of organic debris on channel morphology and bedload transport in a New Zealand forest stream, *Earth Surface Processes and Landforms*, v. 6, p. 571-579.
- Olson, P. L., Legg, N. T., Abbe, T. B., Reinhart, M. A., and Radloff, J. K., 2014, A Methodology for Delineating Planning-Level Channel Migration Zones, No. 14-06-025, Washington State Dept. of Ecology, p. 56-63.
- Petralia, J., 2022, The Effects of Channel Incision and Land Use on Surface-Water/Groundwater Interactions in the Teanaway River Basin, Washington, USA [M.S. thesis]: Central Washington University.
- Porter, S. C., 1965, Day 5, in Schultz, C. B., and Smith, H.T.U., eds., *Guidebook for Field Conference J — Pacific Northwest: INQUA Cong.*, 7th, Boulder, Colo., p. 35-37.
- Porter, S.C., 1976, Pleistocene glaciation in the southern part of the North Cascade Range, *Washington: Geological Society of America Bulletin*, v. 87, p. 61, doi:10.1130/0016-7606(1976)87<61:PGITSP>2.0.CO;2.

- Roni, P., Beechie, T., Pess, G. and Hanson, K., 2015, Wood placement in river restoration: fact, fiction, and future direction. *Canadian Journal of Fisheries and Aquatic Sciences*, no. 3, p. 466-478.
- Russell, I.C., 2016, *Rivers of North America*: Creative Media Partners, LLC.
- Schanz, S.A., Montgomery, D.R., and Collins, B.D., 2019, Anthropogenic strath terrace formation caused by reduced sediment retention: *Proceedings of the National Academy of Sciences*, v. 116, p. 8734–8739, doi: 10.1073/pnas.1814627116.
- Stearns, J. A., Wagner, H.C., and Batatian, D.L., STATE OF WASHINGTON DEPARTMENT OF NATURAL RESOURCES Boyle, B.J., Commissioner of Public Lands, Diss. Washington State University Pullman, Washington, 1983.
- Swanson, F. J., Lienkaemper, G. W., & Sedell, J. R., 1976, History, physical effects, and management implications of large organic debris in western Oregon streams, v. 56, Department of Agriculture, Forest Service, Pacific Northwest Forest and Range Experiment Station.
- Tabor, R. W., Waitt, R. B., Frizzell, V. A., Swanson, D. A., Byerly, G. R., & Bentley, R. D. (1982). Geologic map of the Wenatchee 1:100,000 quadrangle, Central Washington. map, Reston, VA; The United States Geologic Survey.
- U.S. Department of the Interior Bureau of Reclamation Pacific Northwest Region and State of Washington Department of Ecology Central Regional Office, 2012, Yakima River Basin Integrated Water Resource Management Plan Final Programmatic Environmental Impact Statement BENTON, KITTITAS, KLICKITAT AND YAKIMA COUNTIES, Ecological Publication Number: 12-12-002:
<https://www.usbr.gov/pn/programs/yrbwep/reports/FPEIS/fpeis.pdf>, (accessed March 2023).
- Waitt, R. B., 1979, Late Cenozoic deposits, landforms, stratigraphy, and tectonism in Kittitas Valley, Washington, No. 1127, US Govt. Print. Off.
- YBIP, Yakima Basin Integrated Plan, 2021, <https://yakimabasinintegratedplan.org/> (accessed December 2021)

APPENDICES

Appendix A - Stratigraphic Profiles

North Fork Teanaway River and Dickey Creek Confluence

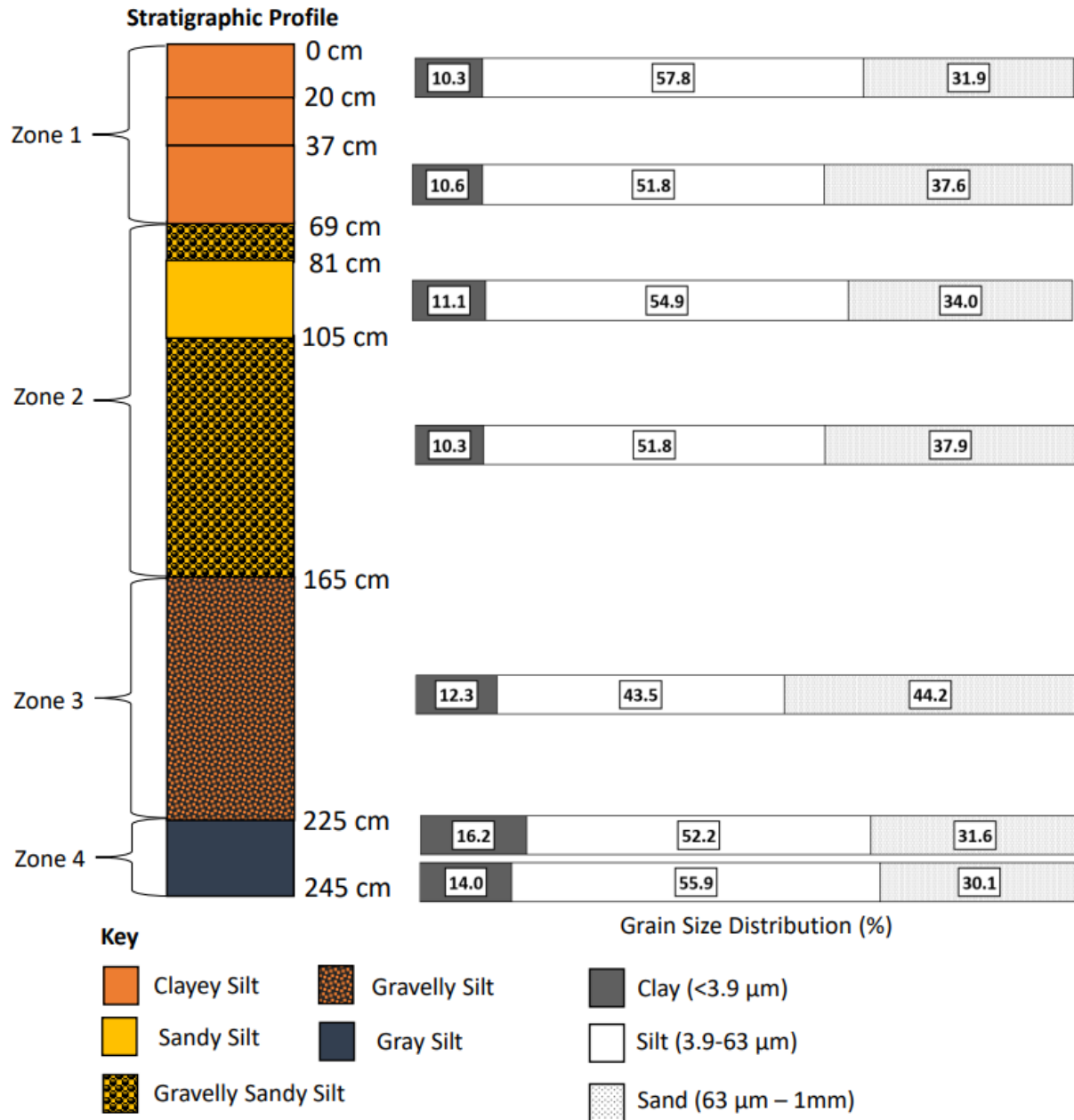


Figure A1. Stratigraphic profile and grain-size distribution bars for the North Fork Teanaway River and Dickey Creek Confluence.

North Fork Teanaway River and Indian Creek Confluence

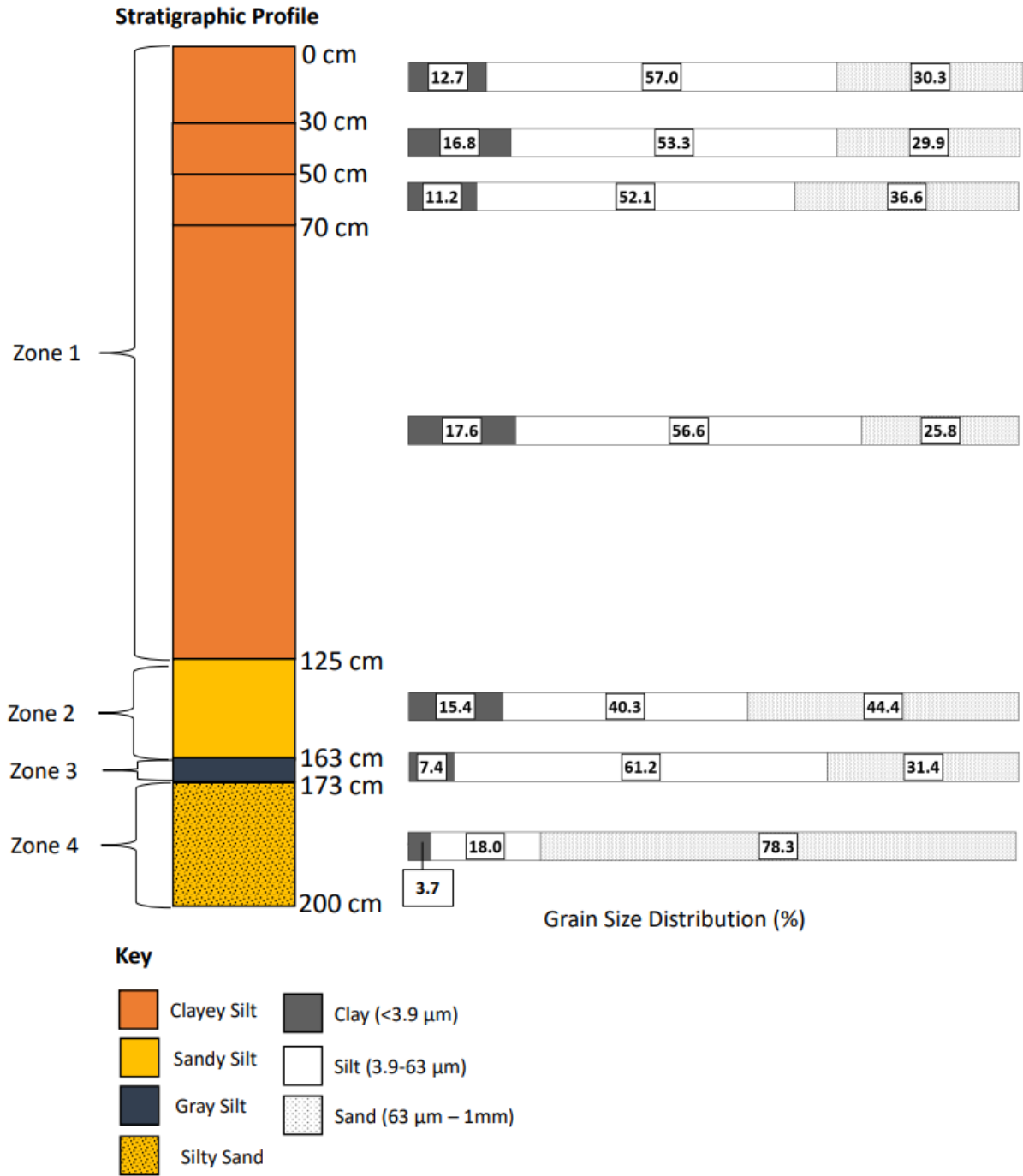


Figure A2. Stratigraphic profile and grain-size distribution bars for the North Fork Teanaway River and Indian Creek Confluence.

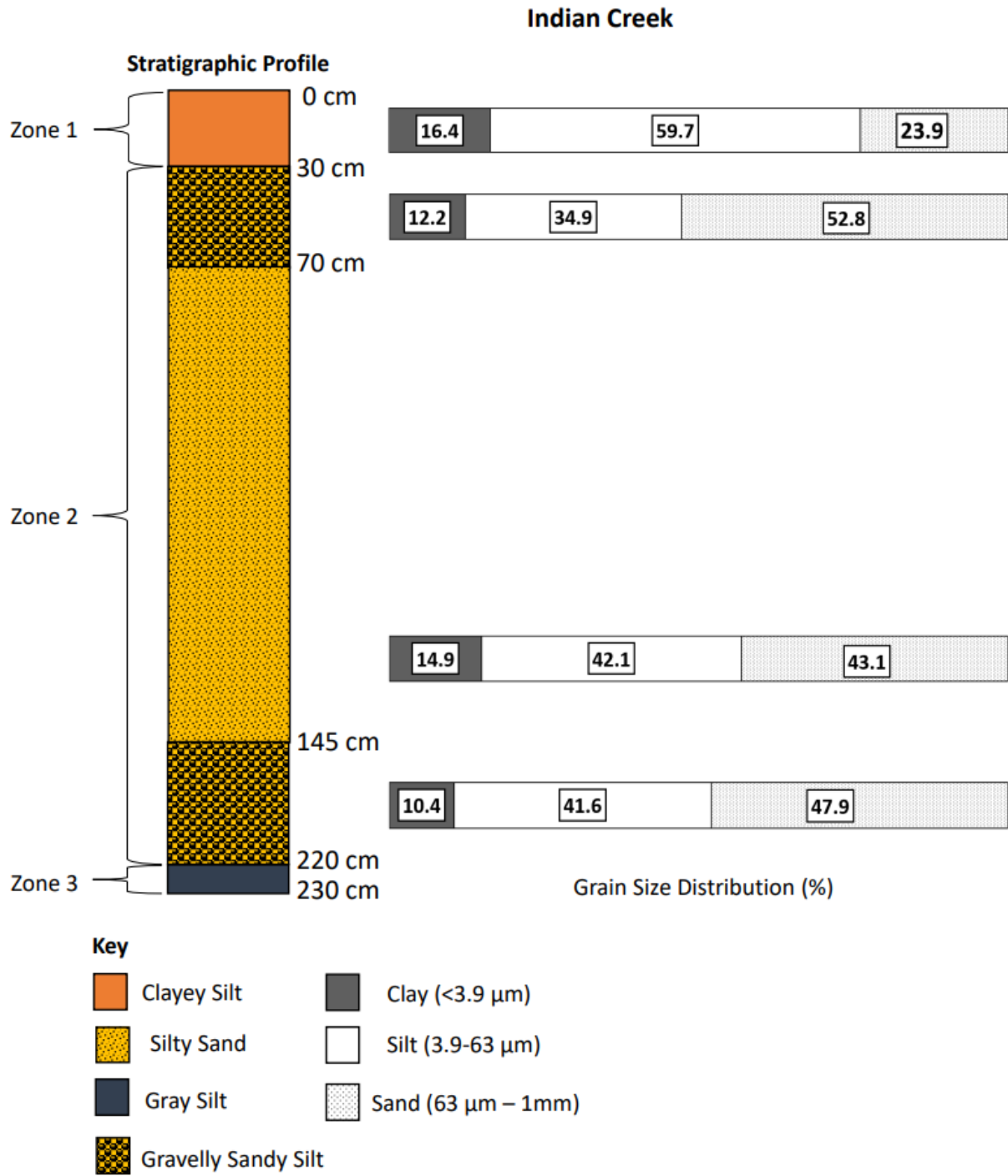


Figure A3. Stratigraphic profile and grain-size distribution bars for Indian Creek.

Jack Creek

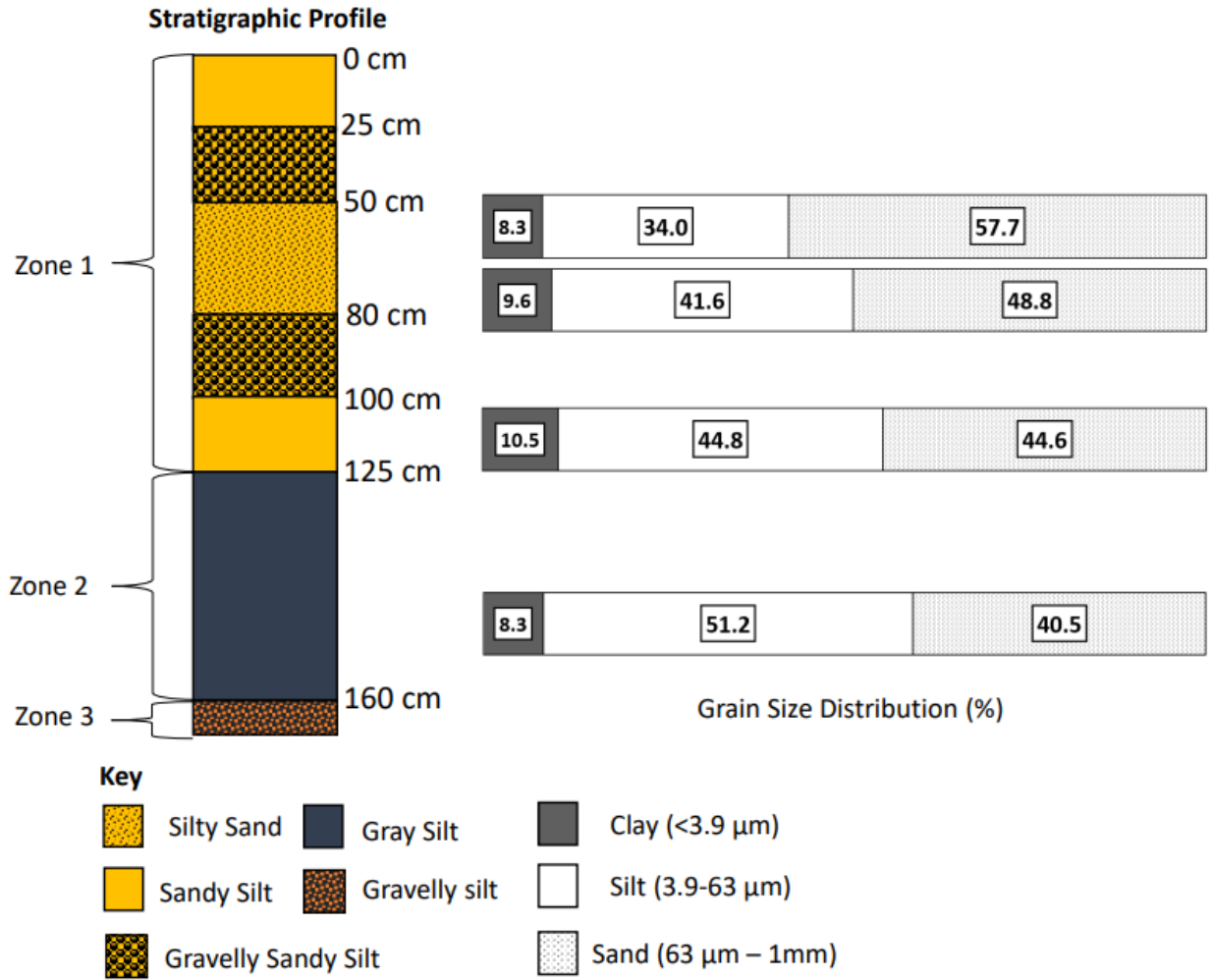


Figure A4. Stratigraphic profile and grain-size distribution bars for Jack Creek.

Middle Reach Taneum Creek #1

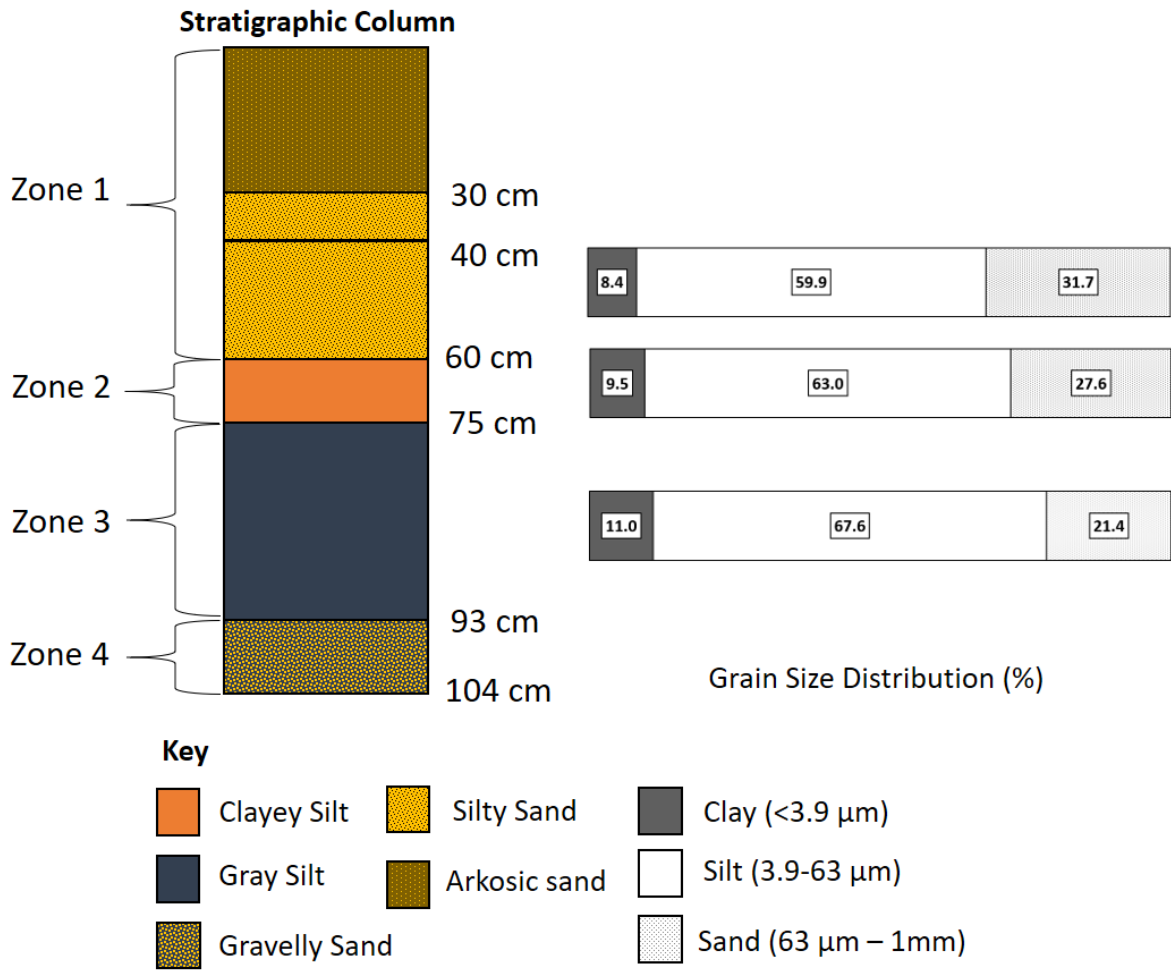


Figure A5. Stratigraphic profile and grain-size distribution bars for Middle Reach Taneum Creek #1.

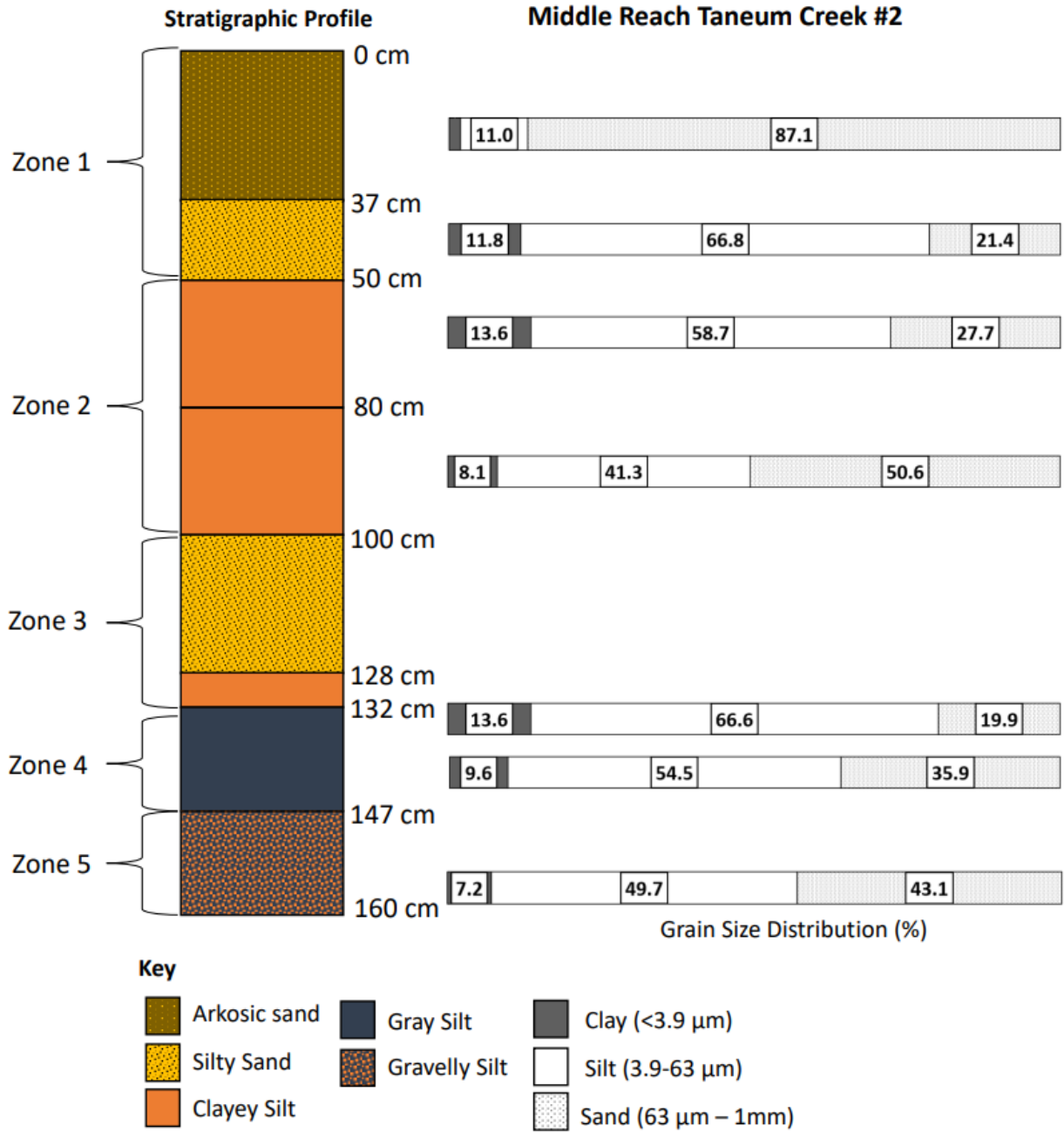


Figure A6. Stratigraphic profile and grain-size distribution bars for Middle Reach Taneum Creek #2.

Appendix B - Grain-Size Distribution Graphs

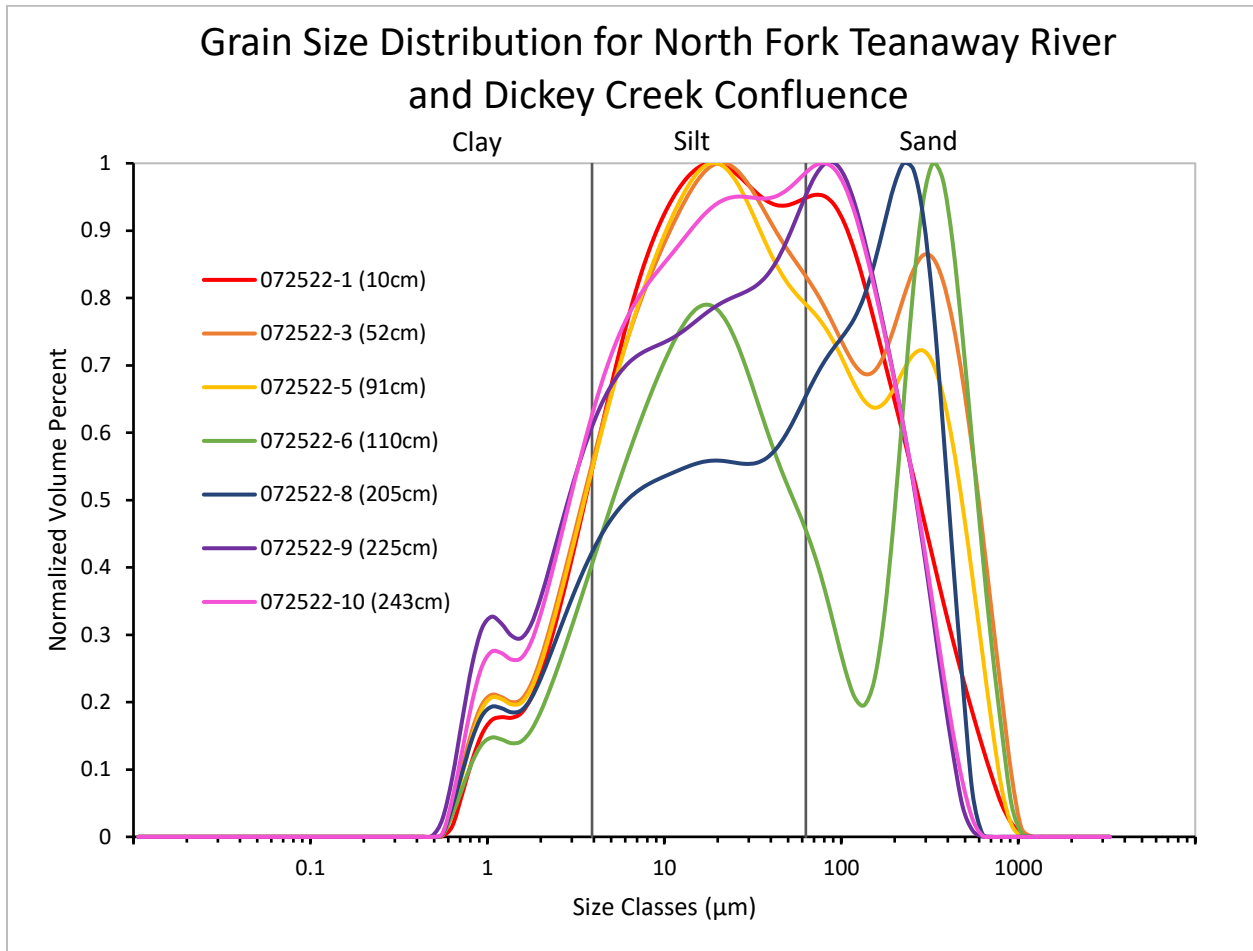


Figure B1. Grain-size distribution graph for the North Fork Teanaway River and Dickey Creek Confluence.

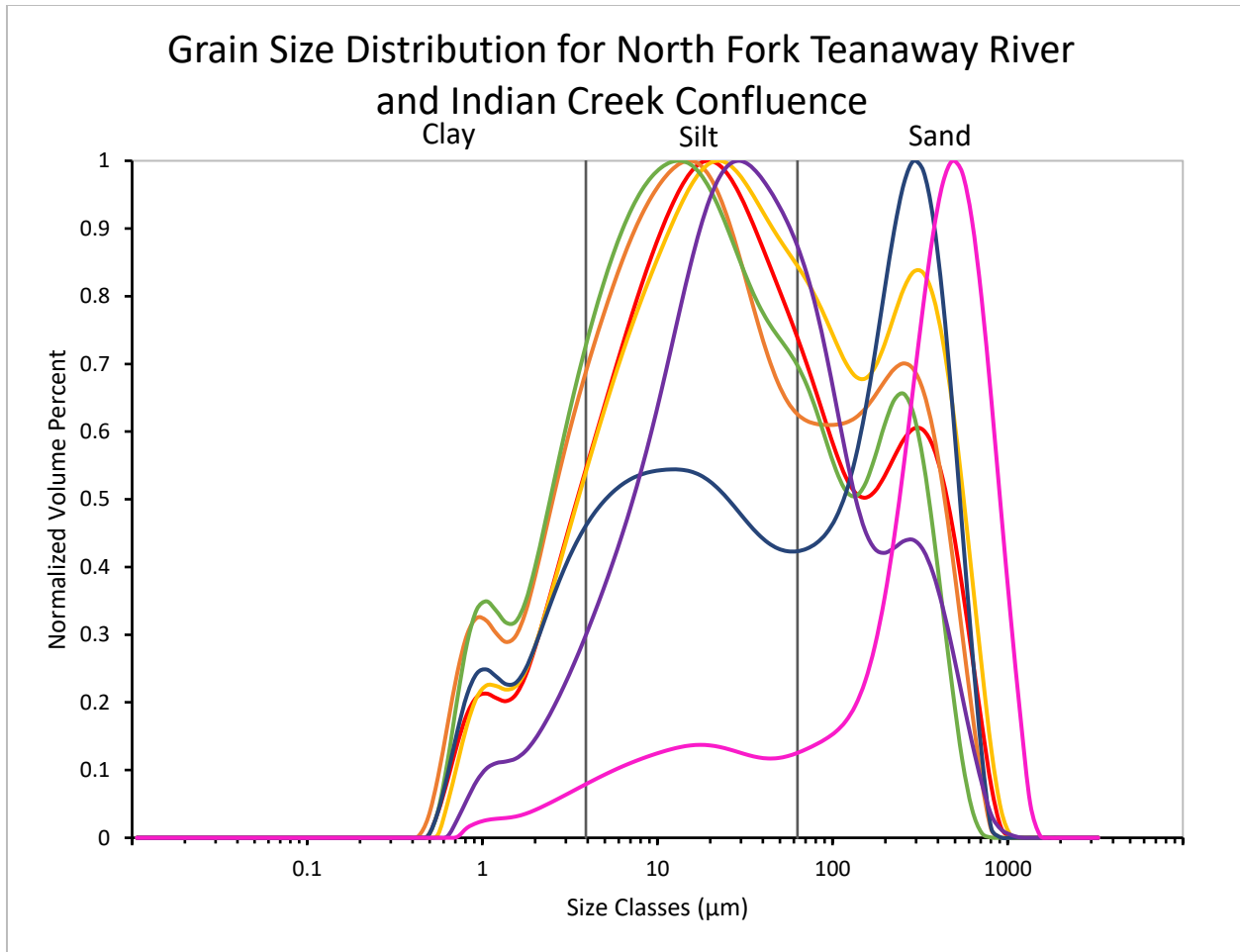


Figure B2. Grain-size distribution graph for the North Fork Teanaway River and Indian Creek Confluence.

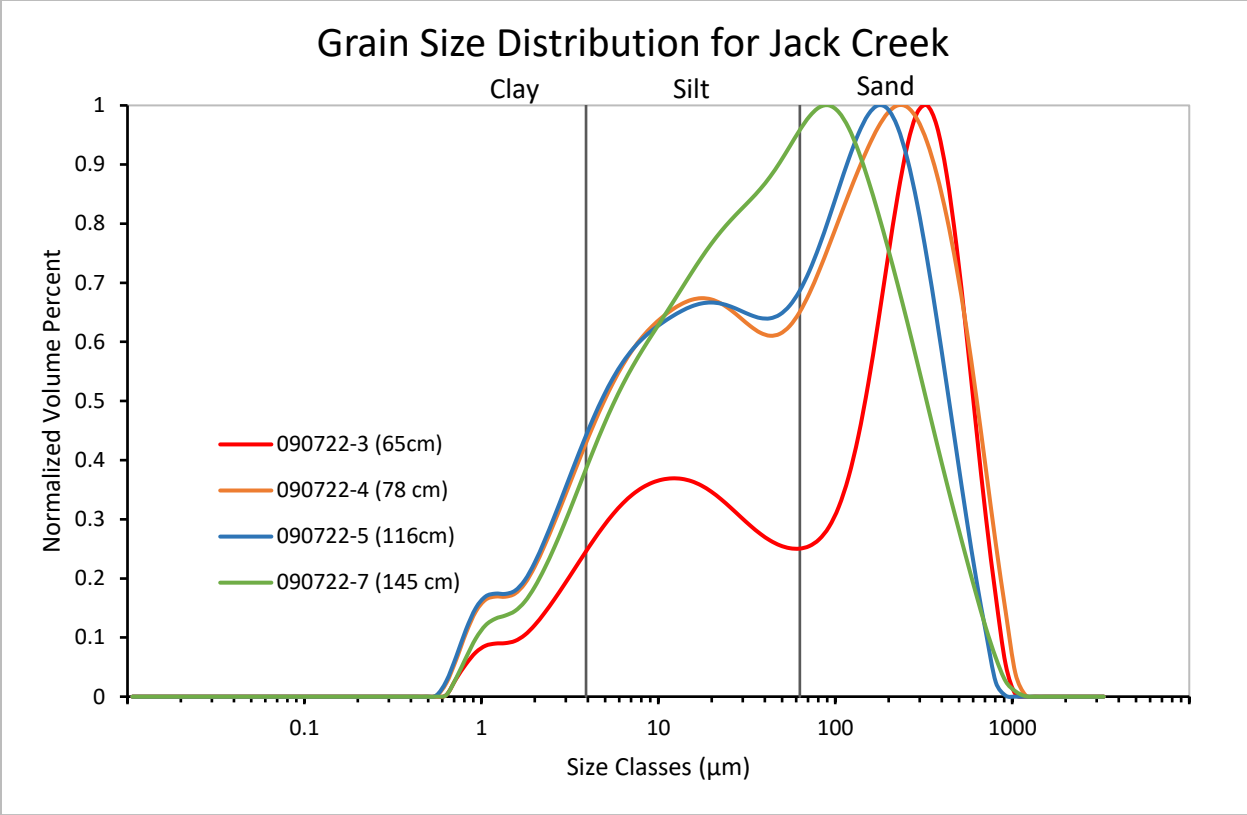


Figure B4. Grain-size distribution graph for Jack Creek.

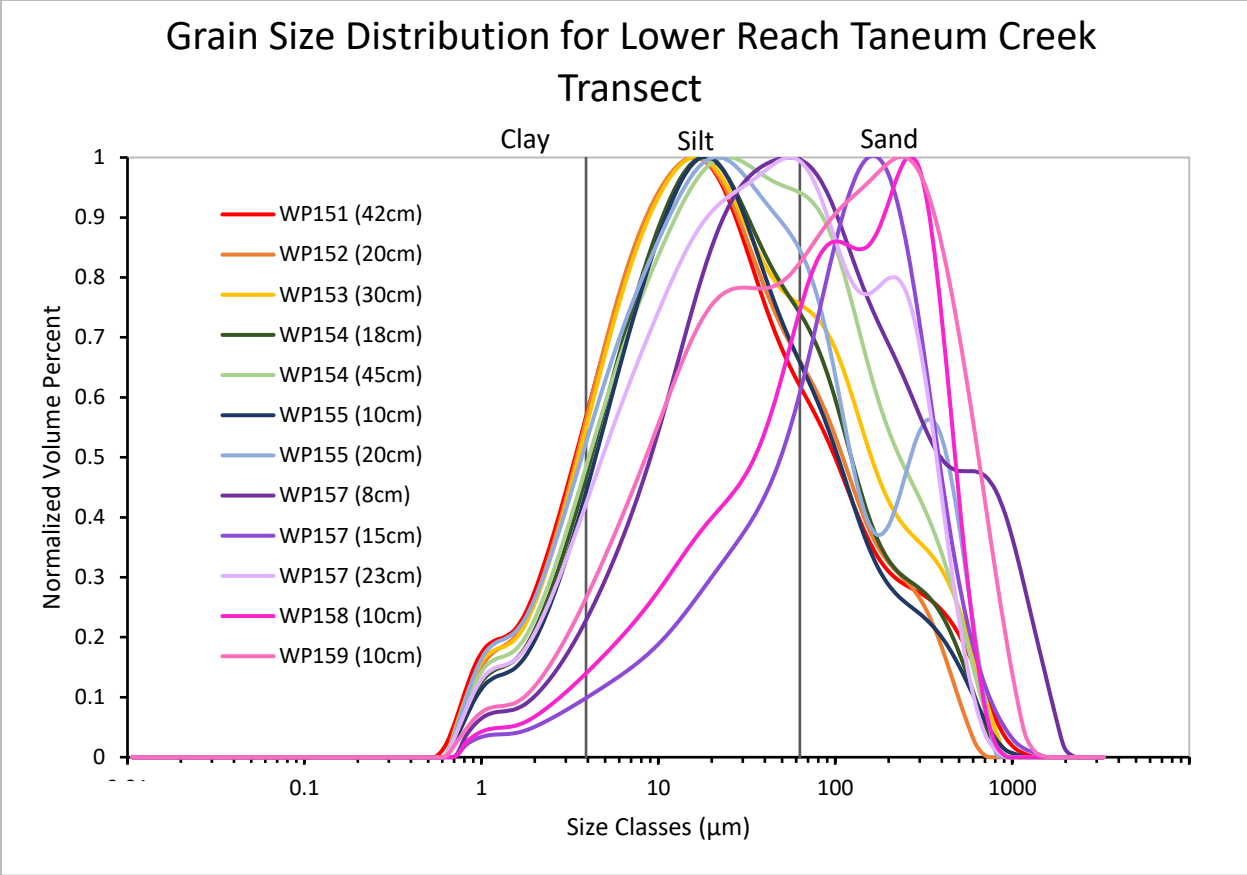


Figure B5. Grain-size distribution graph for Lower Taneum Creek Meadow Transect.

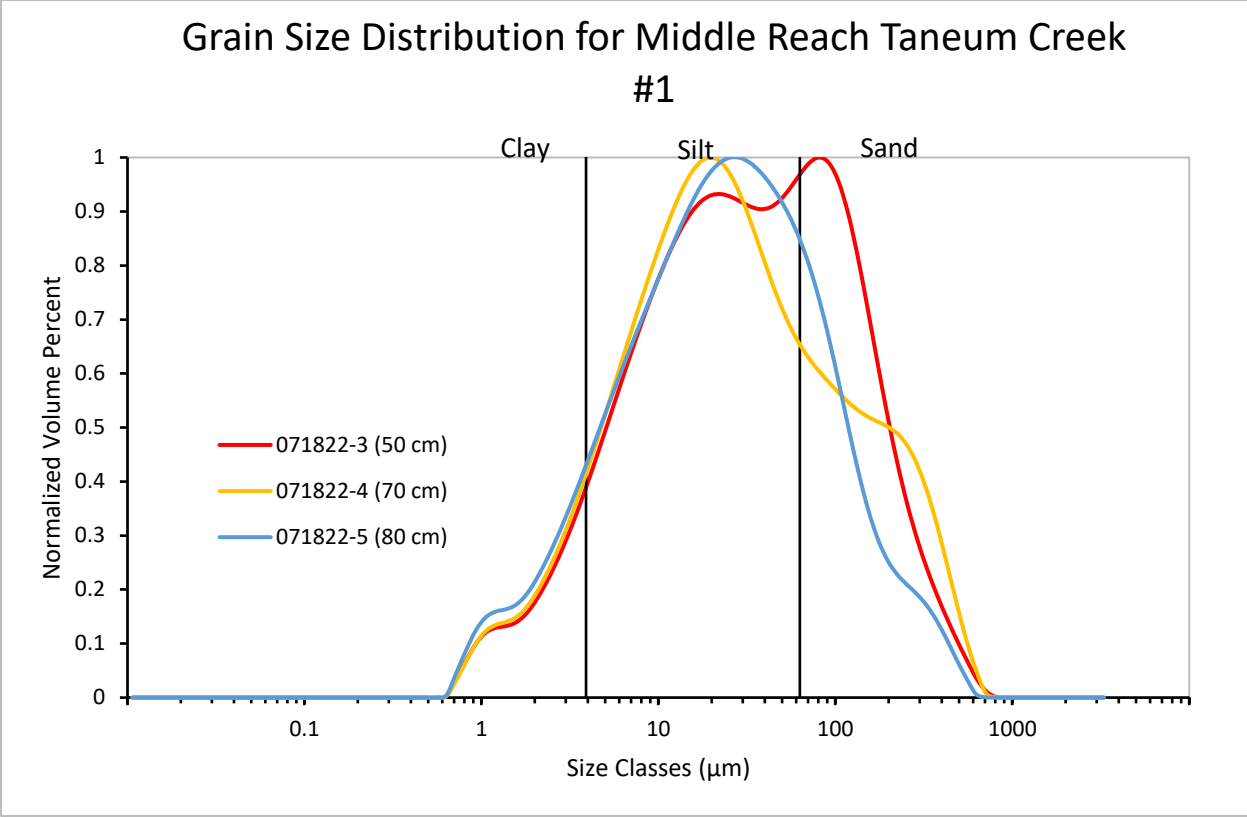


Figure B6. Grain-size distribution graph for Middle Reach Taneum Creek #1.

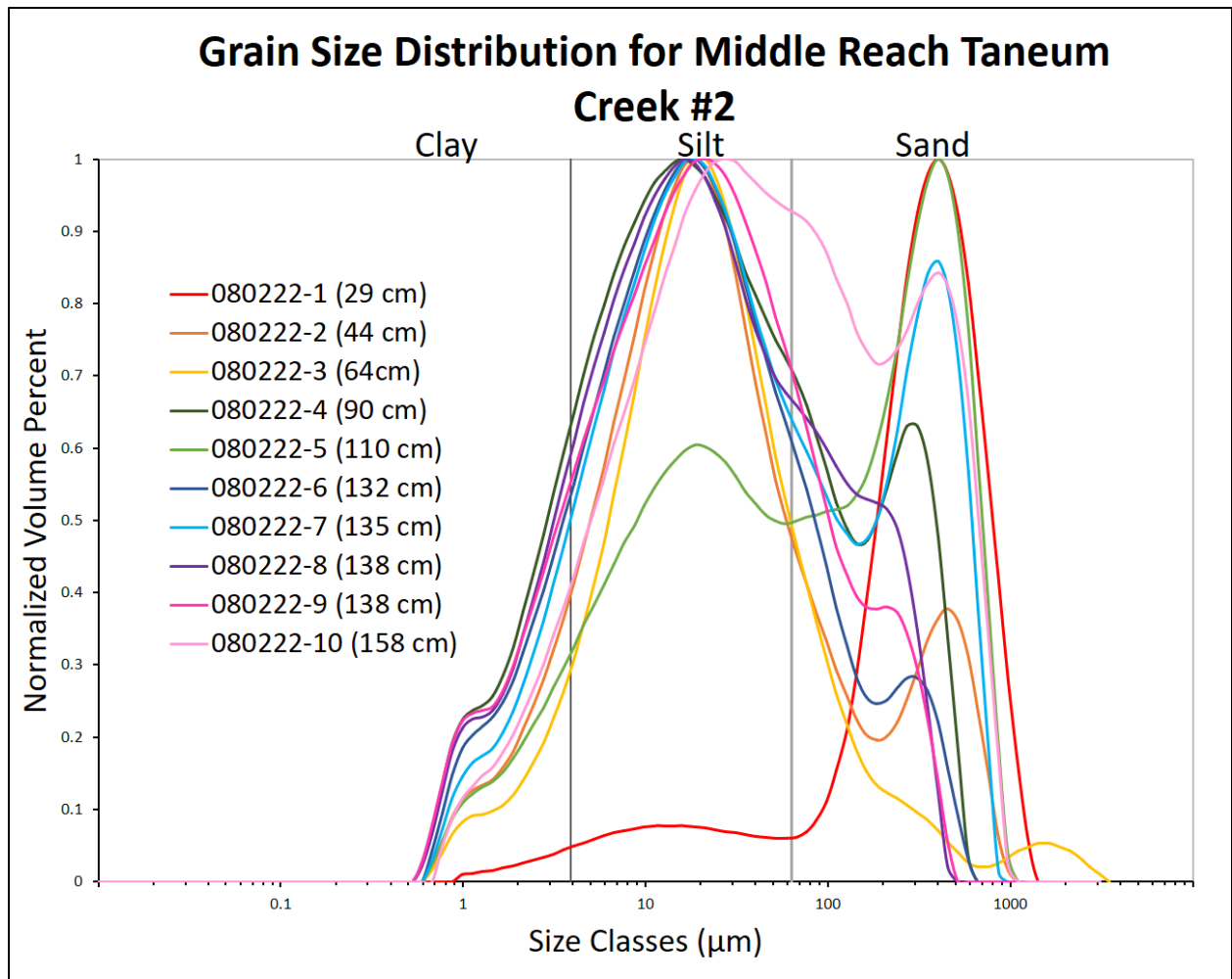


Figure B7. Grain-size distribution graph for Middle Reach Taneum Creek #2.

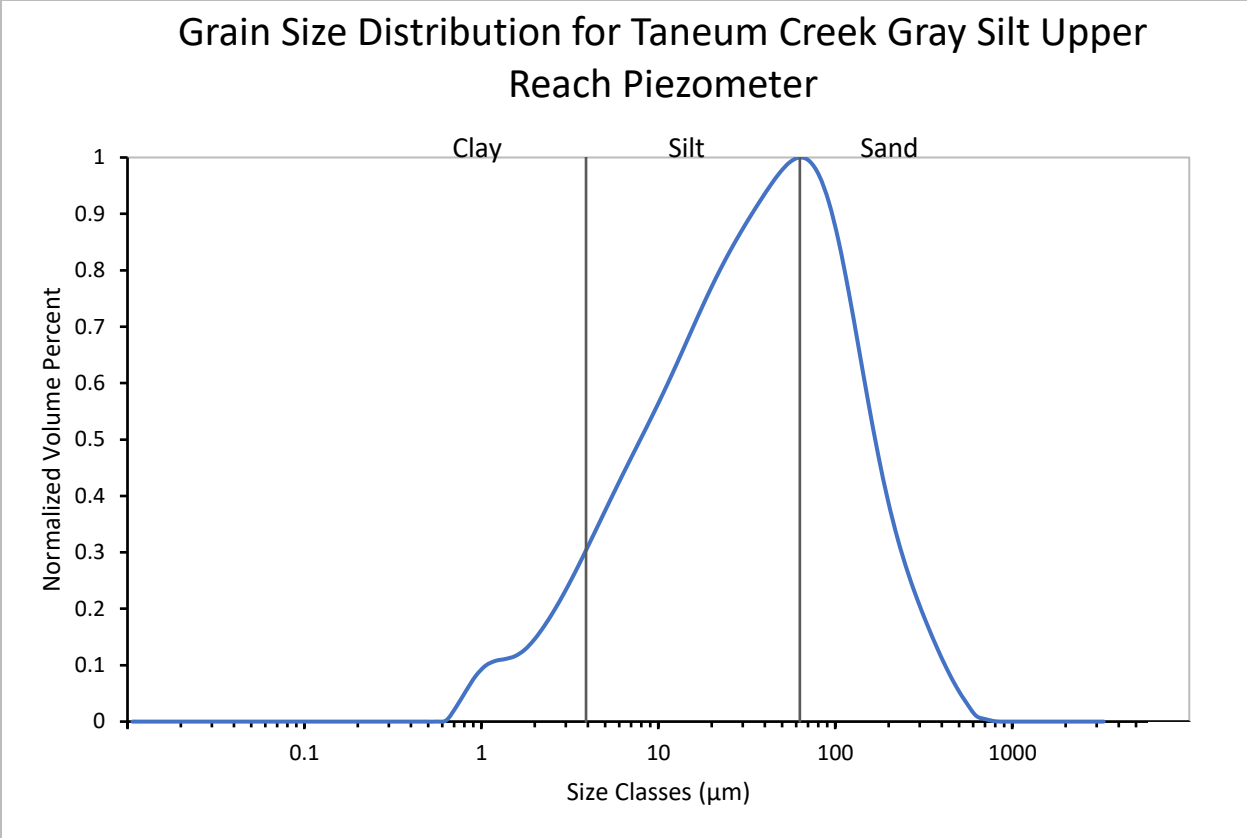


Figure B8. Grain-size distribution graph for Upper Reach Taneum Creek gray silt piezometer location.

Appendix C. REM to Floodplain Area Instructions

How to get a floodplain area value from a relative elevation model (REM) in ArcGIS Pro

References:

- Dilts, T. E., Yang, J., and Weisberg, P. J., 2010, Mapping riparian vegetation with lidar data predicting plant community distribution using height above river and flood height: ArcUser Online.
- Olson, P. L., Legg, N. T., Abbe, T. B., Reinhart, M. A., & Radloff, J. K., 2014, A methodology for delineating planning-level channel migration zones: Washington State, Dept. of Ecology, No. 14-06-025.

Requires

- ArcGIS Pro Software
- LiDAR data without hillshade (I used a dtm from WA DNR LiDAR Portal)
- For better visualization during digitizing process use hillshade and bathymetric hillshade data
- Patience – based on the size of the project and how many separate DEM files you’re using this may take some time and troubleshooting

Modified from the Kernel Density Method by Dilts et al. (2010) and the Inverse Distance Weighting Method, developed at the Washington Department of Ecology by Jerry Franklin and Patricia Olson.

Part 1: Extraction of Channel Water Surface Elevations

Step 1: Manually trace the channel line* - I used the bathymetric hillshade from WADNR to gain a better idea of water subsurface. Could also use a normal hillshade model.

Step 1a: Create new line feature class or shapefile.

Step 1b: Draw a line feature along the lowest elevation in the channel (thalweg). Make line all one feature, if you need to do separate lines combine using the merge tool in the editing tab. If digitizing tributaries they should be a separate line feature class.

Step 2: Generate points along the channel line and extract elevation

Step 2a: Use the Generate Points Along Lines tool in Data Management

- Input Features: Thalweg line feature class
- Output Feature Class: Name your output and direct to correct folder location (ex. thalweg_points)
- Point Placement: By distance
- Distance: determine the average width of your channel and use that number with correct unit
- Check the box “Include End Points”
- Click “Run”

Step 2c: Extract elevations to points using Extract Multi Values to Points Tool

NOTE: In this step you can assign the elevation values to all the points at once using multiple DEMs that the thalweg runs through but, in Parts 2 and 3 you can only process one DEM at a time.

- Make sure the previous editing session is no longer active.
- Navigate to or search the Extract Multi Values at Point Tool (Spatial Analyst > Extraction)
- Choose the “thalweg_points” as the input points and the DTM files as the input rasters. For the output names make sure to label which raster it came from (ex. raster input = DEM_1 and output = emvp_1). This tool will extract the elevation at each point and place the elevation value in a new field in the attribute table.

NOTE: Where the extent of the LiDAR dataset is much larger than the spatial extent of the point features, limit the processing extent under Environment – limit the extent to the extent of the DTM you are using

Part 2: Detrend the DEM using new elevation point values

This step will allow the computer to see what exactly you are comparing the raw DEM to when you go to make your REM based on your chosen search radius. By detrending the DEM you are creating a new base level (the channel) to then compare the raw DEM to.

Step 3: Inverse Distance Weighting (IDW) Tool (Spatial Analyst Tools > Interpolation>IDW)

- Input Point Features: Channel Point feature class with elevation values (thalweg_points)
 - NOTE: if performing this more than once keep in mind that elevation values are saved as a new attribute field. This means each time you run the EVMP tool choose the correct attribute field in the Z value field below.
- Z value field: Choose the name of the attribute field containing elevations from a drop down list.
- Output Raster: Specify the output raster directory and name
- Output cell size: The same as the raw LiDAR DTM
- Power: The default power is 2. Changing the power value will change the distance weighting factor, with higher powers giving a greater weight to closer elevation points.
- Search radius: “The default search radius is variable such that the 12 closest elevation points to a grid cell are used in the IDW calculation. We recommend that the search radius be changed to “Fixed” in the drop down. The Search Radius should then be assigned a Distance based on the width of the floodplain area. It is important that the search radius be set so that the search distance extends well beyond the floodplain area. The IDW algorithm will produce pronounced steps in the detrended DEM within the floodplain area on the inside of meander bends if the search distance is set too small.” (Olson et al., 2014)
 - I measured the width of the entire floodplain area left and right of the channel to come up with the best number (4,000-6,000 ft worked best for my river). When choosing a value you need to think about what you want your data to include: just the floodplain, adjacent terraces or hillslope too? This value needs to be in the unit the data is in. Go to the layer properties to find the correct unit. (WA DNR is in feet). A larger search radius also results in more smoothing of the data

NOTE: Where the extent of the LiDAR dataset is much larger than the spatial extent of the point features, limit the processing extent under Environment – limit the extent to the extent of the DTM you are using

Part 3: Creating the REM

The REM is generated using the minus tool, which subtracts the raw DEM from the detrended DEM. Because the detrended DEM is based on elevations of the water surface within the stream channel, relative elevation values will generally be positive, except in low-lying floodplain areas that sit below the adjacent channel.

Inputs to the Minus Tool (Spatial Analyst) are:

- Input Raster 1 (the raster from which raster 2 values will be subtracted): Raw DEM
- Input Raster 2 (the raster values which will be subtracted from raster 1): Detrended DEM
- Output: Your REM!

Part 4: Symbology – how to best display your REM

This part requires some experimenting with the symbology tab to find how to best represent your data.

- Navigate to the symbology tab (right click on layer name in the contents panel)
- Under Primary symbology select Classify
- Now mess around with the method, classes and numerical breaks within the classes to see which displays the most difference in your area (distinctness of the channels and terraces of the floodplain)
 - Look in the histogram tab under symbology to use the sliding scale for customizing your breaks, much easier than typing the ranges of values for each class.
 - Make your REM 50% transparent using the Rater Layer tab at the top and layer it over the hillshade for optimal viewing

NOTE: When using multiple DEMs to create multiple REMs that are next to each other they will not look continuous with the same symbology breaks. The detrending step will skew upstream and downstream values so the seams between two REMs will show very different elevation patterns for the channels.

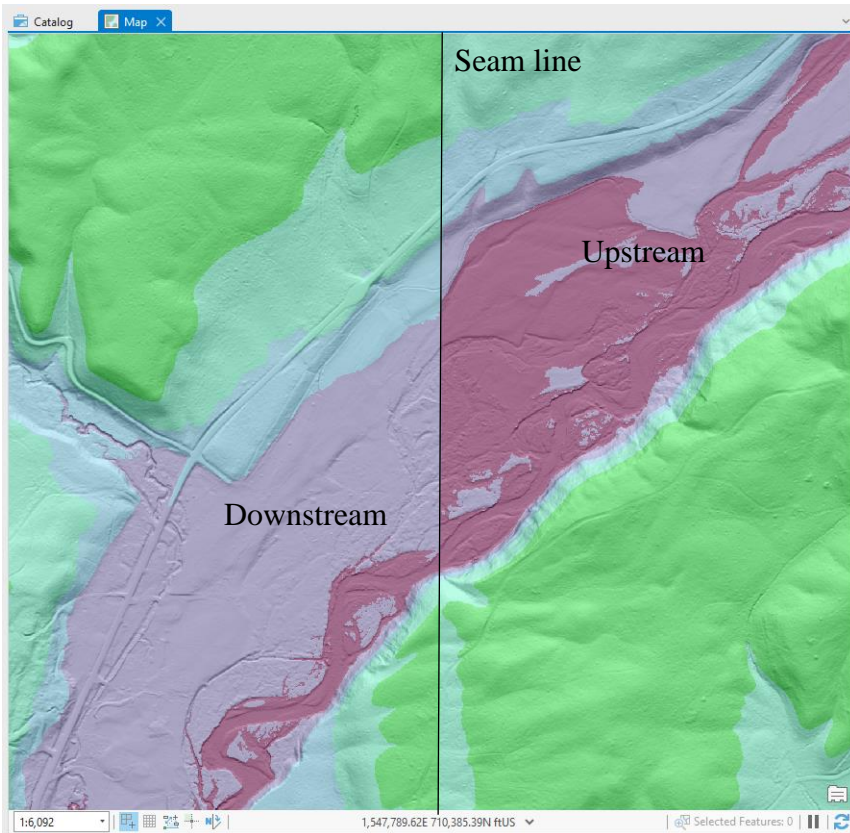


Figure C1. ArcGIS Pro 3.0 screenshot showing skewing between the seams of two REMs.

Part 5. REM Floodplain Extraction and Area Calculation

Once you have an REM to get a value for the floodplain area, you must transform the data from raster to vector to calculate the area. The instructions use Middle Creek (mc) REM as an example to follow.

Step 1. First you must use the “Raster Calculator” in the Spatial Analyst toolbox to change the numeric value from decimal to integer.

- $\text{Rem_mc} * 1,000,000$ (no commas but spaces are okay)
- $\text{Output} = \text{rem_mc_rct}$

Step 2. The use the “Int” tool in the Spatial Analyst toolbox

- $\text{Input} = \text{rem_mc_rct}$
- $\text{Output} = \text{rem_mc_int}$

Step 3. Then you must use the “Raster to Polygon” conversion tool

- $\text{Input} = \text{rem_mc_int}$
- Uncheck “Simplify Polygon”

- Check “Create multipart features”
- Output = rem_mc_cvt

Step 4. Now we are going to divide the new output rem_mc_cvt by 1,000,000 to get the decimal values back for the area calculation

- Add an attribute field in your table called “Conversion”
- Make this field a double data type and numeric
- Right click highlighted column and select Calculate Field
- Gridcode / 1000000

Step 5. For Layer with only the potentially inundated floodplain

- Select by attribute
- Where Conversion is less than or equal to 10
- And conversion is greater than 0
- Apply
- Right click over layer in contents panel and hover over selection
- Choose Make layer from selected feature

Step 6. Then we need to make a new attribute field for Inundation Area

- Add an attribute field called “In_Area”
- Make this field double and numeric
- Save
- Select Column and Calculate Geometry

Step 7. Then to export attribute table to excel use the “Table to Excel” tool

- Make sure to specify your output destination and change the suffix from .xls to .xlsx

Step 8. If you want to assign symbology to the polygon layer follow instructions below. This may not work if you don’t have a many to many relationship in place

- Symbology tab to advanced options (furthest icon to right on symbology pane looks like a paint brush)
- Data exclusion conversion ≥ 40 to isolate the lowest floodplain
- Graduated colors, work from bottom of list up replacing the max value (15, 10, 5, 0)